# FLOOD VULNERABILITY IN PUNJAB, PAKISTAN: A GEOSPATIAL ANALYSIS AND CARTOGRAPHIC APPROACH

MASTER'S THESIS

submitted in partial fulfillment of the requirements for the degree of

Master of Science (MSc)

**PARIS-LODRON UNIVERSITY SALZBURG (PLUS)**

Faculty of Digital and Analytical Sciences

Department of Geoinformatics

and

**PALACKÝ UNIVERSITY OLOMOUC (UPOL)**

Faculty of Science

Department of Geoinformatics

PLUS supervisor: Zahra Dabiri, Ph.D.

UPOL supervisor: prof. RNDr. Vít Voženílek, CSc.

submitted by

Gernot Nikolaus

Salzburg & Olomouc, May 2025

With the support of Erasmus+ programme of the European Union. This Master's Thesis has been developed in the framework of the Erasmus Mundus Joint Master Degree (EMJMD) "Copernicus Master in Digital Earth", jointly coordinated by Paris-Lodron University Salzburg, Department of Geoinformatics, Austria together with University of South Brittany, Computer Science Department, France and Palacký University Olomouc, Department of Geoinformatics, Czech Republic.

# ANNOTATION

The primary objectives of this research are to assess flood vulnerability in Punjab, Pakistan, with a developed Flood Vulnerability Index (I). Furthermore, different cartographic visualization techniques are used to present flood vulnerability and are evaluated in user testing (II). An atlas is compiled, presenting the results for a broader audience, and a digital product is developed (III).

To achieve these goals, open-access data is collected and processed in a GIS environment. The Analytical Hierarchy Process is combined with geospatial analysis and overlay analysis to generate flood vulnerability maps. Different cartographic approaches are visualized with the outcome of the analytical part and tested with users from the general public and climate risk analysts. The maps are enhanced based on the feedback; all results of the master thesis, numbers, and visualizations are compiled into an atlas, featuring maps, figures, and tables.

# KEYWORDS

Floods, Flood Vulnerability, Climate Change, Analytical Hierarchy Process (AHP), Weighted Overlay Analysis, Thematic Atlas, Remote Sensing, Earth Observation, Cartography, Punjab (Pakistan), Disaster Mitigation, Flood Risk Management.

Number of pages: 63

Number of attachments: 4

This thesis has been composed by Gernot Nikolaus for the Erasmus Mundus Joint Master's Degree Program in Copernicus Master in Digital Earth for the academic years 2023/2024 and 2024/2025 at the Department of Geoinformatics, Faculty of Natural Sciences, Paris Lodron University Salzburg, and Department of Geoinformatics, Faculty of Science, Palacký University Olomouc.

Hereby, I declare that this piece of work is entirely my own, the references cited have been acknowledged, and the thesis has not been previously submitted to the fulfillment of the higher degree.

02.05.2025, Olomouc Gernot Nikolaus

I would like to dedicate this work to my late grandfather. He was always very keen on hearing about my work, what I do, and my bachelor's and master's studies. He would have been very interested in reading this thesis, and we would both have enjoyed discussing it with each other.

I would like to sincerely thank both my supervisors. Thank you, Mr. Prof. RNDr. Vít Voženílek, CSc, for your time, the meetings to discuss and receive feedback, and for reading through the thesis. Thank you, Ms. Zahra Dabiri, Ph.D, for your time and the almost biweekly meetings to discuss and refine my work. I am deeply grateful to the experts in Pakistan, who took the time to rate the parameters for the AHP. Without their feedback, based on local experience in Pakistan, the study would not have been possible in its current form. Furthermore, I would like to thank my colleagues at the UNU-EHS for being part of the AHP rating and taking their time for the user testing. I am also thankful to Mr. Radim Tolasz and Mr. Petr Dobrovolný for discussing my master's thesis idea at the beginning. Also, I would like to extend my gratitude to everyone at the Department of Geoinformatics, who gave me feedback and were always ready to discuss anything throughout this journey.

I would like to thank my family and friends, especially my parents, who supported me during these two years of study. Special thanks to both my siblings, Karin and Paul, who read not only through the thesis but also carefully reviewed the atlas, helping to identify and correct errors.

Palacký University Olomouc
Faculty of Science
Academic year: 2024/2025

# ASSIGNMENT OF DIPLOMA THESIS

(project, art work, art performance)

| | |
|---|---|
| Name and surname: | **GERNOT NIKOLAUS** |
| Personal number: | **R230911** |
| Study programme: | **N0532A330010 Geoinformatics and Cartography** |
| Work topic: | **Flood Vulnerability in Punjab, Pakistan: A Geospatial Analysis and Cartographic Approach** |
| Assigning department: | **Department of Geoinformatics** |

## Theses guidelines

The aim of this thesis is to analyze the impact of floods on vulnerability in Punjab, Pakistan using geospatial data and tools. The focus will be on identifying and visualising the most vulnerable and flood-prone areas. The student will conduct a review of existing research on flooding and its visualisation, and study relevant vulnerability indicators. Sentinel-1 and Sentinel-2 satellite data will be used to provide information on the extent of flooding and its impact on agriculture, infrastructure and vegetation. The results of the thesis will be reflected in spatial analyses and a cartographic product. In the spatial analyses, the student will focus on determining the main vulnerability factors and identifying flood-prone areas in the province. The main output of the thesis will be the Punjab Region Atlas, a comprehensive printed atlas with maps of vulnerability, risk zones and social impacts of floods as well as coping capacity, accompanied by an electronic version enriched with interactive elements. The atlas will include textual commentary, infographics and images to enhance the interpretation of the results. A simple story map will serve as a digital supplement to the printed atlas. Through user testing, the student will evaluate the usability of the outputs from the perspective of the target users, such as policy makers and emergency response teams.

| | |
|---|---|
| Extent of work report: | **max. 50 pages** |
| Extent of graphics content: | **as needed** |
| Form processing of diploma thesis: | **electronic** |
| Language of elaboration: | **English** |

Recommended resources:


- Allafta, H., & Opp, C. (2021, January). GIS-based multi-criteria analysis for flood prone areas mapping in the trans-boundary Shatt Al-Arab basin, Iraq-Iran. Geomatics, Natural Hazards and Risk, 12(1), 2087–2116. doi: 10.1080/19475705.2021 .1955755
- Hoque, M. A.-A., Tasfia, S., Ahmed, N., & Pradhan, B. (2019, January). Assessing Spatial Flood Vulnerability at Kalapara Upazila in Bangladesh Using an Analytic Hierarchy Process. Sensors, 19(6), 1302. doi: 10.3390/s19061302
- Roy, A., & Dhar, S. (2024, January). Assessment of flood vulnerability and identification of flood footprint in Keleghai River basin in India: a geo-spatial approach. Natural Hazards, 120. doi: 10.1007/s11069-024-06411-9
- Ullah, N., Tariq, A., Qasim, S., Panezai, S., Uddin, M. G., Abdullah-Al-Wadud, M., & Ullah, S. (2024, October). Geospatial analysis and AHP for flood risk mapping in Quetta, Pakistan: a tool for disaster management and miti- gation. Applied Water Science, 14(11), 236
- Saaty, T. (1994, March). How to Make a Decision: The Analytic Hierarchy Process. Aestimum, 24. doi: 10.13128/Aestimum -7138


| | |
|---|---|
| Supervisors of diploma thesis: | **prof. RNDr. Vít Voženílek, CSc.**<br>Department of Geoinformatics |

| | |
|---|---|
| Date of assignment of diploma thesis: | **December 8, 2024** |
| Submission deadline of diploma thesis: | **May 7, 2025** |

L.S.

**doc. RNDr. Martin Kubala, Ph.D.**
Dean

**prof. RNDr. Vilém Pechanec, Ph.D.**
Head of Department

Olomouc December 11, 2024

# Content

# LIST OF ABBREVIATIONS

| **Abbreviation** | **Meaning** |
|---|---|
| AHP | Analytical Hierarchy Process |
| AR | Annual Rainfall |
| CCC | Coping Capacity Component |
| DD | Drainage Density |
| DeP | Dependent Population |
| DH | Distance to Health Facilities |
| DiP | Disabled Population |
| DR | Distance to the river |
| EL | Elevation |
| FP | Female Population |
| FPC | Flood-Prone Component |
| FVI | Flood Vulnerability Index |
| GIS | Geographical Information System |
| LR | Literacy Rate |
| LULC | Land Use Land Cover |
| MCDA | Multi-Criteria Decision Analysis |
| OSM | OpenStreetMap |
| PD | Population Density |
| PSC | Population Susceptibility Component |
| SD | Standard deviation |
| SL | Slope |
| TWI | Topographic Wetness Index |

# INTRODUCTION

Flooding is one of the greatest dangers globally, which not only destroys infrastructure and damages the economy, but also claims human lives (Bates *et al.*, 2008; Kundzewicz *et al.*, 2014; Rentschler, Salhab and Jafino, 2022; Chen *et al.*, 2024). Pakistan, especially the Punjab region, is affected frequently by floods due to its high population density, agricultural activities, and the presence of five major rivers (Rahman *et al.*, 2017; Waseem and Rana, 2023; Chen *et al.*, 2024). Yearly flood events are exacerbated by climate change (Aldous *et al.*, 2011; Arnell and Gosling, 2013; Kundzewicz *et al.*, 2014; Youssef *et al.*, 2021) thus demanding for effective flood assessments and effective mitigation strategies.

To address flooding globally, researchers have turned to flooding models in combining remote sensing data, Geographical Information System (GIS) techniques, and various flood drivers, to assess the flood challenge in a study area (Gigović *et al.*, 2017; Hoque *et al.*, 2019; Burayu, Karuppannan and Shuniye, 2023; Hossain and Mumu, 2024; Ibrahim *et al.*, 2024; Roy and Dhar, 2024; Ullah *et al.*, 2024). While remote sensing provides important data about topographic conditions, the GIS environment gives the opportunity to store and process this data. Depending on the study and the area, different parameters are chosen and their influence on the study's model is determined.

The flood danger and the large number of people affected in the Punjab province were the motivation for this study. Although global research on flooding exists, only a few studies concentrate on Pakistan, and fewer on the highly affected Punjab region. Studies in Punjab mainly focus on the assessment of areas that are prone to floods and where flooding occurs, but the population is not taken into account. As flood events not only affect the landscape but also communities, it is important to investigate flooding from a multi-dimensional perspective. Such a perspective is used in this master's thesis by developing a flood vulnerability framework. This framework consists of three components, which are used to highlight areas most vulnerable to flooding. While one component considers physical and environmental factors, the others reflect the affected population. Another motivation lies in the mapping of the results. Recognizing that good visualizations, which effectively communicate the results, are missing in existing flood research, this study also focuses on creating visually appealing maps. Different mapping techniques are developed and evaluated in user testing to come to a visualization that works for different users.

All results are compiled into a printed atlas, making the outcomes tangible and accessible not only for informing a decision but also for the general or local population.

# 1 OBJECTIVES

The aims of the master's thesis are to analyze the flood vulnerability in Punjab, Pakistan by developing a flood vulnerability assessment by integrating environmental, social, and coping capacity indicators, and using Copernicus satellite- and geospatial data and tools. The main focus of the thesis lies in the identification of the flood-prone and the most vulnerable areas. The study aims to enhance flood risk mapping and visualization to support decision-making and disaster risk management. To achieve this, a review is done on floods, risk, and relevant vulnerability indicators.

The results of the thesis will be presented through spatial overlay analyses and a cartographic product. In spatial analysis, the focus lies on identifying the flood-prone areas and determining the main factors of vulnerability. Through user testing, the usability of the different cartographic visualization techniques is evaluated to improve the communication of flood risk information. The final output of the thesis will be a printed Atlas, featuring maps of hazard and vulnerability areas, demographic impacts of floods, infographics, and textual commentary. A story map will serve as a digital supplement to the printed atlas, embedded with an electronic version of the printed atlas.

The objectives of this master's thesis can be structured and divided as follows:

I. Geospatial Analysis and Mapping of Flood Vulnerability
   1. Mapping of vulnerability indicators.
   2. Analytical Hierarchy Process.
   3. Determine flood-prone and vulnerable areas based on geospatial analysis.
   4. Validate the flood-prone areas with Sentinel-1 SAR data.

II. Cartographic Design and User Testing
   1. Create visual approaches of flood vulnerability.
   2. Conduct user testing to evaluate the effectiveness of the mapping results.

III. Cartographic Project of the Atlas
   1. Compile an atlas that conveys the results effectively.
   2. Create a digital product.

# 2 STATE OF THE ART

This chapter introduces the context of flood vulnerability and its assessment while reviewing recent studies in this field. Furthermore, it gives information on the knowledge and research gaps this research is trying to fill.

## 2.1 Flood Vulnerability

Flooding is one of the most catastrophic events, occurring in different regions and time periods, as well as affecting large populations worldwide (Bates *et al.*, 2008; Kundzewicz *et al.*, 2014; Bathrellos *et al.*, 2018; Rentschler, Salhab and Jafino, 2022). Floods are a physical phenomenon; when rivers overtop their banks, water flows into the floodplain, which is favored for settlements because they are fertile and near water, thereby increasing the likelihood of flood-related disasters (Bathrellos *et al.*, 2018). According to Rentschler, Salhab and Jafino (2022), 23% of the worldwide population is exposed to floodwaters exceeding 0.15 meters in depth. The majority of those exposed live in South and East Asia, where 1.24 billion people are in areas at risk. Moreover, climate change has an impact and influence on floods, increasing both the intensity as well as its occurrence (Aldous *et al.*, 2011; Arnell and Gosling, 2013; Kundzewicz *et al.*, 2014; Youssef *et al.*, 2021). According to Bates *et al.* (2008) flooding is influenced by various climate factors, such as precipitation and temperature patterns. Additionally, drainage also plays a significant role, as well as urbanization, and the presence of flood management structures like dams or reservoirs.

Floods pose a significant risk to both lives and livelihoods, particularly for vulnerable communities (Rentschler, Salhab and Jafino (2022). Vulnerability is a crucial component in risk management and damage assessment (Connor and Hiroki, 2005; Huang *et al.*, 2012). However, the definition is not fixed; different definitions of the term 'Vulnerability' appear in literature, as well as different concepts of it have been created (IPCC, 2012; Nasiri, Mohd Yusof and Ali, 2016). Furthermore, its meaning evolved over time. For example, the IPCC Third Assessment Report defines vulnerability as a function of exposure, sensitivity, and adaptive capacity (IPCC, 2001). Then, the Fifth Assessment Report redefined the vulnerability's definition and excluded exposure from it (IPCC, 2014). Since then, vulnerability is seen as a function of sensitivity and the capacity to cope and adapt (IPCC, 2022). According to Proag (2014), vulnerability is "the degree to which a system, or part of a system, may react adversely during the occurrence of a hazardous event". For UNDP (2004) human vulnerability is the "human condition or process resulting from physical, social, economic and environmental factors, which determine the likelihood and scale of damage from the impact of a given hazard". Balica and Wright (2010) define vulnerability as the interaction between exposure, susceptibility, and resilience of each community in risk conditions. Nasiri et al. (2016) state that a human system is vulnerable to these three factors. Furthermore, several studies define vulnerability as a function of exposure, sensitivity, and adaptive capacity (Balica and Wright, 2009; Thomas *et al.*, 2018). Additionally, some studies equate sensitivity with susceptibility (Nasiri, Mohd Yusof and Ali, 2016; Padhan and Madheswaran, 2023), and capacity with resilience or adaptive capacity (Balica, Douben and Wright, 2009; Padhan and Madheswaran, 2023).

Several terms appear during the definition of vulnerability: exposure, sensitivity, and capacity. The UNDRR defines exposure as the "situation of people, infrastructure, housing, production capacities and other tangible human assets located in hazard-prone areas" (UNDRR, 2009). Other studies defined it as the chance that people and/or physical items will be affected by floods (Padhan and Madheswaran, 2023). Sensitivity is the "extent to which an element of the system is exposed, which in turn influences the chance of being harmed at the time of occurrence of flooding events" (IPCC, 2001). Resilience is defined as "the capacity of a system, community or society to resist or to change in order that it may obtain an acceptable level in functioning and structure." (UNDP, 2004).

## 2.2 Methodologies in Flood Vulnerability Assessment

With the increasing challenges of flooding occurring, the understanding and mitigation of flood events are becoming more and more important. Different approaches for assessing flood exit. For example, the development of hydrologic and hydraulic models, or the use of artificial intelligence and machine learning (Kumar *et al.*, 2023). The use of GIS, remote sensing, and Multi-Criteria Decision Analysis (MCDA) gives the possibility not only to assess the spatial extent but also the vulnerability of the population during a flood event. This is emphasized by multiple studies (Gigović *et al.*, 2017; Hoque *et al.*, 2019; Burayu, Karuppannan and Shuniye, 2023; Hossain and Mumu, 2024; Ibrahim *et al.*, 2024; Roy and Dhar, 2024; Ullah *et al.*, 2024).

GIS and remote sensing data have become important tools for the observation and management of flood catastrophes (Kabenge *et al.*, 2017). GIS provides a framework for integrating, analyzing, and visualizing spatial data, such as topography, land use land cover, precipitation, rivers, or historical flood records (Kabenge *et al.*, 2017; Hoque *et al.*, 2019; Ullah *et al.*, 2024). While satellite imagery might be used to identify flood areas and to evaluate their extent (Kabenge *et al.*, 2017), digital elevation model (DEM) provides information about regions that might be prone to flooding (Coveney and Roberts, 2017). According to Kumar *et al.* (2023), the steps of a remote sensing and GIS model consist of the following: data collection, preprocessing, flood modeling, and forecasting future floods. First, the needed data for the study is gathered, and the remote sensing data is pre-processed. For example, with radiometric calibration. Then, the data is processed in the GIS environment, e.g., georeferenced. Image analysis methods, such as thresholding or image segmentation, detect floods, and affected areas are identified. Flood maps are created to draw an image of the extent and to evaluate the intensity of flooding. These techniques help identify flood-prone areas and develop strategies for flood mitigation (Sanders *et al.*, 2020). While the input data is calibrated to improve the model's accuracy (Jahandideh-Tehrani *et al.*, 2020), the model is validated with field data or other data sets (Molinari *et al.*, 2019). This ensures that the model is able to capture real flood events and to predict future scenarios, to warn possible affected communities (Kumar *et al.*, 2023).

MCDA is a method to make informed decisions (Evers, Almoradie and de Brito, 2018). The combination of GIS and MCDA has become more popular for evaluating different factors in flood modeling (Hossain and Mumu, 2024). A commonly used technique is the Analytical Hierarchy Process (AHP), as shown in several studies (Hoque *et al.*, 2019; Aydin and Sevgi Birincioğlu, 2022; Burayu, Karuppannan and Shuniye, 2023; Kara and Singh, 2024; Ullah *et al.*, 2024; Zhran *et al.*, 2024). The AHP method divides the flood problem into different parameters and then conducts pairwise comparisons among them. Through the judgment of experts, each criterion is assigned relative importance. According to (Ouma and Tateishi, 2014) the AHP consists of four steps: creation of the decision hierarchy, determining the relative importance of the factors, calculating the weight, and checking the consistency with the consistency ratio.

Kumar *et al.* (2023), emphasize the relevance of future flood models, remote sensing data, and GIS. They hold great potential for effective analysis and managing flood risk more effectively. The quality and the accessibility of remote sensing and geo data increase, which provides more possibilities for better modelling. The combination of GIS and AHP holds advantages, too. GIS enables the calculation of parameters. At the same time, AHP allows for prioritizing them (Ouma and Tateishi, 2014).

## 2.3 Relevant Studies

Recent studies have used the combination of GIS, remote sensing, and AHP techniques to assess flooding across various regions.

Ullah *et al.* (2024) conducted a study in the Quetta District in Pakistan, identifying flood-prone areas by combining an AHP and a geographic information system (GIS). To achieve the flood risk result, eight factors, such as topographic wetness index (TWI), elevation, slope, rainfall, land use land cover (LULC), stream distance, drainage density, and soil type, were used. Based on experts' judgment, these factors were rated with a pairwise comparison matrix (scale of 1 to 9), and the weight for its relative importance was calculated with AHP for each factor. A consistency ratio was calculated to ensure that the matrix is reliable. Furthermore, sensitive analysis was conducted with a single-parameter sensitivity analysis (SPSA) and a map removal sensitivity analysis (MRSA). The eight factors were prepared in a GIS and ranked into five classes to produce the flood risk map of the study area. The model was validated with 130 locations of historical flood event. The final output of the study was a flood risk zone map, showing the flood risk zones in a diverging color scheme and as a pixel-based map.

Roy and Dhar (2024) studied the flood vulnerability footprint of the river Keleghai in West Bengal, India. A flood vulnerability map was created with an AHP and seven criteria, consisting of elevation, slope, rainfall, Normalized Different Vegetation Index (NDVI), LULC, distance to river, and TWI. The layers were classified into five susceptibility class categories, ranging from very low to very high. Based on the AHP, the weights were given to each layer, and the flood risk map was calculated in a GIS environment. The flood risk zones pixel map was validated with recent flood data of 10 days, derived via Google Earth Engine (GEE) with Sentinel-1 data. The authors conclude that the combination of remote sensing data and the AHP, with field verification, could be effective for flood risk management.

Burayu, Karuppannan, and Shuniye (2023) developed a flood vulnerability mapping approach by integrating remote sensing data with an AHP in the Southern Oromia Region, Ethiopia. The authors used eight environmental parameters. Drainage density, elevation, rainfall, slope, soil, land use land cover, distance from the river, and a topographic wetness index were used to create a flood vulnerability map. By combining this map with population density and land use land cover, again, a flood risk map was created. Using AHP for the parameters of the flood vulnerability map, slope (32%), elevation (22%), and rainfall (15%) achieved the highest weights. The parameters were classified into 1, very low, to 5, very high, and calculated then the vulnerability map using weighted overlay in ArcGIS environment. The authors conclude that the findings of their study support the effectiveness of integrating AHP and GIS in utilizing spatial data for informed decision-making in flood hazard mapping.

Similar to the previous study, Mshelia et al. (2024) analyzed flood risk hazards by combining remote sensing data, GIS-based spatial analysis, and an AHP, in the Zambezi Region, Namibia. The study used ten parameters, such as elevation, slope, rainfall, distance from the river, drainage density, topographic wetness index, land use land cover, distance to road, modified soil adjusted vegetation index, and soil type. Each parameter was classified into five susceptibility levels, ranging from very low to very high. Based on the parameters' weight obtained with the AHP, the flood susceptibility map was generated using the weighted overlay in the GIS environment. The GIS results were validated with qualitative surveying interview data. The authors concluded that the study revealed that some areas are safer compared to others and propose for the government to move people away from the high risk region to reduce the impact of flooding.

Hamidi *et al.* (2022), conducted a study in the Charsadda District, Pakistan, incorporating physical as well as social vulnerability parameters, termed as exposure, susceptibility, and resilience. The authors used a GIS and an equal weighting method for weighting the different indicators, such as elevation, proximity to rivers, dependent population, female-male ratio, and literacy. This data, belonging to socio-demographic, was collected via a household questionnaire survey. After assigning weights, the different components were aggregated and mapped, and the vulnerability was calculated and classified from low to high. The study showed that areas with the highest vulnerability were indicators of exposure. Therefore, the authors conclude that several components of exposure, resilience, and adaptability, which in their interplay influence the vulnerability of an individual or a society, contribute to vulnerability, and do not only rely on susceptibility. Furthermore, the authors state the importance of understanding dominant physical and social vulnerabilities that can help mitigate in the study area.

Another study, by Kablan, Dongo, and Coulibaly (2017) assessed social vulnerability to floods in Cocody, Côte d'Ivoire using exposure, susceptibility, and lack of resilience parameters, such as elevation, percentage of women, percentage of people under 5 and 65, and literacy rate. Data was collected per sub-district area, and the different indicators were weighted using an unequal weighting method. The maps were classified into five classes, ranging from very low to very high. The authors explain in the study that the lack of resilience did not correlate with vulnerability but with susceptibility and exposure. However, also some important data for resilience, such as for medical care, were not taken into account due to data availability. Furthermore, the authors also state that their assessment is based on sub-district-level data, creating artificial boundaries in their vulnerability analysis. Using more precise data, such as at the household level, might improve the research.

Hoque et al. (2019) analyzed their study parameters in the physical and social vulnerability, as well as coping capacity criteria. The study area was in the local administrative region Kalapara Upazila in Bangladesh, and the authors conducted the study with GIS and AHP. The physical vulnerability consisted of five parameters, such as elevation, slope, and precipitation. The social vulnerability included eight factors, i.e., population density, dependent population, and disabled population; while three parameters belonged to the coping capacity, such as the literacy rate and the distance to health complexes. In GIS, each criterion was mapped in layers, resampled in a 30 m resolution, and classified into five vulnerability levels. Five experts and one user weighed the criteria with a pairwise comparison matrix; a consistency ratio ensured the consistency of the responses. The weights were used to calculate the different criterion layers separately with the weighted overlay technique and classify them again into five groups. Final maps were created; one by multiplying the physical and social vulnerability layer together, and the other by taking the just mentioned layer and dividing it by the coping capacity layer. These outputs were normalized in values of zero to one and were once again categorized into five vulnerability classes. These maps (raster maps) were validated with a field visit.

These studies demonstrate that assessing flood impacts with different components, such as environmental and socio-demographic factors, is essential. While many studies employ a broad set of socio-economic indicators, some focus mainly on analyzing flood-prone areas with physical components. Furthermore, it was shown that the use of flood vulnerability varies across studies. While some studies use environmental parameters, such as rainfall and drainage density, the authors term their output flood vulnerability; in other studies, the vulnerability is with the combination of socio-economic factors. The literature forms the basis for this study's approach, which aims to assess flood-prone areas and directly analyze how populations are affected by floods in Punjab, Pakistan.

## 2.4 Knowledge and Research Gap

Due to climate change and global warming, floods occur more often, exposing people of communities (Seneviratne *et al.*, 2021). Therefore, flood vulnerability assessment has taken an important position in identifying risk. Studies have used remote sensing data in a GIS, using factors and evaluating criteria with an AHP to assess flood areas and vulnerabilities.

However, many studies focus on a smaller area, such as a district, and not a whole region. This study aims to evaluate a whole region and analyze flood vulnerability. There are only a few studies analyzing flood-prone areas in Pakistan, and there are fewer assessing population susceptibility and coping capacity, especially in the Punjab region. To address this gap for the study area in Punjab, this study develops a Flood Vulnerability Index (FVI) integrating a Flood-Prone Component (FPC), a Population Susceptibility Component (PSC), and a Coping Capacity Component (CCC), aiming to assess both flood exposure and human vulnerability, while considering data availability constraints. Several studies evaluate the study's flood extent with previous flood data, but take only one flood event into account for validating their results (Roy and Dhar, 2024). This study aims as well to address this gap by deriving Sentinel-1 data in order to produce flood hazard maps of the last years and use this data for validation. While some studies take a coarser study resolution, e.g., doing the analysis on an administrative level (Kablan, Dongo and Coulibaly, 2017; Padhan and Madheswaran, 2023) causing artificial boundaries in their results, this study uses a dasymetric mapping technique to map data, usually on boundaries level, to places where settlements are. This approach will increase the value of the study, as the data reflects where people live.

A major research gap exists in the communication of the results. Existing research largely relies on raster-based maps, which might be scientifically robust but may not be accessible or easy to interpret by decision-makers and the general public. As Baptista (2014) states that the approach of the vulnerability assessment should be tangible to users without technical background, so should also the output of the results be as tangible as possible. Effective flood vulnerability assessments should not only be methodologically robust, but also visually communicative to lighten decision-making. Therefore, this study aims to develop and assess different cartographic approaches with cartographic principles, visualizing the different components of the FVI, while evaluating it through user testing to enhance the clarity and usability of these flood vulnerability maps. This approach can contribute to the field of flood mapping by providing new ways of thinking about and presenting flood risk and vulnerability. Secondly, besides the research papers, there rarely exists any other output that delivers the message of the danger of floods. Therefore, the study will also compile an atlas, using the results of the analysis combined with the visual maps to bridge the gap between data analysis and visual communication, making the conducted findings more accessible and impactful.

The main aim of the study is twofold; firstly, to analyze flood vulnerability, and secondly, by the communication of the results. The study addresses gaps in previous research by

1. Analyzing flood-prone areas in Punjab, Pakistan, while integrating population susceptibility and their capacity to cope.
2. Evaluate the identified flood-prone areas with high-resolution Sentinel-1 Synthetic Aperture Radar (SAR) data from multiple flood events.
3. Enhancing the study by using a dasymetric mapping technique.
4. Creating, visualizing, and conducting user testing of different cartographic approaches to present different ways of presenting flood vulnerabilities.
5. And compiling an atlas to enhance the visual communication of flood risk and their people in Punjab, Pakistan.

# 3 METHODOLOGY

The chapter describes the datasets and sources to develop the framework for the flood vulnerability assessment in Punjab. It begins by presenting the study area and the data used in this study. Furthermore, it gives an overview of the software used and the study's workflow.

## 3.1 Datasets and Sources

Different datasets were used for the different parameters used in this study (Table 1). PERSIANN-CSS (Precipitation Estimation from Remotely Sensed Information using Artificial Neural Networks - Cloud Classification System) data was used for the Annual Rainfall, downloaded via the CHRS data portal (CHRS, no date). Drainage Density, Elevation, Slope, and Topographic Wetness Index were obtained from the FABDEM (Forest And Buildings removed Copernicus 30m DEM). FABDEM is a product from the Copernicus GLO 30 Digital Elevation Model (DEM), delivering a resolution of 1 arc-second grid spacing (approximately 30m at the equator), whereas errors of buildings and vegetation were removed (Hawker *et al.*, 2022). The WorldCover V2 2021 was used for the Land Use Land Cover (Zanaga *et al.*, 2022). Health facilities were downloaded, provided by the Humanitarian OpenStreetMap Team via the Humanitarian Data Exchange portal; the same applies to the river stream data. The census data of 2023 was accessed at the Pakistan Bureau of Statistics website (PBS, 2023) and downloaded as PDFs. Sentinel-1 SAR data was used for validating part of the model (Copernicus Sentinel data, 2021-2024), and retrieved via Google Earth Engine (https://earthengine.google.com/).

**Table 1** Description of datasets, their sources, and outputs.

| Source | Output | Temporal Resolution | Spatial Resolution |
|---|---|---|---|
| Sentinel-1 SAR data; Copernicus Sentinel data, 2021-2024 | Previous Flood extent for validation | 2021-2024 | 10 m |
| ESA WorldCover 10m; Zanaga et al., 2022 | Land Use Land Cover | 2021 | 10 m |
| FABDEM (Forest And Buildings removed Copernicus DEM); Hawker et al., 2022 | Drainage Density, Elevation, Slope, TWI | 2023 | 30 m |
| OpenStreetMap, HOT OSM; https://data.humdata.org/dataset/hotosm_pak_waterways | Distance to the River | Modified: 8 January 2025 | Lat., Long. |
| PERSIANN-CCS; https://chrsdata.eng.uci.edu/ | Annual Rainfall | 2015-2023 | 0.04° x 0.04° (4km) |
| 2023 Census, Pakistan Bureau of Statistics (PBS); https://www.pbs.gov.pk/digital-census/detailed-results | Dependent Population, Disabled Population, Female Population, Population Density, | 2023 | Admin3 (Tehsil) |
| | Literacy Rate | | |
| OpenStreetMap, HOT OSM; https://data.humdata.org/dataset/hotosm_pak_health_facilities | Distance to Health Facilities | Modified: 8 January 2025 | Lat., Long. |

## 3.2 Software and Tools

### 3.2.1 ArcGIS PRO

ArcGIS Pro (Version 3.2.1) is mainly used for processing data and for geospatial analysis. The data and parameters are classified and mapped. The different mapping approaches are visualized here at first hand, before they are post-processed in another software.

### 3.2.2 Google Earth Engine

Google Earth Engine (GEE) is used for deriving large datasets. Large datasets were already pre-processed in the GEE and downloaded for the study area. For example, the flood extent of previous years is used for the validation process.

### 3.2.3 Excel

Excel (Version 2503) is used for the AHP. Pairwise comparison matrices were created, the weights were calculated, and their consistency ratio was checked. Excel is also used to calculate the percentage and the area extent of the different classes in the study area, and to create the graphs used in the study.

### 3.2.4 Affinity Designer and Affinity Publisher

Affinity Designer (Version 2.6.2) is used for creating all visual flowcharts, symbols, or figures. Furthermore, the maps are exported as PDF format from ArcGIS Pro and then post-processed in the software. The poster is also created here. Affinity Publisher is used for compiling the atlas.

### 3.2.5 Leaflet

The digital product is created using Leaflet, a java script library for creating interactive maps.

### 3.2.6 GitHub

GitHub is used to host the digital interactive flood vulnerability product. Furthermore, the atlas can also be viewed and downloaded there.

### 3.2.7 QuestionPro

The online survey tool QuestionPro is used for creating a survey to evaluate the importance of the different parameters for the AHP.

## 3.3 Methods and Processing Procedure

The workflow of this study followed a structured approach, integrating literature review, expert consulting, spatial data analysis, and user testing to develop and visualize a flood vulnerability assessment (Figure 1).

Based on literature review, freely available data, and meetings with experts in disaster risk, climatology, and meteorology, 13 parameters are defined for this study. These indicators are derived from various data sources. Each parameter is mapped, classified, and ranked into classes, ranging from 1, very low, to 5, very high (Hoque *et al.*, 2019; Allafta and Opp, 2021; Ullah *et al.*, 2024).

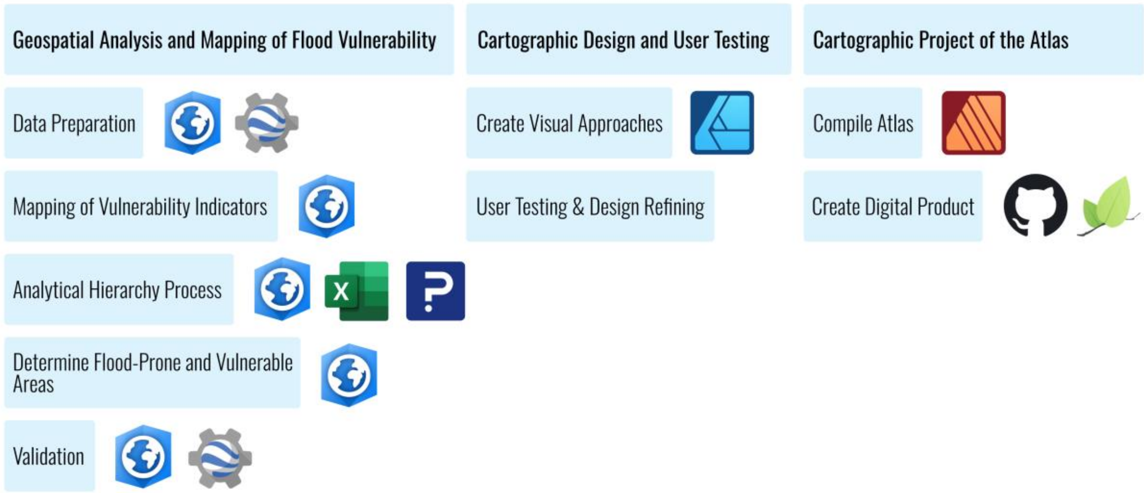


**Figure 1** Workflow of the study.

The component maps are generated by a weighted overlay analysis based on multi-criteria decision analysis, using AHP and applying normalized weights to the indicators. The importance of each parameter is derived using a survey. Similar to other studies (Hoque *et al.*, 2019; Allafta and Opp, 2021; Roy and Dhar, 2024; Ullah *et al.*, 2024), a pairwise comparison matrix is created, relative scores are calculated, and the consistency of the matrix is determined.

After each map is generated, the flood vulnerability is assessed with different approaches, including formula-based results, as well as different cartographic ways. As the study region is very large, it is important to still be able to show regions that have a high vulnerability and to make this message not only available to researchers but also understandable to people. Therefore, the creation of accessible and legible information is important. To achieve that, data has to be generalized to present it in a way that shows high vulnerability areas in a static format. The vulnerability cartographic mapping approach is rated and evaluated with two user groups: the general public and climate risk analysts, identifying which mapping techniques are preferred.

The analysis, the parameter maps, the cartographic maps, as well as the results of the analysis, are compiled into an atlas. Furthermore, a digital product is created.

# 4 GEOSPATIAL ANALYSIS AND MAPPING OF VULNERABILITY

The chapter describes the geospatial techniques for developing the index for flood vulnerability assessment for Punjab. It begins by presenting the study area and the FVI. Furthermore, it explains the processing steps of each parameter, the AHP, and how the component maps and the FVI were calculated.

## 4.1 Study Area

The study area – Punjab, Pakistan – is one of the five provinces of Pakistan (Figure 2). According to the Pakistan Bureau of Statistics (PBS), almost 130 million people live in the region. Although it is not the largest region, it is the most populated one in Pakistan (PBS, 2023). The region spans an area of 205,345 km² and borders India on the eastern side. The PBS divides the province in their census into 36 districts, as well as 146 Tehsils; these are the administrative regions below the district level. The presence of the five major rivers – Indus, Jhelum, Chenab, Ravi, as well as Sutlej – has made Punjab an agricultural center of the country, but prone to catastrophic flooding (Rahman *et al.*, 2017).

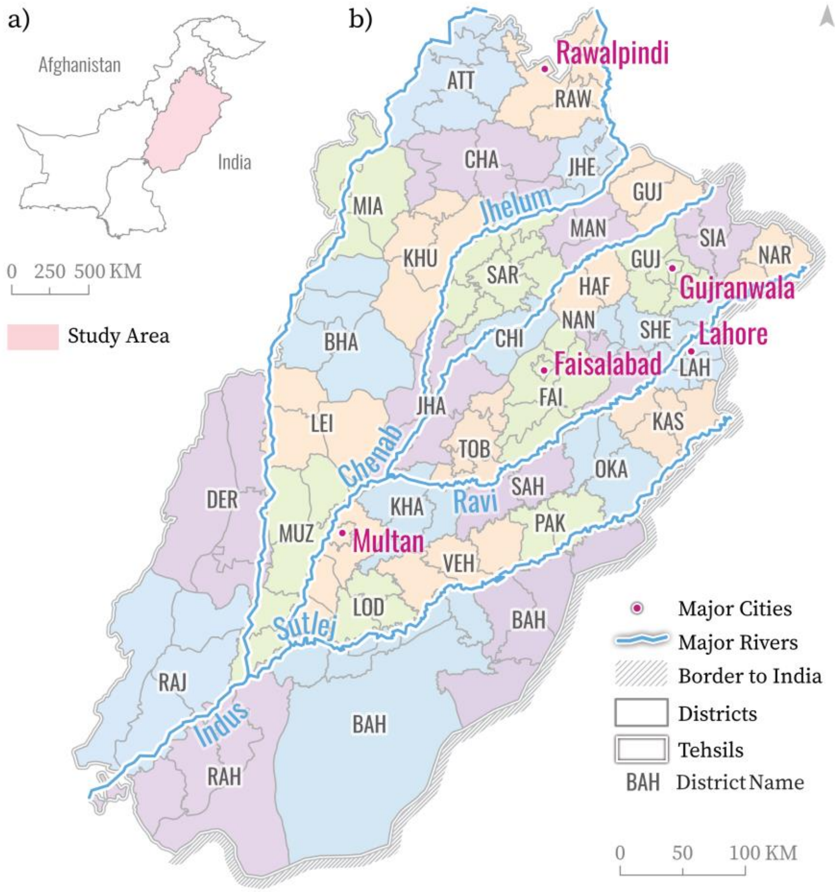


**Figure 2** Study area; (a) the province's location in Pakistan; (b) study area Punjab.

Flood risk and vulnerability are a central concern in the province. According to Rentschler et al. (2022), Pakistan is among the top ten countries where the population is exposed to high flood risk. In particular, the Punjab region is in third place among the subnational administrative areas with the highest absolute number exposed to floods: 38% of the population lives in high-risk flood zones. 2022 was the severest flood since the 2010 flooding (Waseem and Rana, 2023), affecting 33 million people (WFP, 2024). Almost every three years

Pakistan is hit by flood events; between 1950 and 2021 around 21 extreme flood events occurred in the country (Waseem and Rana, 2023). The monsoon season is from June to September and brings severe rainfall (Latif and He, 2025). In the last three years, the average monsoon rainfall was above average (PMD, 2024). This is also reflected in the flood severity. Last year's floods, in 2024, caused 94 deaths in Punjab, among them 46 children, while 238 people were injured, including 86 children (Islamic Relief, 2024).

## 4.2 Flood Vulnerability Index (FVI)

The different criteria were selected based on the literature review, studies, and consultation with experts. As literature has shown that flood vulnerability is a multidimensional concept that includes environmental, demographic, and socioeconomic factors, a the FVI was compiled, using three parts (Figure 3): FPC, PSC, and CCC.

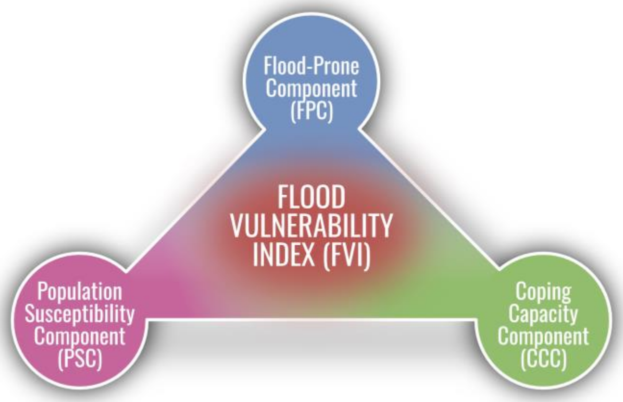


**Figure 3** Flood Vulnerability Index and its components.

This framework explicitly incorporates human vulnerability factors to flood-prone parameters, ensuring a holistic perspective on flood impacts. Furthermore, recognizing the lack of communication, this study employs mapping approaches that prioritize clarity and usability. Based on user testing, different visualization techniques were evaluated, merging the three components together or visualizing them separately, to determine effective ways to represent flood vulnerability.

### 4.2.1 Flood-Prone Component (FPC)

One component of the FVI Model is the FPC. As vulnerability is determined by physical and natural factors (Hoque *et al.*, 2019), the FPC represents the physical and environmental factors influencing flood occurrence. According to (Ullah *et al.*, 2024), the mapping of flood-prone areas is a crucial method for flood management and risk reduction planning, as it helps in generating more effective results. To assess the exposure of the study area to flooding, seven environmental and hydrological parameters were integrated that influence the occurrence of floods (Table 2): Annual Rainfall (AR), which represents the precipitation of rainfall, considering that more extreme rainfall is a driver of flooding (Bathrellos *et al.*, 2016; Kara and Singh, 2024); the Distance to the River (DR) which is the proximity to channels influencing flood-prone (Fernández and Lutz, 2010); the Drainage Density (DD) measures the extent of drainage networks affecting runoff concentration and therefore with higher drainage to a higher flooding (Subbarayan and Saravanan, 2020); the Elevation (EL) as lower elevation experiences higher flood risk (Sanyal and Lu, 2006; Rahman *et al.*, 2019; Allafta and Opp, 2021); the Land Use Land Cover (LULC) – classifying objects, such as buildings, vegetation, and cropland – determining surface permeability and potential water retention capacity (Price, Jackson and Parker, 2010; Owuor *et al.*, 2016; Mojaddadi *et al.*, 2017; Ogato *et al.*, 2020; Allafta and Opp, 2021; Chen *et al.*, 2024; Ullah *et al.*, 2024); the Slope (SL) as flat surfaces are more at risk (Gigović *et al.*, 2017); and the Topographic Wetness Index (TWI) quantifies the topography and soil moisture (Roy and Dhar, 2024).

### 4.2.2 Population Susceptibility Component (PSC)

While there has been extensive research into physical vulnerability, social vulnerability aspects have only been given more attention in recent years (Ajtai *et al.*, 2023). Social vulnerability can be influenced by factors such as age, medical conditions, education, gender, race and ethnicity, income, and residential property (Cutter, Boruff and Shirley, 2003). Therefore, another component of the study's FVI is the PSC, assessing the demographic and socioeconomic characteristics that affect a population's ability to withstand floods, consisting of four parameters focusing directly on population characteristics (Table 2): the Dependent Population (DeP), the Disabled Population (DiP), the Female Population (FP), and the Population Density (PD). While the DeP, DiP, and FP have difficulties in emergency situations (Neumayer and Plümper, 2007; Hoque *et al.*, 2019), higher PD is considered as a higher risk (Hoque *et al.*, 2019). While social vulnerability consists of a broader range of socio-economic, demographic, and infrastructural factors (Cutter, Boruff and Shirley, 2003; Ajtai *et al.*, 2023), other studies also use factors of economic and infrastructural kind, such as housing conditions and building characteristics (Fernandez, Mourato and Moreira, 2016; Hamidi *et al.*, 2022), their exclusion in this study is due to data availability limitations. Therefore, this index is termed PSC, as it does not cover all aspects of social vulnerability but focuses on key demographic indicators to provide a human-centered approach, representing a measure of human susceptibility to flood risks in the study area, given the possibility of measuring flood vulnerability directly at the population.

**Table 2** Flood Vulnerability Index components and their criteria.

| Components of FVI | Criteria |
|---|---|
| Flood-Prone Component (FPC) | Annual Rainfall (mm/y) |
| | Distance to River (m) |
| | Drainage Density (m/km$^2$) |
| | Elevation (m) |
| | Land Use Lanc Cover |
| | Slope (°) |
| | TWI |
| Population Susceptibility Component (PSC) | Dependent Population (%) |
| | Disabled Population (%) |
| | Female Population (%) |
| | Population Density (km$^2$) |
| Coping Capacity Component (CCC) | Distance To Health Facilities (m) |
| | Literacy Rate (%) |

### 4.2.3 Coping Capacity Component (CCC)

The third component of the FVI is the CCC. According to UNISDR (2009), the coping capacity is the "ability of people, organizations, and systems, using available skills and resources, to face and manage adverse conditions, emergencies or disasters". Due to data limitations, two capacity coping parameters were chosen (Kablan, Dongo and Coulibaly, 2017; Hoque *et al.*, 2019): the Distance to Health Facilities (DH) and the Literacy Rate (LR).

## 4.3 Mapping of Parameters

To ensure that the study delivers results as accurately as possible, each parameter map was projected in the study coordinate system – Kalianpur 1962 UTM Zone 43N – and resampled to a resolution of 30 m. In the beginning, a snap raster of this resolution was generated and used in all the following processing steps, ensuring that each pixel of each map lies directly above each other. Each parameter was processed in the GIS environment and classified into five classes, ranging from 1 to 5; which meant for the different components: 1, very low flood-prone, to 5, very high flood-prone for the FPC; 1, very low population susceptibility, to 5, very high population susceptibility for the PSC; and 1, very low coping capacity, to 5, very high coping capacity for the CCC. The interval of the parameter's classes was achieved with different methods, e.g., natural breaks, quantile, or manual intervals. To increase the readability of the maps and the data, the values of the different classifications were rounded to two digits. This was done to deliver results as tangible as possible and achieve good communication, while also not disturbing the correctness of the assessment and the final output.

**Table 3** Classification of components: FPC = Flood-Prone Component, PSC = Population Susceptibility Component, CCC = Coping Capacity Component.

| Class | FPC | PSC | CCC |
|---|---|---|---|
| 1 | Very low flood-prone | Very low population susceptibility | Very low coping capacity |
| 2 | Low flood-prone | Low population susceptibility | Low coping capacity |
| 3 | Moderate flood-prone | Moderate population susceptibility | Moderate coping capacity |
| 4 | High flood-prone | High population susceptibility | High coping capacity |
| 5 | Very high flood-prone | Very high population susceptibility | Very high coping capacity |

With 'Tabulate Area', the percentage and the area size of the different classes within the parameters, component maps, and the FVI were calculated. The total study area calculated using the GIS method derived an area of 205,697 km², which slightly differs from the officially reported area of 205,345 km². This small discrepancy is possible due to variations in the data sources, as no official shapefile was available. This small difference (0.17%) is negligible and does not impact on the overall results.

### 4.3.1 Flood-Prone Component Parameters

In this study, seven FPC parameters were selected (i.e., Annual Rainfall, Distance to the River, Drainage Density, Elevation, LULC, Slope, and Topographic Wetness Index).

#### 4.3.1.1 Annual Rainfall

PERSIANN-CSS data were downloaded as yearly rainfall from each year 2015 to 2023 via the CHRS data portal. These nine data sets were loaded into ArcGIS Pro and reprojected with 'Project Raster'. As a resampling technique, the Bilinear interpolation was used, as the technique is preferred for continuous data (esri, no date f). The average AR was calculated with the 'Raster Calculator' by adding all rasters together and dividing by their number. The 'Raster To Points' tool was used for the 'Kriging' tool. According to Hoque et al. (2019), the kriging interpolation is a common method for interpolating precipitation data sets.

More extreme rainfall is considered to cause flood events (Bathrellos *et al.*, 2016; Kara and Singh, 2024). The precipitation data in the study area ranged from 269.35 mm/year to 1037.09 mm/year, with a mean of 558.01 mm/year and a standard deviation (SD) of 145.84 mm/year. The data was classified using the Natural Breaks (Jenks), as this method minimizes variances within classes, and maximizes variances between classes (esri, no date a), making it suitable for skewed data distribution in the AR data set. After applying the interval, the classes were slightly adjusted for better interpretation.

#### 4.3.1.2 Distance to the River

River and drainage channel data from OSM were used to calculate the proximity of the DR layer, in accordance with a study by Ghorbani *et al.* (2015). The DR layer was calculated with 'Distance Accumulation', calculating the distance for each cell in the raster to the input layer (esri, no date b). After the calculation, the layer was clipped to the study area.

A closer distance to waterbodies means a higher risk (Fernández and Lutz, 2010). The DR ranged from 0 m to 86,103.05 m, with a mean of 5657.92 m, and a SD of 10,351.99 m, indicating very skewed data in the lower distance. The dataset was classified into intervals with manual classes, in accordance with other literature (Hoque *et al.*, 2019; Ullah *et al.*, 2024).

#### 4.3.1.3 Drainage Density

The DD is calculated with the Equation 1 (Hossain and Mumu, 2024).

$$drainage\ density = \frac{total\ length\ of\ drainage\ channels}{total\ area} \tag{1}$$

The elevation profile, which was created for the elevation map as described below (4.3.1.4 Elevation) was used in the calculation process. The DEM was filled with 'Fill', and then the 'Flow Direction' and the 'Flow Accumulation' were run. With the 'Raster Calculator Tool', equal or greater than 1% of the highest value of the Flow Accumulation layer is extracted and saved into a new layer. Then, the 'Stream Order' and the 'Stream to Feature' are executed. Finally, the 'Line Density' tool was executed.

Higher drainage leads to higher surface runoff (Subbarayan and Saravanan, 2020). The DD values ranged from 0 to 122.07 m/km$^2$, with a mean of 31.29 m/km$^2$ and a SD of 26.99 m/km$^2$. This indicated a skewed distribution towards lower density values. To ensure balanced classification and meaningful differentiation across the areas, the quantile method was used. This interval method classifies the data into equal-sized categories (esri, no date a), addressing skewness in the distribution and making meaningful flood vulnerability levels. For better understanding and interpretation, the values were slightly rounded.

#### 4.3.1.4 Elevation

The FABDEM data was loaded into GEE, clipped to the study area, projected on the CRS, and loaded into the GIS environment.

The EL ranged from 68.50 to 2323.25 m above sea level, with a mean elevation of 222 m and a SD of 193.60 m. Indicating very skewed data in the low elevation. Low-elevated regions are at a higher flood risk (Sanyal and Lu, 2006; Rahman *et al.*, 2019; Allafta and Opp, 2021).

#### 4.3.1.5 Land Use Land Cover

For the LULC layer, the WorldCover V2 2021 was used (Zanaga *et al.*, 2022). The different tiles covering the study area were downloaded from the ESA WorldCover Viewer and loaded into ArcGIS Pro. While reprojecting the files to the used CRS in this study with the Project Raster tool, the cell size was resampled to 30 m. As a resampling technique, the Nearest Neighbor was used, as this is best for discrete data (esri, no date f). After the 'Mosaic to New Raster' tool merged all the tiles into one, the layer was clipped to the study area, all while ensuring that the output was snapped correctly.

The given WorldCover layer is classified into tree cover, shrubland, grassland, cropland, built-up, bare/sparse vegetation, permanent waterbodies, and herbaceous wetland (Figure 19a). According to Ogato *et al.* (2020), waterbodies are at a very high and built-up areas are at a high flood risk. Since more than half of the floods in 2022 in Pakistan were on cropland (Chen *et al.*, 2024), cropland has been classified as highly prone to flooding in this study. Furthermore, bare land is at a moderate risk, as precipitation hits the bare ground (Allafta and Opp, 2021), resulting in a higher risk of flooding and runoff (Owuor *et al.*, 2016), as the rain might lead to the formation of a surface crust reducing the infiltration and hydraulic conductivity (Price, Jackson and Parker, 2010). Vegetation is less prone, as it can store water for a period of time (Ullah *et al.*, 2024), and its negative correlation between vegetation density and flooding (Mojaddadi *et al.*, 2017). Less prone also applies to shrublands, due to their high roughness and seepage rates (Allafta and Opp, 2021).

#### 4.3.1.6 Slope

SL was created with the FABDEM data in ArcGIS Pro. With 'Fill', artificial sinks were removed (esri, no date c). Degrees were used as the output measurement, and the geodesic method for calculation, as this gives a more precise output on a larger region (esri, no date g).

Slope plays an important role in the rate and duration of water flow (Ogato *et al.*, 2020). Flatter surfaces have a higher risk, as water moves slower, collects longer, and builds up (Gigović *et al.*, 2017). The SL ranged from 0° to 75.50°, with a mean of 1.56°, and a SD of 4.72°. Natural breaks were chosen as classification intervals and slightly manually adjusted, for better interpretation and readability. Given the skewed data in the lower slope areas, as well as the fact that flat areas are at higher risk, the focus was set on shallow areas.

#### 4.3.1.7 Topographic Wetness Index

The TWI quantifies the topography of hydrological processes and the variability in terrain in soil moisture (Roy and Dhar, 2024). The TWI was created with the FABDEM data in ArcGIS Pro. First, the layer was filled with the Fill tool to remove sinks or depression which could cause errors in the flow of water. Then, the Flow Direction tool was run to create the flow direction for each raster cell (esri, no date e), followed by the Flow Accumulation tool (esri, no date d). Then, the tangent of the new slope radians layer was calculated again with the Raster Calculator. Finally, the Topographic Wetness Index was calculated with the Equation 2 (Beven and Kirkby, 1979),

$$TWI = \ln\left(\frac{a}{\tan(b)}\right) \tag{2}$$

where $a$ is the flow accumulation and $b$ is the slope in radians (Roy and Dhar, 2024). While the index does not have a unit, higher values mean a higher potential for flooding (Roy and Dhar, 2024). In the end, the raster was clipped to the study area.

The TWI ranged from -1.35 to 34.55, with a mean of 7.88 and a SD of 3.69. While the index does not have a unit, higher values mean a higher potential for flooding (Roy and Dhar, 2024). By using quantiles, each class represents a reasonable distribution of the values. The values were slightly rounded for better interpretation.

### 4.3.2 Population Susceptibility Component Parameters

In this study, the component of the PSC is based on four parameters: Dependent Population, Disabled Population, Female Population, and Population Density. Based on the downloaded census data, an Excel sheet was created putting all the required data together. For the DeP, the number of people under 15 and over 60 were counted and the percentage was calculated for each Tehsil. Furthermore, the number of disabled, for DiP, and female population, for FP, was transferred, and the share in each Tehsil was calculated. The PD was calculated with the total amount of the population and the area of the Tehsils. Then, this table was joined with the administrative boundaries' shapefile of the Tehsils. A map was created for each PSC parameter. As the census data was available on administrative boundaries (Tehsils), a dasymetric map was created for all PSC parameter maps. A dasymetric map is a thematic mapping technique in which statistical data is redistributed on the basis of additional spatial information to provide a more accurate representation of population distribution within administrative boundaries (Eicher and Brewer, 2001). To get this information, the Tehsil map was masked out with settlement data, derived from the LULC. A settlement layer was created based on the LULC, consisting of buildings (1) and no-buildings (0); each PSC parameter map was then calculated with the Equation 3:

$$PSC\ paramter\ map\ masked = settlements\ \times PSC\ parameter\ map \tag{3}$$

The PSC represents human-related vulnerability, therefore, the dasymetric mapping method ensures that the analysis of PSC is only represented in settled areas. This prevents overestimation in large, sparsely populated Tehsils and provides a more realistic spatial representation of human vulnerability.

#### 4.3.2.1 Dependent Population

The DeP is comprised of people under 15 and over 60. According to Hoque et al. (2019), these age groups are dependent, as they may not earn money and are dependent on other family members. The share of DeP ranged from 37.80% to 59.20%, with a mean of 44.77% and a SD of 3.31%. Given the skewed distribution, Natural Breaks was chosen as an interval method.

#### 4.3.2.2 Disabled Population

Disabled populations face challenges in emergency situations (Hoque *et al.*, 2019). The share of DiP ranged from 1.67% to 15.73%, with a mean of 4.21% and a SD of 2.00%. Natural Breaks was chosen as an interval method.

#### 4.3.2.3 Female Population

Women might have more difficulties in flooding situation and their mobility during evacuation, e.g., during pregnancy (Neumayer and Plümper, 2007). The share of the FP ranged from 46.12% to 52.02%, with a mean of 49.00% and a SD of 0.91%. Natural Breaks were chosen as an interval method.

#### 4.3.2.4 Population Density

Higher Population Density is considered more vulnerable (Hoque *et al.*, 2019). The values of PD ranged from 8.56 pop./km² to 18,945.59 pop./km², with a mean of 1276.36 pop./km² and a SD of 2866.66 pop./km². Natural Breaks was chosen as an interval method.

### 4.3.3 Coping Capacity Component Parameters

The component of the coping capacity consists of two criteria. The DH was calculated with 'Distance Accumulation'. Similar to the PSC parameters, the LR was derived from the 2023 census data and combined with the administrative boundaries of the Tehsils. As the coping capacity is also related to the population and its ability to respond to floods, the data were also masked with the settlements using the Equation 3 to focus only on relevant populated areas.

#### 4.3.3.1 Distance to Health Facilities

The values of DH ranged from 0 m to 140,110.78 m, with a mean of 24,995.72 m and a SD of 22,050.09 m. The layer was classified in accordance with other literature (Hoque *et al.*, 2019).

#### 4.3.3.2 Literacy Rate

Through low LR, warnings can be missed (Hagenlocher *et al.*, 2016). The values of the LR layer ranged from 8.60% to 88.20%, with a mean of 63.94% and a SD of 13.30%. Natural Breaks were chosen as an interval method.

## 4.4 Analytical Hierarchy Process

The relative importance of the seven parameters of the FPC, the four parameters of the PSC, and the two parameters of the CCC was assessed using an AHP technique. Similar to other studies (Hoque *et al.*, 2019; Ogato *et al.*, 2020; Allafta and Opp, 2021; Ullah *et al.*, 2024) the present study uses the AHP technique to compute relative scores of the parameters, create pairwise comparison matrices, and assess the matrix consistency.

### 4.4.1 Survey

A survey was carried out in order to weigh each parameter for its importance based on experts' opinions. The survey was created with the online survey tool QuestionPro. The survey was filled out by two different groups: Experts in Pakistan (n=8), working in sectors such as disaster risk management, urban planning, environmental sciences, forestry, and healthcare, as well as climate risk analysts (n=5) of the United Nations University – Institute for Environment and Human Security (UNU-EHS). The experts were asked to fill out a bipolar matrix, rating the relative importance of one sub-criterion against another based on the scale of Saaty's 1 to 9 weighting (Table 4).

**Table 4** Importance scale (based on Saaty, 1990)

| Importance Intensity | Definition |
|---|---|
| 1 | Equal importance |
| 3 | Moderate importance |
| 5 | Strong importance |
| 7 | Very strong importance |
| 9 | Extreme importance |
| 2, 4, 6, and 8 | Intermediate values for finer judgments |

Thereby, each component of the FVI was evaluated individually, and the experts were able to give their opinion about which indicators are more important, and how much more important it is.

### 4.4.2 Pairwise comparison matrix

The comparison matrices were created in Excel for each criterion. The geometric average of the responses was taken, and the corresponding matrix was filled out for FPC (Table 5), PSC (Table 6), and CCC (Table 7).

**Table 5** Pairwise comparison matrix for FPC; AR = Annual Rainfall, DR = Distance to River, DD = Drainage Density, EL = Elevation, LULC = Land Use Land Cover, SL = Slope, TWI = Topographic Wetness Index.

| Parameter | AR | DR | DD | EL | LULC | SL | TWI |
|---|---|---|---|---|---|---|---|
| **AR** | 1 | 2 | 1 | 1 | 1 | 1 | 1 |
| **DR** | 1/2 | 1 | 1 | 1 | 1 | 1 | 1 |
| **DD** | 1 | 1 | 1 | 3 | 1 | 3 | 2 |
| **EL** | 1 | 1 | 1/3 | 1 | 1 | 1 | 1 |
| **LULC** | 1 | 1 | 1 | 1 | 1 | 3 | 2 |
| **SL** | 1 | 1 | 1/3 | 1 | 1/3 | 1 | 1 |
| **TWI** | 1 | 1 | 1/2 | 1 | 1/2 | 1 | 1 |

**Table 6** Pairwise comparison matrix for the PSC; DeP = Dependent Population, DiP = Disabled Population, FP = Female Population, PD = Population Density.

| Parameter | DeP | DiP | FP | PD |
|---|---|---|---|---|
| **DeP** | 1 | 1 | 2 | 4 |
| **DiP** | 1 | 1 | 4 | 4 |
| **FP** | 1/2 | 1/4 | 1 | 3 |
| **PD** | 1/4 | 1/4 | 1/3 | 1 |

**Table 7** Pairwise comparison matrix for the CCC; DH = Distance to Health Facilities, LR = Literacy Rate.

| Parameter | DH | LR |
|---|---|---|
| **DH** | 1 | 2 |
| **LR** | 1/2 | 1 |

### 4.4.3 Matrix Consistency

According to Brunelli (2015), the eigenvalue ($\lambda_{max}$) indicates the deviation of the matrix from the consistency. First, the normalized vector of the matrices (Table 5, Table 6, Table 7) was calculated by dividing each element in the column by its corresponding column sum. Then, the weights of each parameter were calculated by taking the product of each parameter in the row and taking the average. The normalized vector of each parameter, as well as its respective weight, can be seen in Table 8, Table 9, and Table 10. The weighted sum was calculated by the summation of the row of each parameter; and the consistency vector of each parameter by dividing the product by the respective weight. Furthermore, $\lambda_{max}$ was computed by dividing the sum of the consistency vectors by the number of parameters.

**Table 8** Normalized vector for FPC; AR = Annual Rainfall, DR = Distance to River, DD = Drainage Density, EL = Elevation, LULC = Land Use Land Cover, SL = Slope, TWI = Topographic Wetness Index.

| Parameter | AR | DR | DD | EL | LULC | SL | TWI | Weight |
|---|---|---|---|---|---|---|---|---|
| **AR** | 0.15 | 0.25 | 0.19 | 0.11 | 0.17 | 0.09 | 0.11 | 0.15 |
| **DR** | 0.08 | 0.13 | 0.19 | 0.11 | 0.17 | 0.09 | 0.11 | 0.13 |
| **DD** | 0.15 | 0.13 | 0.19 | 0.33 | 0.17 | 0.27 | 0.22 | 0.21 |
| **EL** | 0.15 | 0.13 | 0.06 | 0.11 | 0.17 | 0.09 | 0.11 | 0.12 |
| **LULC** | 0.15 | 0.13 | 0.19 | 0.11 | 0.17 | 0.27 | 0.22 | 0.18 |
| **SL** | 0.15 | 0.13 | 0.06 | 0.11 | 0.06 | 0.09 | 0.11 | 0.10 |
| **TWI** | 0.15 | 0.13 | 0.10 | 0.11 | 0.09 | 0.09 | 0.11 | 0.11 |

**Table 9** Normalized vector for PSC; DeP = Dependent Population, DiP = Disabled Population, FP = Female Population, PD = Population Density.

| Parameter | DeP | DiP | FP | PD | Weight |
|---|---|---|---|---|---|
| **DeP** | 0.36 | 0.40 | 0.27 | 0.33 | 0.34 |
| **DiP** | 0.36 | 0.40 | 0.55 | 0.33 | 0.41 |
| **FP** | 0.18 | 0.10 | 0.14 | 0.25 | 0.17 |
| **PD** | 0.09 | 0.10 | 0.05 | 0.08 | 0.08 |

**Table 10** Normalized vector for CCC; DH = Distance to Health Facilities, LR = Literacy Rate.

| Parameter | DH | LR | Weight |
|---|---|---|---|
| **DH** | 0.67 | 0.67 | 0.67 |
| **LR** | 0.33 | 0.33 | 0.33 |

Lastly, the consistency of the matrices was determined by the consistency ratio ($CR$), as in the Equation 4:

$$CR = \frac{CI}{RI} \tag{4}$$

where $CR$ is the consistency ratio, $RI$ is the random index (Table 11), and $CI$ is the consistency index, calculated in the Equation 5:

$$CI = \frac{\lambda_{max} - n}{n - 1} \tag{5}$$

where $\lambda_{max}$ is the maximum eigenvalue, and $n$ is the number of parameters.

**Table 11** Random index (Saaty, 1987).

| N | 1 | 2 | 3 | 4 | 5 | 6 | 7 | 8 | 9 | 10 |
|---|---|---|---|---|---|---|---|---|---|---|
| **Random index (RI)** | 0 | 0 | 0.58 | 0.90 | 1.12 | 1.24 | 1.32 | 1.41 | 1.45 | 1.49 |

The FPC matrix achieved $CR$ of 0.04, the PSC a $CR$ of 0.04, and the matrix a $CR$ of 0. All of the matrices have $CR$ < 0.10, which indicates an informed judgement (Saaty, 1994).

**Table 12** Matrix consistency.

| FVI Component Matrix | λ_max | N | RI | CI | CR |
|---|---|---|---|---|---|
| **Flood-Prone Component (FPC)** | 7,31 | 7 | 1.32 | 0.05 | 0.04 |
| **Population Susceptibility Component (PSC)** | 4,12 | 4 | 0.90 | 0.04 | 0.04 |
| **Coping Capacity Component (CCC)** | 2 | 2 | 0 | 0 | 0 |

## 4.5 Validation of FPC

The validation of the FPC was done with a hazard flood layer, indicating where historical flooding happened. A previous flood extent layer was obtained by GEE. Sentinel-1 data was loaded from 2021 to 2024 to ensure that the validation is based on multiple flood events, and the data was filtered based on the monsoon period to pre-flood (May-June) and post-flood (September-October). Furthermore, the layer was generated with VV polarization and IW mode. In order to improve the accuracy of the validation layer, slopes with > 3° were filtered out to reduce false positives, and the data were smoothed with a focal median filter (100 m radius). Finally, flooded areas were identified using a threshold of –3 dB, and all images were merged to capture all the flooding events during these years. With 'Tabulate Intersection', the percentage of historical flooding events in the classes of the flood-prone areas was calculated.

## 4.6 Generating of Maps

### 4.6.1 Flood-Prone, Population Susceptibility, and Coping Capacity Maps

The FPC Map, PSC Map, and CCC Map were calculated with the weighted overlay analysis, with the Equation 6:

$$Component_{map}(x,y) = \sum_{i=1}^{n} W_i \times CR_i(x,y) \tag{6}$$

where $Component_{map}(x,y)$ represent the respective map at each pixel location, $W_i$ is the weight assigned for the corresponding parameter (Table 5) and $CR_i(x,y)$ is the class rank (1 to 5) to the corresponding parameter.

### 4.6.2 Flood Vulnerability Index map

FVI is calculated in accordance with other study (Hoque *et al.*, 2019) with the Equation 7:

$$FVI = \frac{(FPC \times PSC)}{CCC} \tag{7}$$

where $FVI$ represents the Flood Vulnerability Index, $FPC$ the Flood-Prone Component, $PSC$ the Population Susceptibility Component, and $CCC$ the Coping Capacity Component (CCC).

Since the PSC and the CCC outputs were masked with settlements to make sure to focus on actual human populations, a lot of Null values would exist in the results of this formula. In order to avoid computational issues and bias in the flood vulnerability calculation, areas with no data in PSC were given the lowest vulnerability class (1) to reflect the absence of population at risk. Areas with no data in the CCC were assigned with the highest coping capacity class (5) to indicate that uninhabited areas do not require coping mechanisms. This makes sure that higher FPC and PSC values indicate worse conditions (more vulnerable), and higher CCC reduces it, respectively. The approach ensures that the FPC remains for the whole area, while PSC and CCC-related factors only apply to actual human populations, preventing distortions in the final vulnerability assessment.

# 5 CARTOGRAPHIC DESIGN AND USER TESTING

The chapter describes the cartographic principles to visualize flood vulnerability in Punjab. It begins by explaining the color choices. Furthermore, it explains the different cartographic visualization techniques, how the user testing was conducted, and summarizes the responses of the user.

## 5.1 Colors

Colors help visualize data, both quantitative and qualitative. While different color hue differentiates categories, the color value (lightness/darkness) describes the intensity order of a phenomenon (Brewer, 1999). Several color combinations were tested to find options that looked good in print while also capturing the semantics of each component.

For the FPC initially, a red color was chosen, with the aim of giving the feeling that the higher the prone of a flood, the more dangerous the risk is. However, the user testing indicated that the red is too dominant. To enhance the readability, the color was switched to blue, also to link the thematic connections to water. To maintain visual consistency, the blue color scheme is used throughout this thesis. The component uses a sequential scheme to show the different intensities of flood-prone areas, while a higher intensity of blue means more flood-prone (Figure 4b). The PSC is represented using a pink color. When showing the different classes of population susceptibility, a sequential pink color scheme was used (Figure 4c). A higher intensity of pink colors indicates a higher susceptibility of the population. The CCC is visualized in green. A sequential color scheme was chosen when visualizing the different classes of the coping capacity (Figure 4d). A higher intensity of green indicates a higher coping capacity, reinforcing this positive association.

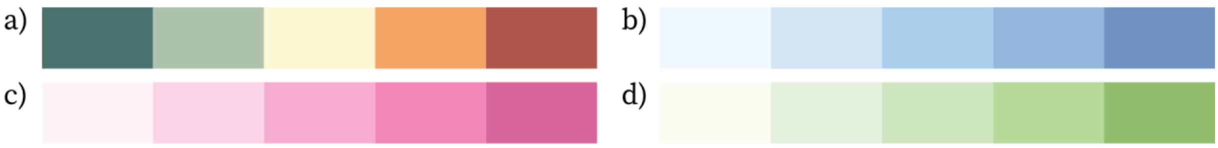


**Figure 4** The color scheme of (a) Flood Vulnerability Index, (b) FPC, (c) PSC, and (d) CCC.

For the FVI, a divergent color scheme was chosen (Figure 4a), from dark green (very low vulnerability), to light yellow (moderate), to dark red (very high vulnerability).

The aim of the given colors was to make them not only effective in conveying the spatial relationship but also intuitively interpretable for users, and to provide as effective communication of the data as possible. Therefore, these color hues are used systematically throughout the text and in the atlas to make the connection to the component and the meaning directly possible.

## 5.2 Processing steps Cartographic Visualizations

### 5.2.1 Flood Component Maps and FVI Map Across Tehsils

In order to visualize the spatial distribution of the different components and the FVI, 'Zonal Statistics' was used to calculate the mean values at the Tehsil level (administrative level 3). This method calculates the respective average value of the FPC, PSC, CCC, and FVI within each Tehsil with the Equation 8:

$$Tehsil_{mean} = \frac{\sum(Pixel\ Value \times Pixel\ Count}{Total\ Pixel\ Count\ in\ the\ Zone} \tag{8}$$

This approach ensures that each Tehsil is represented by an aggregated average level, making the regional comparison possible.

Furthermore, the FVI was normalized with the Equation 9:

$$FVI_{norm} = \frac{FVI - FVI_{min}}{FVI_{max} - FVI_{min}} \tag{9}$$

where $FVI$ is the pixel value of the FVI, $FVI_{min}$ the minimum value of the FVI map, and $FVI_{max}$ the maximum value, respectively. This was done after the aggregation at the Tehsil level.

### 5.2.2 FPC Background with Pie Charts of People Exposed Across Tehsils

Different approaches of maps were visualized using the FPC in the background, while symbols of PSC and CCC are mapped at the Tehsil level.

The first map uses pie charts, indicating the proportion of PSC and CCC calculated by averaging their pixel map at the administrative boundary. Furthermore, the size of the charts serves as a proxy for people affected. This was calculated using the settlements layer, indicating buildings and no-buildings, and counting the amount of 30 m pixels across each Tehsil. Based on that, the respective number of hectares of settlements was calculated, and the charts were scaled accordingly.

### 5.2.3 FPC Background with Half-Circles of People Exposed Across Tehsils

A second map uses the FPC as background as well. This time, PSC and CCC are represented as scaled half circles, representing the classes of PSC and CCC, respectively.

The pie chart and the half-circle map draw the major river for better orientation. Furthermore, the Tehsils with the highest FPC were labeled with their first three letters.

### 5.2.4 Kriging Map of FVI and FPC

A different mapping approach was tested out to ignore administrative boundaries, as flooding or other climate change-related hazards do not stop at borders, for each component and the FVIM as follows: With 'Generate Tessellation' a hexagon grid was created, covering the study area. Based on the grid, 'Zonal Statistic' was run to get the average mean values of each hexagon cell. 'Feature to point' created points inside each hexagon cell, while 'Extract Multi Values To Points', saved each value of the aggregated grid of each map layer into respective fields. Finally, 'Kriging' created an interpolation for each map. The Geometric interval method was used for their data classification. Different resolutions were used in this approach with hexagon grids of 10 km², 50 km², and 100 km².

### 5.2.5 Kriging Map of FPC with Wurman Dots of People Exposed

Similar to those mentioned above, a kriging of FPC was calculated with a 100 km² hexagon grid. Furthermore, the values of the Tehsil average of PSC and CCC were taken and saved into a point layer. The same hexagon grid was used, so that both layers share the same uniform grid size and ensure that they represent comparable spatial units. Graduated symbols visualized people's exposure, with the dividing PSC by CCC. Given that formula, a larger circle means higher exposure to the population, while a smaller one means the opposite.

## 5.3 Process of the User Testing

As different mapping approaches of flood vulnerability were visualized, user testing was conducted to assess two main aspects as follows:

- Is assessing vulnerability with administrative boundaries better, or is it better to have the data interpolated (Kriging map)?
- Is it preferred to use the formula to analyze flood vulnerability or to have the three components separately visualized (pie charts, half circles, Wurman dots) to represent each underlying factor individually?

These questions were examined in user testing with two different user groups: climate risk analyzers (n=10), and people of the public (n=6) who are not familiar with the topic. Five maps were tested in the user testing: (a) FVI across Tehsils and (b) interpolated with 50 km², (c) FPC background with pie charts of people exposed across Tehsils, (d) FPC background with half-circles of people exposed across Tehsils, and (e) kriging map of FPC with Wurman Dots of people exposed. These maps were printed out in the style they would also appear in the Atlas. The user testing was per person, with 20 to 25 minutes planned, recorded, and conducted as follows: First, the user received a quick explanation of the study, the components, the FVI formula, as well as the pixel map. Then, the user looked at each map one by one. An explanation was only given if it was necessary. They had to think out loud and briefly describe what they saw. Once a map was done, the next map was shown. Depending on the map, questions were asked by the tester to get also a better understanding of the user's understanding:

a. FVI across Tehsils: Do administrative boundaries help in understanding flood risk, or do they make it misleading?
b. FVI Interpolated: Does this map feel more accurate than the Tehsil-based one? Why or why not?
c. FPC background with half-circles of people exposed across Tehsils: Does adding human exposure make the risk clearer, or do they make it harder to interpret? Do the pie charts give more insight into vulnerability compared to the previous maps?
d. FPC background with half-circles of people exposed across Tehsils: Does this way of visualizing Population Susceptibility and Coping Capacity make sense to you? Do the half-circles make it easier or harder to understand than the pie charts?
e. Kriging map of FPC with Wurman Dots of people exposed: Does this map summarize the others well? Is this the easiest map to understand? Does the dot representation work, or is it misleading?

After all maps were shown, the users were asked some additional questions:

- Which map was the most useful? Why?
- Which map was the hardest to understand? Why?
- If you had to pick one map for decision-making, which would it be?
- If you had to show one of these maps to the public, which would it be?

Finally, the user rated all the maps once again on a sheet of paper with a two-dimensional grid. The user had to place a dot in the scale of from 0 to 100 of these two dimensions, while the x-axis indicates the ease of understanding and the y-axis the level of spatial data.

## 5.4 Cartographic Visualizations and User Testing Responses

For the user testing, two pages were created to give a quick summary of the research and its components (Figure 5). On the left side, the three different indices were enumerated with their color scheme and respective maps drawn. A small text gives a short summary. Furthermore, the formula of the FVI was explained and visualized. On the right page, the FVI Map is drawn with its five vulnerability classes. These two pages were used at the beginning of the user testing for explanation to the participants. A very short explanation was given, and questions were answered if it was necessary.

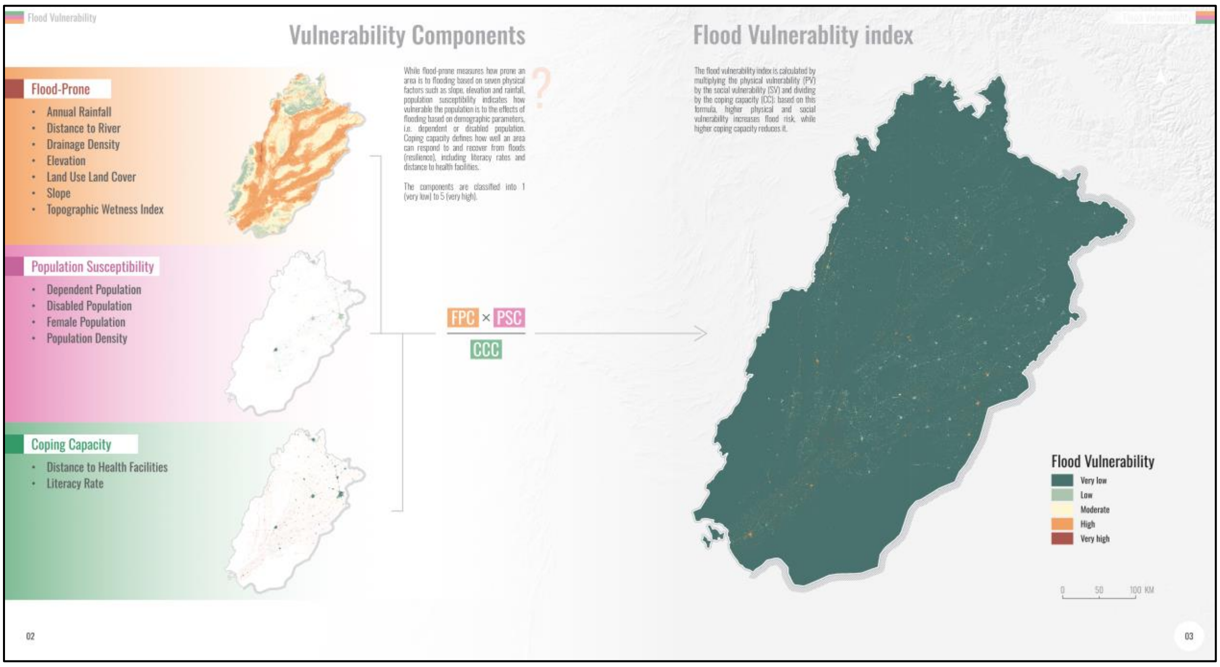


**Figure 5** Starting map of the user testing; showing the three different components with its parameters (left), and the calculated FVI Index Map (right) based on its components.

### 5.4.1 FVI Map Across Tehsils

The FVI Map was aggregated to Tehsils with the average (Figure 6). As a classification method, the Equal interval was used to ensure a straightforward as well as consistent interpretation of their flood vulnerability values across administrative boundaries. Policymakers and local authorities often use administrative boundaries to compare the different regions. While this visualization style was generally well-received by both the general public as well as climate risk analysts, their reasons for preference differed.

In the user testing, the participants of the general public think that it makes the risk clearer as it is better to recognize patterns compared to the previous pixel map, and therefore to identify high-risk areas quickly. Several participants stated that using administrative boundaries helped them to interpret the risk more clearly. One participant noted that using administrative boundaries would be more accurate and interesting for the people living in the respective Tehsil. Furthermore, participants stated that the map was immediately clear at first sight, as this technique effectively highlighted risk zones. One participant mentioned that adding the river also contributed to the understanding of the risk in the study area. Some participants stated that this map was the easiest to read, and that it would be suitable for public communication, as it clearly shows the different vulnerability zones.

For climate risk analysts, this mapping approach was valued for its alignment with administrative boundaries for the decision-making process. One participant stated that this map makes it easy for government officials to understand flood risk in Tehsils. Another participant emphasized that this visualization makes risk clearer, as the pixels in the previous pixel map are very small. This was supported by another participant who said that this approach is good for printing maps, when zooming is possible due to a digital product, the previous one is better for retaining spatial detail.

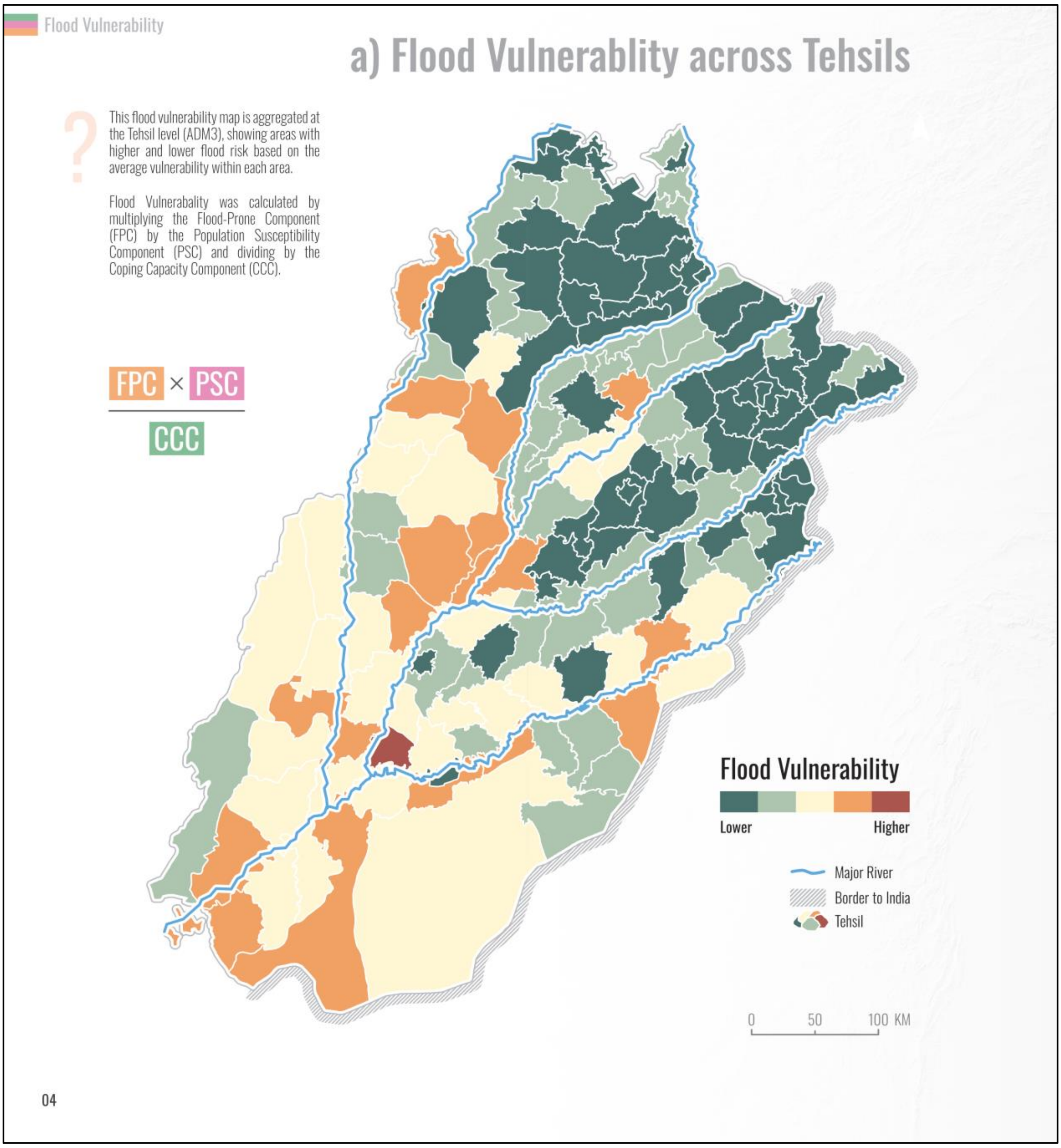


**Figure 6** FVI aggregated to Tehsils. Before the user testing.

### 5.4.2 Kriging Map of FVI Map

The FVI was interpolated in 50 km² hexagons and mapped, drawing the Tehsils, and the districts above (Figure 7). This mapping approach was generally found to be more accurate than the previous one by both user groups. This can be directly seen when comparing the Tehsil in the bottom-right corner. In the previous map, it is just classified as low vulnerability; considering the interpolated map, it shows much more differentiation in the different vulnerability classes in this Tehsil. This makes sense, as the aggregated Tehsils map takes the whole average of its area, which causes the low classification, while the interpolation mapping approach uses the same spatial unit across the study area.

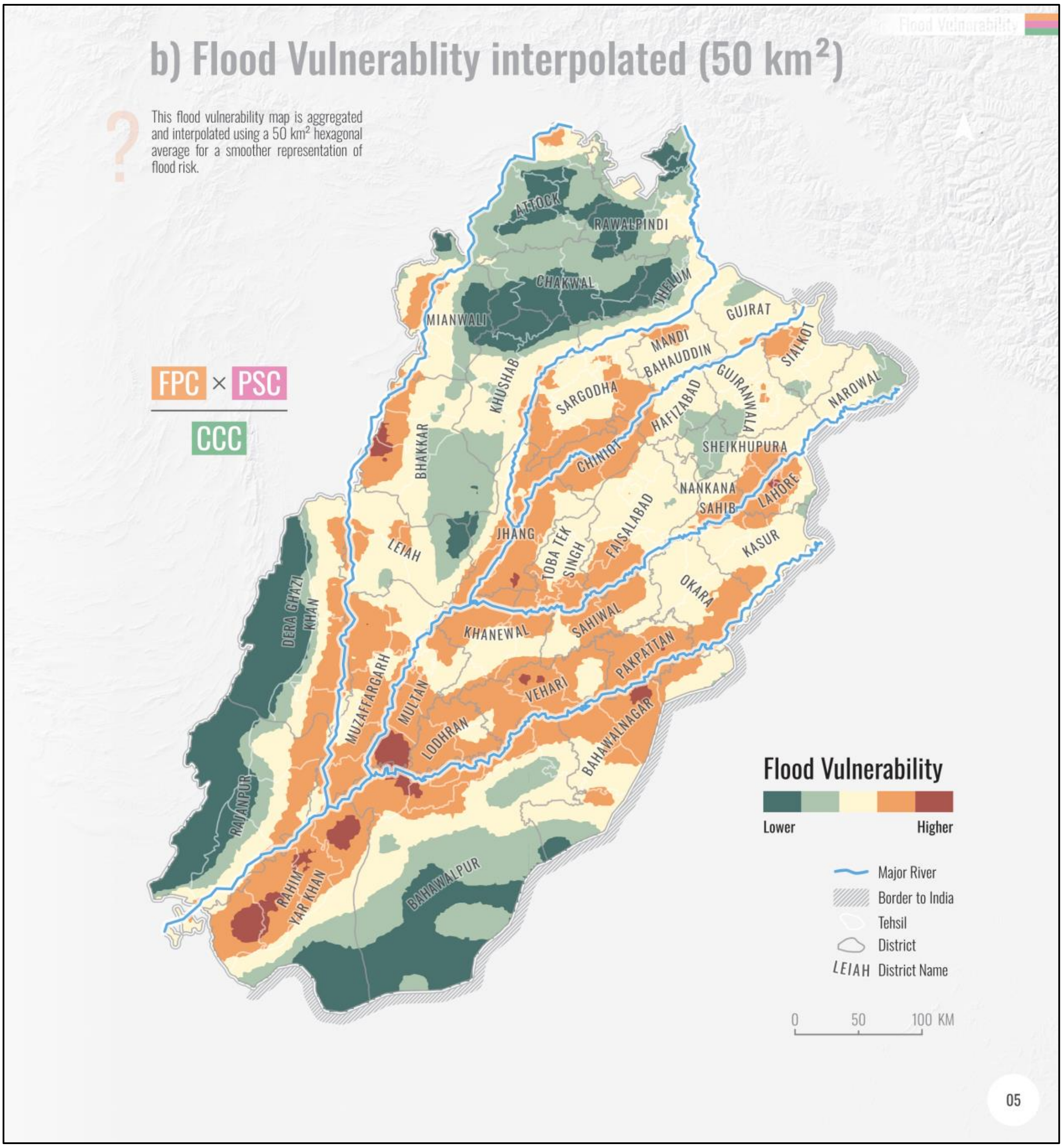


**Figure 7** FVI interpolated. Before the user testing.

The general public stated that this map is more accurate than the previous one. One participant stated that the differences are easier to understand, also, he liked that the districts are labeled. Someone else has correctly recognized that vulnerability "goes beyond boundaries", making this a more accurate approach. However, more explanation of what interpolation does is needed. Therefore, more attention should also be paid to providing more information in the atlas and more explanatory text on how everything was done and calculated. Another participant mentioned that it depends on the user group; people might be interested in their Tehsil, and other people might prefer the interpolation for more accuracy to know where the risk is.

The climate risk analysts' user group draws a similar picture. It was said that this map draws a clearer picture. One participant stated that this map is "more plausible", as aggregated to the admin 3 level; it was justified by this that in the previous map, very high risk is neighboring low-vulnerable zones. However, for a short look, the previous one was better to know immediately where which kind of risk is: “[…] you need a bit more time, but […] this [FVI interpolated] is more accurate”. Someone else said that this approach is more helpful as “[someone] can look more specific” and “see better the vulnerability levels in the Tehsils”. Another one liked this map much better, however, he has drawn attention to carefully using interpolation for its consumption techniques. Furthermore, someone stated that this approach “tracks more [the vulnerability] and makes more sense”.

### 5.4.3 FPC Background with Pie Charts of People Exposed Across Tehsils

The FPC was aggregated to the Tehsil level, while pie charts drew the PSC and the CCC of the Tehsils. The size of the pie charts gives information on the settlement area at the administrative level (Figure 8).

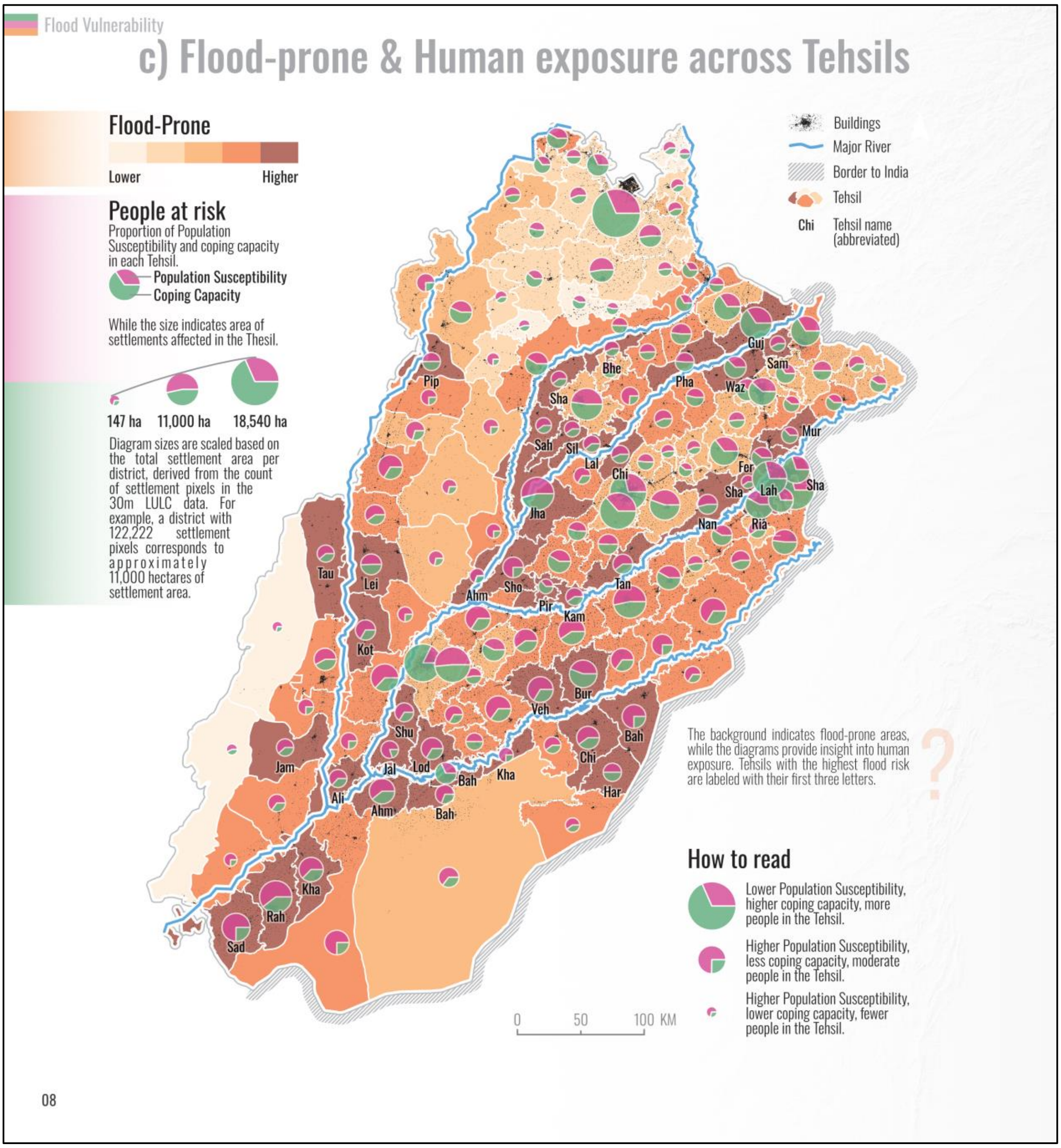


**Figure 8** Flood Vulnerability is split into its three components; visualized with a choropleth background, and pie charts. Before the user testing.

Generally, both user groups found that his map gave more information, but needed more time for understanding.

One participant of the general public stated that in the previous map, the vulnerability is seen immediately. In this map, users have to look closer, but more information is provided. The user said that “for research purposes or people who want to know why exactly there is this vulnerability, this map gives more insights”. This was supported by other participants who said that this map is more difficult to understand and mentioned its complexity, but when more time is spent, it will provide more insights. Someone said that the color of the background should be different, or making it more transparent, to enhance the visibility of the pie charts. Another one said that the background should also be interpolated to make this also more accurate. However, this was done to have the same spatial unit of the components. For some people, an explanation was needed that this mapping approach does not use the formula anymore. In the atlas, there should be an intention to explain the three different components better. After telling the user that the color refers to the three components seen in the first sheet, they understood this reference. It should be emphasized more to explain this better.

The climate risk analysts' user groups' responses draw a similar picture. They emphasized that this map is more complex than the previous one, but it gives more insights into the three components. A participant stated that “for a decision-maker, it is also important to see [...] where tolerable damages are”, and where prioritization is needed. He mentioned that this map is still complex but “[decision makers are] able to prioritize where people need support as fastest”. Several participants said that the pie charts are overlapping, making them too complex. Another participant that it is “super much”, and it is complicated to identify patterns of PSC and CCC with this map. Someone said that there is too much information and had the suggestion that the building layer could maybe be removed, as this information is not necessary and would maybe improve the readability. Someone mentioned that the pie charts suggest that one of the components (PSC, CCC) resolves the other, and users might not have a picture of the values beneath it, as pie charts only give their proportion.

### 5.4.4 FPC Background with Half-Circles of people Exposed Across Tehsils

Similar to the previous map, Figure 9 draws the FPC in the background, however, the PSC and the CCC are mapped above using a different visualization approach. Half circles give information about the index value with its size as well as its color intensity. Generally, this map was more difficult to understand in both user groups, however, some participants also preferred this one over the previous one.

A participant of the general public mentioned that this map is more difficult to understand, as looking more at the legend is needed. While several people said that pie charts are better as this map uses color intensity, which makes it difficult to distinguish the differences with the background below, someone said that this approach is preferred. Due to color blind impairment, the participant looked at the size and not the color. Someone mentioned that the pie charts are better at first sight, however, accuracy is better here, as there is no problem with proportion. The participant suggested using only the size to distinguish the different levels and not changing the color intensity. Another participant supported that this map is more accurate for the population.

Generally, participants in the climate risk analysts user group preferred this map over the pie chart visualization approach. A participant stated that this approach makes more sense and is more accurate than the previous one. However, some participants also had difficulties with the color intensity, especially in the lower PSC and CCC classes. A participant mentioned that coping capacity is visible, especially in the higher classes, but PSC is hard to identify and read. Several participants recommended changing the color of the PSC to a more prominent intensity to make it more visible, and only using one color for each component. Another participant finds that the map is better compared to the pie charts. The PSC and the CCC are independent of each other; they "stand in competition with each other [in the pie-charts], and you do not really know about the index values". Someone mentioned that this visual approach works, hence, it is not a commonly seen approach. A participant finds this map "less busy" and had the recommendation to add an inset map to the areas where symbols accumulate. A user mentioned that this is more visually appealing, but checking the legend is more needed: "[…] have a look back and forth". Nevertheless, one participant had a problem understanding the map due to the color intensity and was not very satisfied with it.

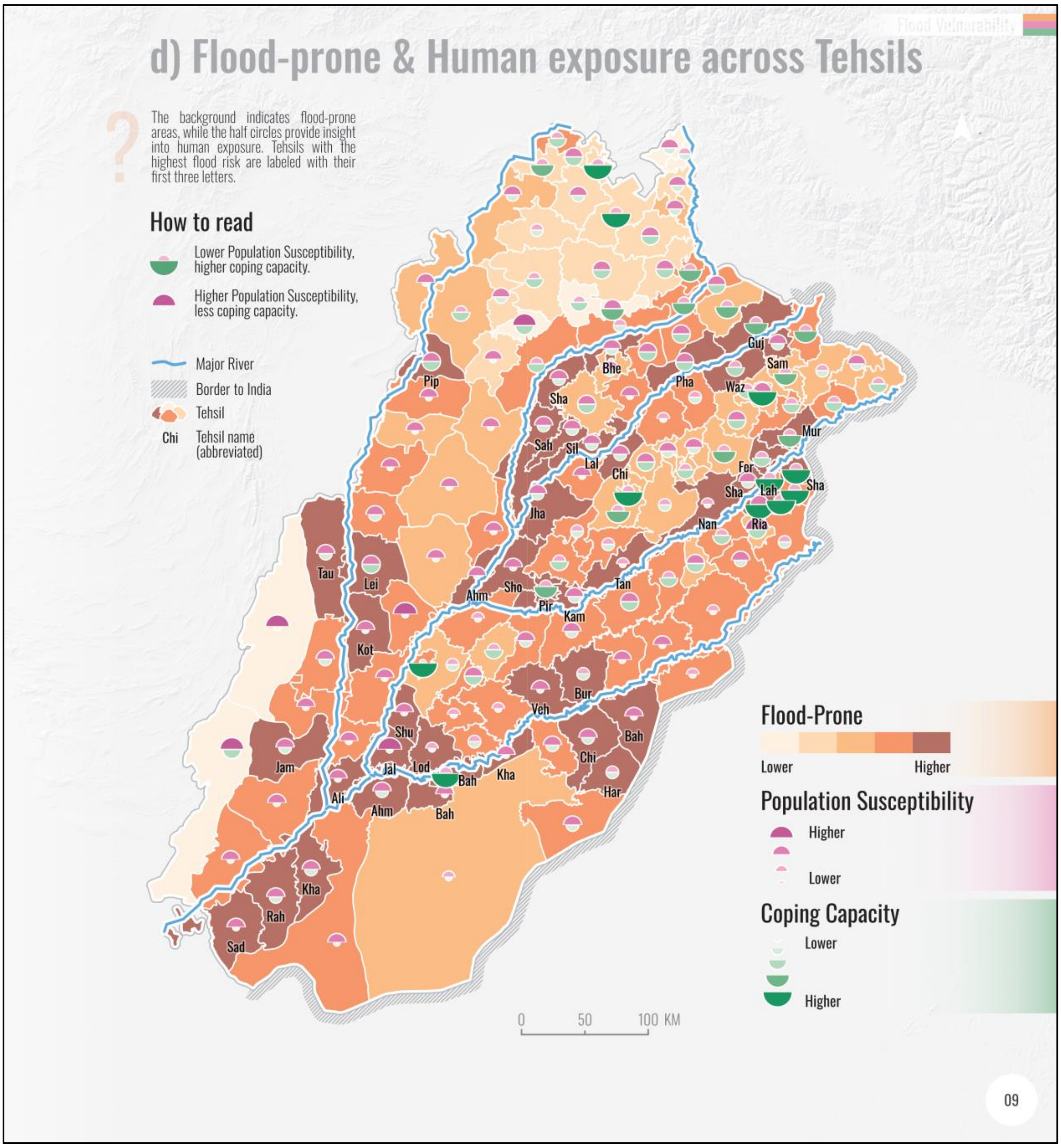


**Figure 9** Flood Vulnerability is split into its three components; visualized with a choropleth background, and half circles. Before the user testing.

## 5.4.5 Kriging Map of FPC with Wurman Dots of People Exposed

Another visualization approach used Wurman Dots to give information about the PSC and the CCC combined, while the background draws the FPC, both aggregated to 100 km² (Figure 10). Generally, both user groups found this map as a good summarization and a visually appealing way. However, the majority of the participants, especially the climate risk analysts, were misled by the legend title of PSC and CCC combination.

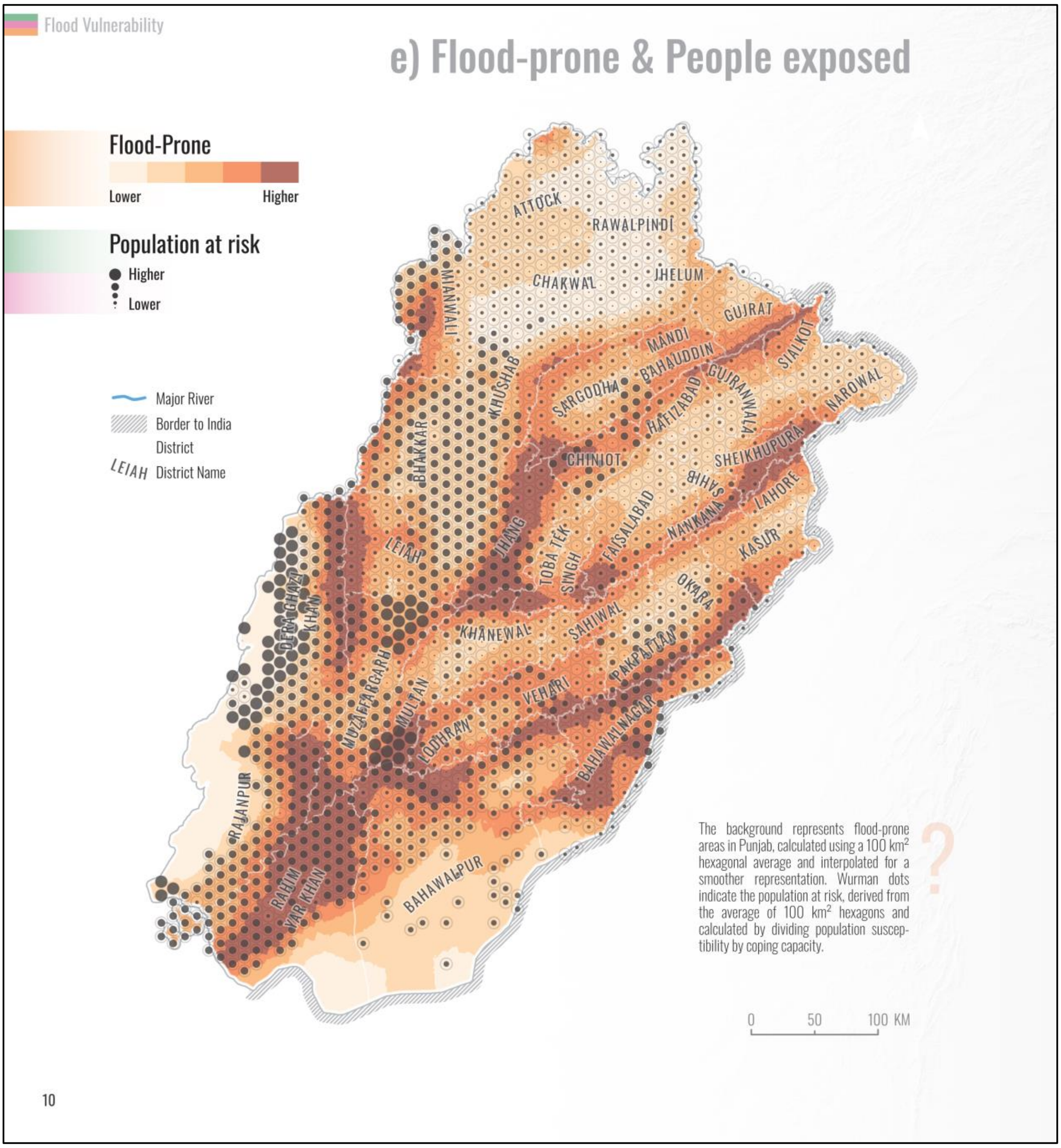


**Figure 10** Flood Vulnerability is split into its three components; visualized with a choropleth background, and Wurman dots. Before the user testing.

Several participants of the general public liked this map the most, as this summarizes the components well, it gives insights into vulnerability, and is still easy to read. However, one participant had difficulties understanding the visualization of the Wurman Dots. In the atlas, a focus should be drawn on a better explanation of this technique and how exactly it visualizes the components. One participant emphasizes that the sizes of the circles give a first look at information how people are at risk, highlighting the possibility of reading information on risk areas, but also how the people are here at risk.

Several participants of the climate risk analysts thought at first that the Wurman Dots show the number of people. Participants state that the title “Population at risk” is misleading, and it sounds like it indicates how many people live there. After an explanation, they understood it. One participant emphasizes that the map summarizes well and highlights that the calculation given already makes it more useful and easier to understand. One participant questioned if it would be possible to increase the resolution, decreasing the hexagon $km^2$, to have better accuracy. While this would give more spatial detail, it has to be considered that the study area is large, making it difficult to communicate with this large area in a less generalized way. Another participant mentioned that adding the river to this map might enhance the interpretation. Some participants had also wondered if it would be possible to visualize the number of people living there, given valuable information, and make this map very valuable. Furthermore, it was noted that the analytics participants mostly only looked at the legend and not at the explanation text. As they were misled by the Wurman dots legend title, some participants rated this map less in understanding. In the explanation text, it was written how the dots were calculated and what they show; the general public looked more at the text and therefore understood it better.

Furthermore, several participants mentioned that the red color of the flood-prone background is too dominant. Moreover, it was observed that some participants struggled to make the connection between the flood-prone but rather to the FVI color scheme, as the reds are similar to those of the FPC. Especially, when the maps went away from the formula, and showed the components not separately. Therefore, to improve clarity and enhance the thematic references, a different color scheme for the FPC was chosen – a blue one – which also enhances the connections to water and aligns more intuitively with flood-prone areas.

# 6 CARTOGRAPHIC PROJECT OF THE ATLAS

The chapter describes the purpose of the atlas and its structure. Choices in the creation process are discussed, and the layout of the digital product is drawn.

## 6.1 Specification of the Objectives and Purposes

The atlas and its maps serve as a tool for understanding and communicating flood vulnerability in Punjab. This is done by structuring the results of the thesis into a clear and visually engaging format, which enhances the accessibility for the general public, stakeholders, and experts. Analysis and methods are divided into different text blocks, giving the user the possibility to choose how much information they want; furthermore, a quick summary is also provided for each parameter and the mapping approaches. This aligns with the study's objective of improving flood risk assessment and decision-making methods by ensuring that the spatial data is effectively integrated into visual insights. Due to the user-centered design as well as user testing for the maps, the atlas ensures that it is not only methodological but also a practical medium.

## 6.2 Title and Thematic Focus of the Atlas

The title of the atlas slightly changed from the master's thesis title. As the atlas is a separate product but contains all the results of the thesis and its analysis, the atlas was termed "Flood Vulnerability in Punjab, Pakistan: An Atlas of Geospatial Analysis and Cartographic Approaches". The thematic focus of the atlas lies in visualizing all the parameters and the FVI maps.

## 6.3 Determination of the Map Scale

Different map scales are chosen, depending on the map shown. As the study area is large, and to cover one atlas page, the scale for maps showing the whole province is 1:3.300.000. Inset maps, showing areas with the highest vulnerability are in 1:500.000.

## 6.4 Choice of Map Projection

As the study worked in the "Kalianpur 1962 UTM Zone 43N" to provide accurate processing and analysis, the projection is the same in the atlas.

## 6.5 Atlas Layout

Generally, the layout structure follows two primary formats. The first structure (Figure 11a) is suitable for the parameter maps, it provides one map for each page. While the right page visualizes the parameter values, the left map shows the classification. Description text and explanation how the data was processed accompany each parameter. Moreover, space for figures gives the possibility to provide deeper insights into the data.

The second (Figure 11b) provides more space for map frames, making it suitable for the vulnerability maps. A hillshade background is drawn, enhancing the orientation for the reader through the perception of the elevation. Furthermore, given the grey background, a white color can be displayed. Moreover, a color-coded navigation system can be found in the right upper corner, indicating the chapter of the atlas, such as FPC or FVI, which helps users quickly locate the sections within the atlas.

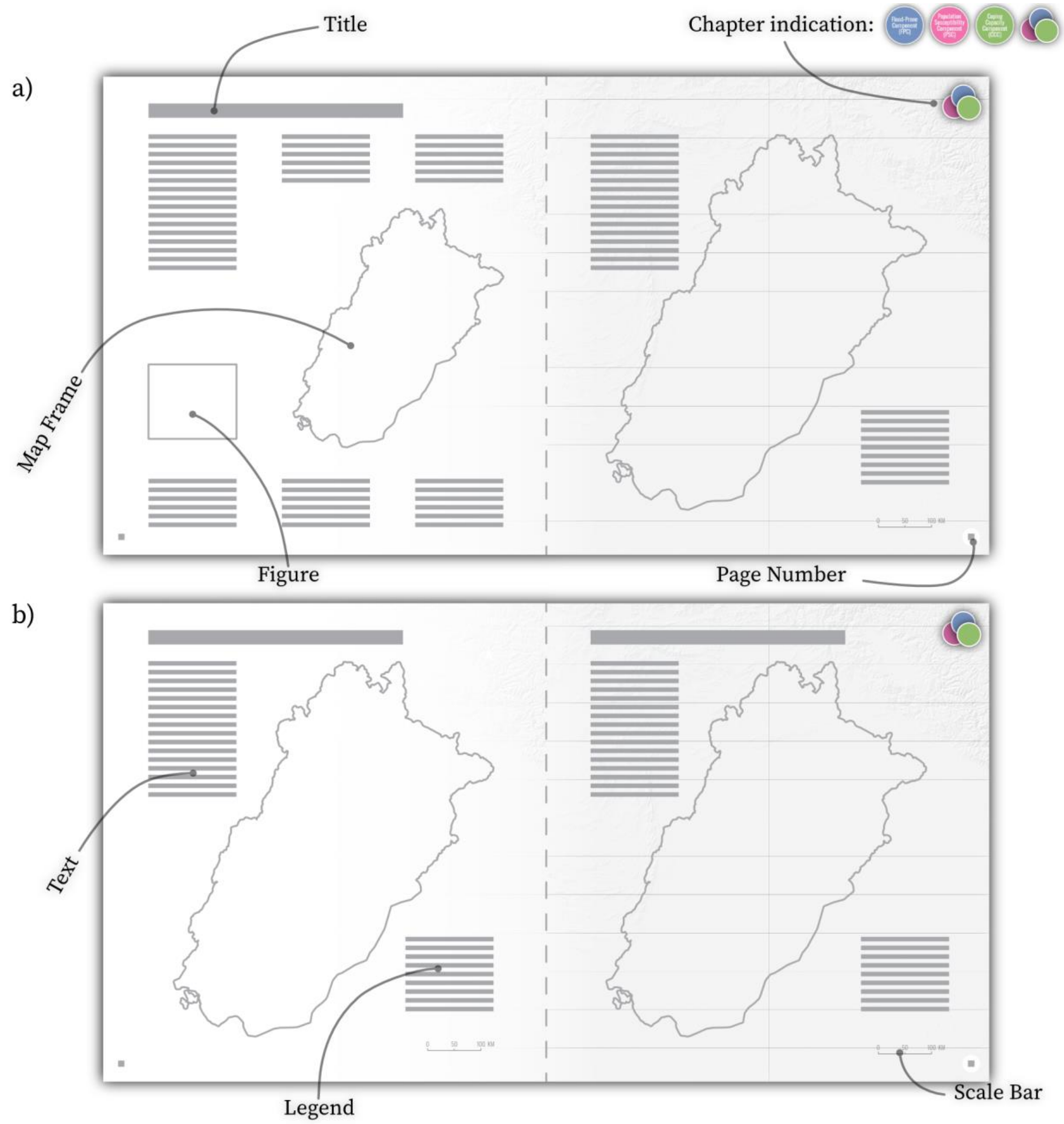


**Figure 11** (a) layout structure for parameter, (b) and for visualizing approaches.

The atlas measures a size of 25 x 27 cm. This size was chosen, as it still provides space for visualizing, but still, it is not too large for difficult handling.

## 6.6 Compilation of the Atlas/Map content

The aim of the layout was to provide a logical flow, offering detailed explanations of the methodology of the study's analysis and results, while ensuring accessibility for both the general readers and experts. Therefore, the atlas starts by introducing the topic and the study area, emphasizing why flood risk research is important. The different parameters were presented and their maps visualized, as well as the analysis and the discussion of their characteristics were provided. Following this line, the final section of the atlas visualizes and discusses the different vulnerability maps (Figure 12).


**Figure 12** Structure of the atlas; Introduction, Guidelines, FPC = Flood-Prone Component, PSC = Population Susceptibility Component, CCC = Coping Capacity Component, Flood Vulnerability Index.

In summary, the atlas consists of the following:

- Introduction: Overview of the study area and additional information;
- Guidelines for the use of the atlas.
- Parameter Maps of the FPC: Seven maps with accompanying analysis;
- Parameter Maps of the PSC: Four maps with accompanying analysis;
- Parameter Maps of the CCC: Two maps with accompanying analysis;
- Vulnerability Maps: Final results with different mapping approaches.

## 6.7 Symbology

For clarity and easy interpretation, the atlas uses a color-coded system. The pages are identified with the respective symbol of the component or the FVI (see Figure 12). Furthermore, the component maps and the FVI maps use the same color hue, for finding directly where in the atlas the user is.

## 6.8 Data Sources

The data sources shown in the atlas are all the data used in the analysis of this study, as summarized in Table 1. Furthermore, further OSM data and open from Natural Earth (https://www.naturalearthdata.com/) was chosen for displaying additional information, such as cities.

## 6.9 Applied Technology

The main technology was ArcGIS Pro for mapping and visualizing the maps in its early state. The maps were exported into Affinity Designer for post-production, such as adding the title and a correct legend. In Affinity Publisher, the maps were combined with additional text, figures, and tables (Figure 13). Leaflet was used for the creation of the interactive dashboard. GitHub provides a dashboard, and a digital version of the atlas can be downloaded there.

## 6.10 Organizational and Economic Aspects

To ensure a high-quality product, cartographers and experts who have experience in the atlas creation were consulted. This discussion and feedback comprise the layout structure, considerations, and rules for printing, and overall usability. From an economic perspective, all the data used was open access. The visualization software license was obtained. Nevertheless, the creation could have been possible using free and open-source software.

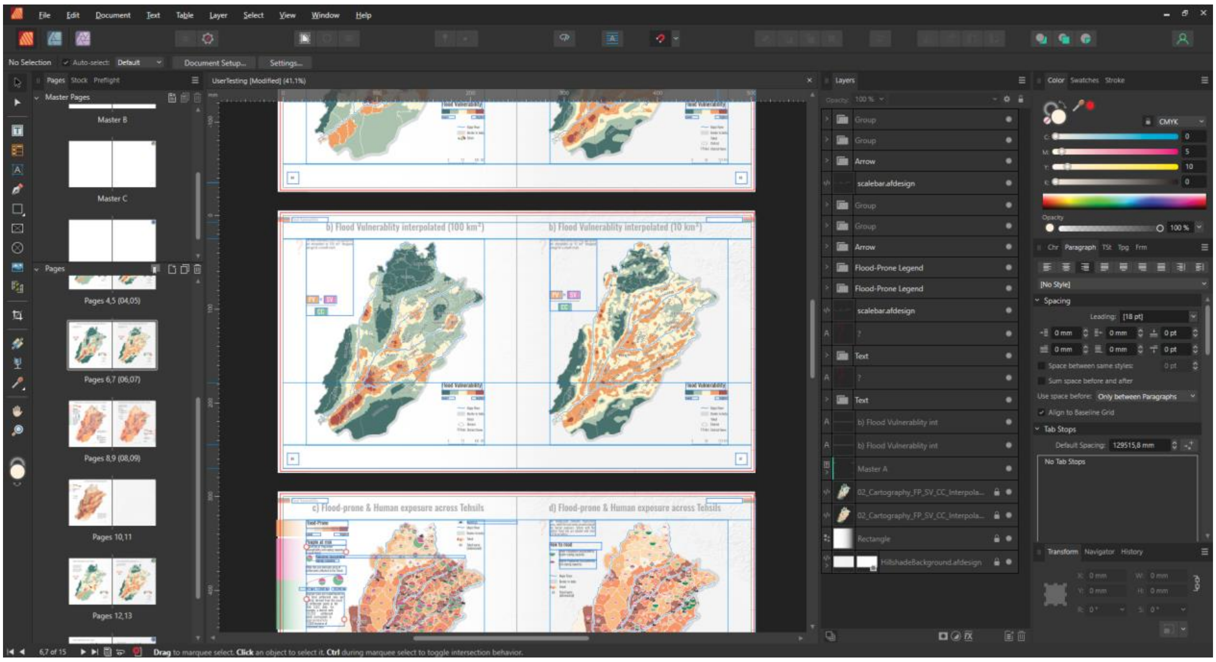

**Figure 13** Screenshot in Affinity Publisher.

## 6.11 Digital Product Layout

In addition, a digital product accompanied the atlas, presenting the maps and the atlas in a digital form, enabling the user to scroll through the analysis and to interact with the results. One part of it is a dashboard created with Leaflet. This page allows the user to interact with the FPC, PSC, CCC, and FVI and receive information on the different values across the Tehsils (Figure 14). The user is able to switch on and off the different layers, while a description text provides more context to the user.

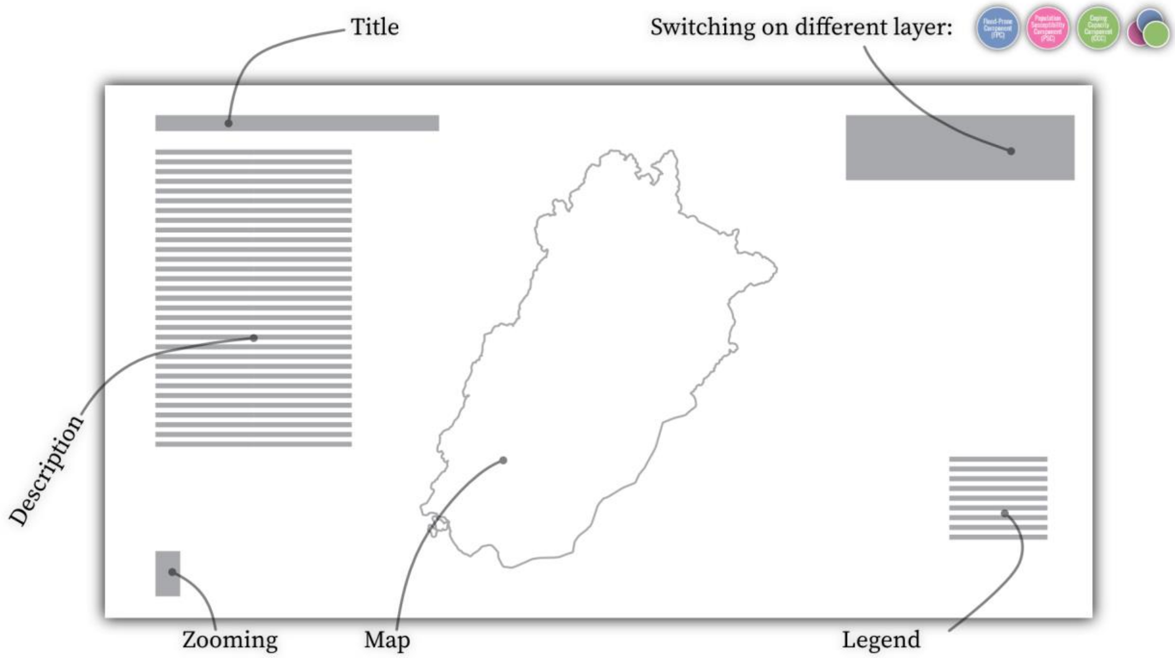


**Figure 14** (a) layout structure for parameter, (b) and for visualizing approaches.

This digital dashboard is uploaded to a GitHub page, making it easily accessible. Furthermore, on this page, additional information is presented, and the atlas can also be downloaded there.

# 7 RESULTS

This chapter gathers the outcomes of the study. Starting with the analysis of each parameter, it goes to the component maps, and then to the FVI results. The results of the user testing of the different mapping approaches are presented, and the feedback is discussed. Furthermore, the design of the Atlas and the digital product is presented.

## 7.1 Geospatial Analysis and Mapping of Vulnerability

### 7.1.1 Mapping of Parameter

Each FVI parameter was mapped and ranked into very low to very high and classified into different categories as previously described in Chapter 4. The following is a detailed summary of the results achieved for each parameter.

#### 7.1.1.1 Flood-Prone Component

##### 7.1.1.1.1 Annual Rainfall

The AR layer of the study area was divided into five classes (Table 13, p. 56): ≤ 400 mm/year (very low), 400–500 mm/year (low), 500–600 mm/year (moderate), 600–700 mm/year (high), and > 700 mm/year (very high). The classification shows that 15.46% (31,795.92 km²) of the study area falls very low, 26.94% (55,411.50 km²) is low, 19.23% (39,557.46 km²) is moderate, 17.22% (35,427.93 km²) is high, and 21.15% (43,504.21 km²) is very high (Figure 15b, c). Precipitation is a driver of flooding (Bates *et al.*, 2008; Bathrellos *et al.*, 2016; Kara and Singh, 2024). Most of the AR occurs in the northern and the southwestern part of Punjab, while the lowest can be found in the center of the province (Figure 15c).

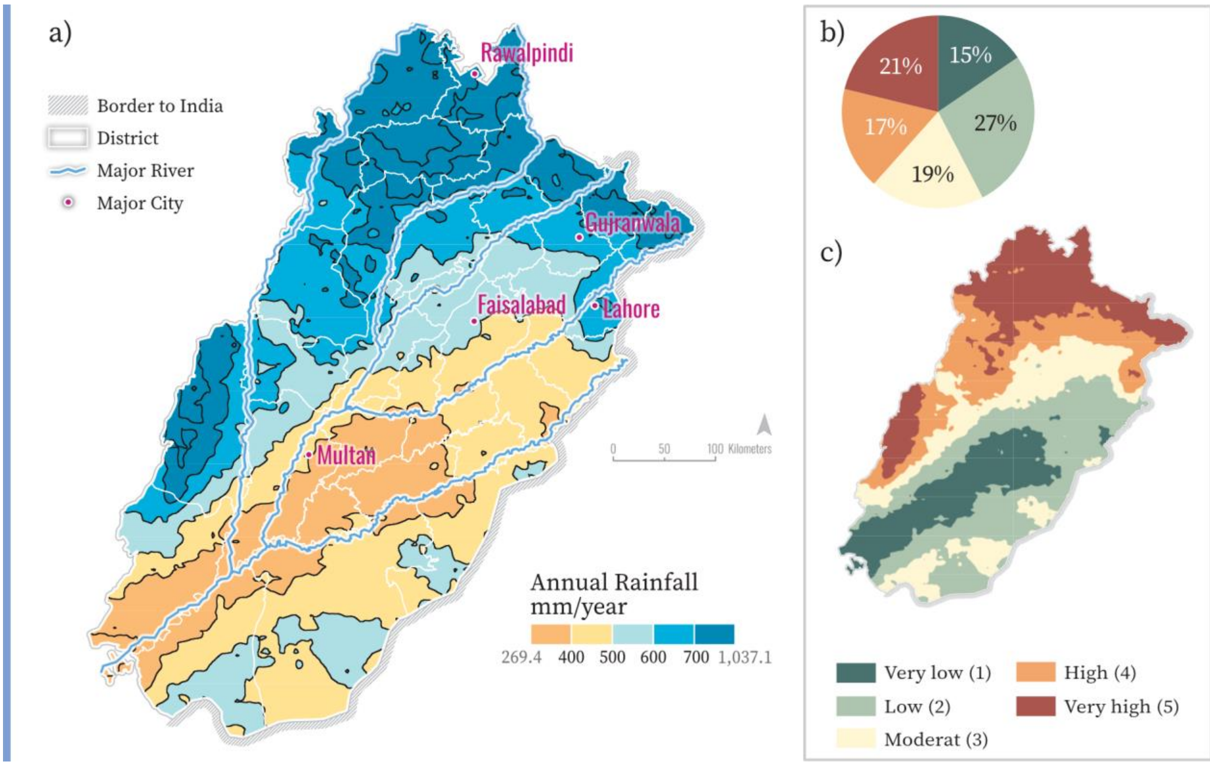


**Figure 15** (a) Annual rainfall map (b) percentages of classes, and (c) distribution of classes in Punjab.

#### 7.1.1.1.2 Distance to the River

The DR layer was classified into five groups (Table 13, p. 56): ≤ 1000 m (very low), 1000–3000 m (low), 3000–6000 m (moderate), 6000–10,000 m (high), > 10,000 m (very high). 12.75% (26,222.92 km²) of the study area is very low, 8.62% (17,728.13 km²) is low DR, 18.56% (38,177.38 km²) is moderate, 31.65% (65,109.38 km²) is high, and 28.42% (58,459.22 km²) very high (Figure 16b, c). Proximity to the river is a greater risk (Fernández and Lutz, 2010). The higher classes can be found as a result of the five major rivers, and additionally, a lot of channels and streams, especially in crop field areas. These areas are mostly in the northeastern and southwestern parts of the region, which are characterized by farmland (Figure 19).

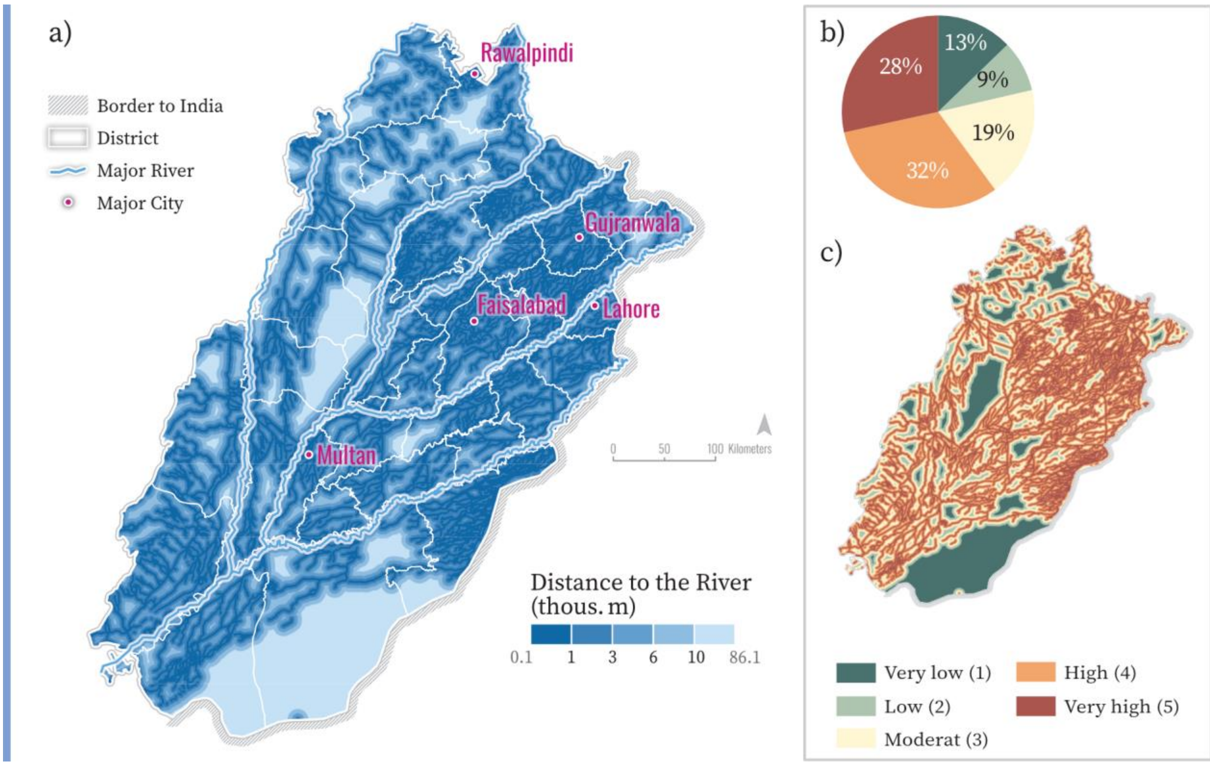


**Figure 16** (a) Distance to a river map, (b) percentages of classes, and (c) distribution of classes in Punjab.

#### 7.1.1.1.3 Drainage Density

The DD in the study area was divided into five classes (Table 13, p. 56): ≤ 6.34 m/km² (very low), 6.34–27.76 m/km² (low), 27.76–39.25 m/km² (moderate), 39.25–56.96 m/km² (high), > 56.96 m/km² (very high). Higher drainage contributes to higher surface runoff (Subbarayan and Saravanan, 2020). The DD layer captures mostly the five major river basins (Figure 17a). The classification describes 29.75% (61,193.51 km²) of the study area as very low, 15.00% (30,849.03 km²) as low, 18.43% (37,918.43 km²) as moderate, 18.61% (38,285.65 km²) as high, and 18.21% (37,450.41 km²) as very high (Figure 17b, c).

#### 7.1.1.1.4 Elevation

The EL values were manually classified into five classes (Table 13, p. 56), focusing on low elevation ranges: ≤ 150 m (very high), 150–200 m (high), 200–300 m (moderate), 300–400 m (low), and > 400 m (very low). The northern and the southwestern parts of Punjab are characterized by high elevation, while the center is low-elevated (Figure 18a). The classification describes 11.27% (23,179.51 km²) of the study area as very low, 3.88% (7990.26 km²) as low, 15.04% (30,937.53 km²) as moderate, 30.18% (62,085.42 km²) as high, and 39.62% (81,504.31 km²) as very high (Figure 18b, c). Lower elevation is more prone to flooding

(Sanyal and Lu, 2006; Rahman *et al.*, 2019; Allafta and Opp, 2021), as the mid to southern part of the Punjab is categorized with low topography, the large number in this category makes sense.

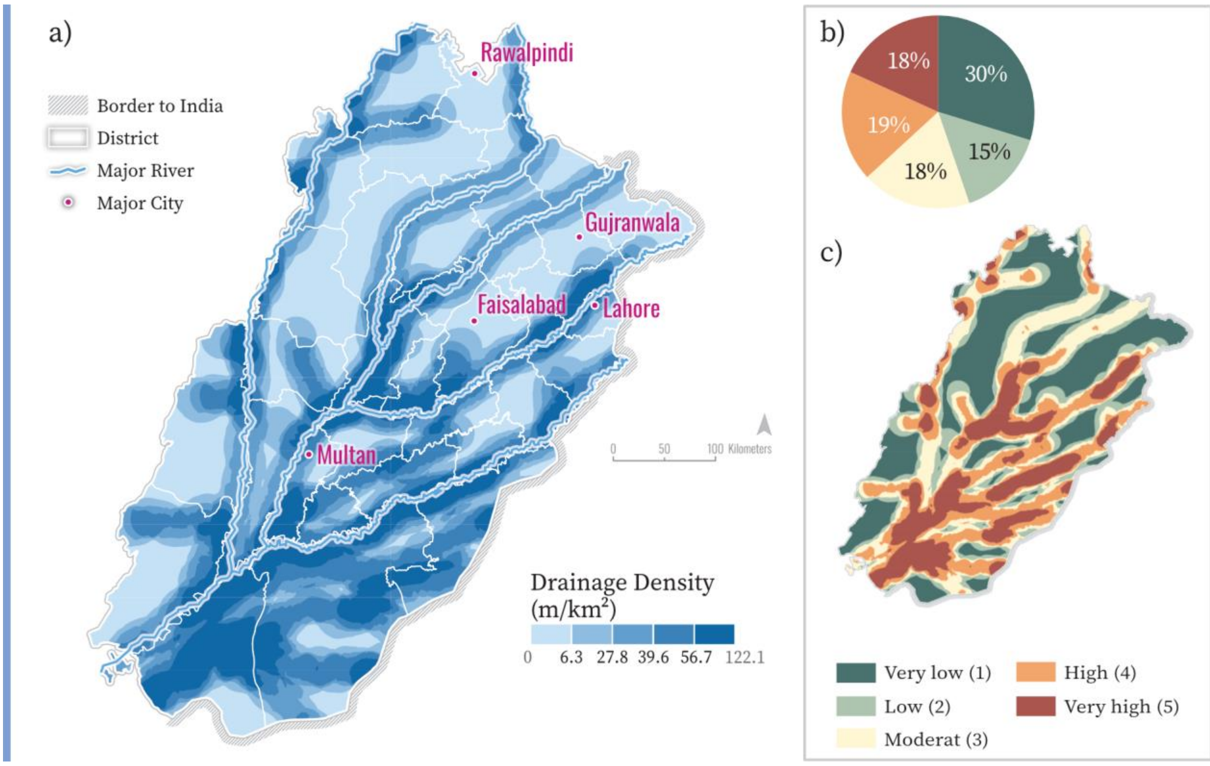


**Figure 17** (a) Drainage density, (b) percentages of classes, and (c) distribution of classes in Punjab.

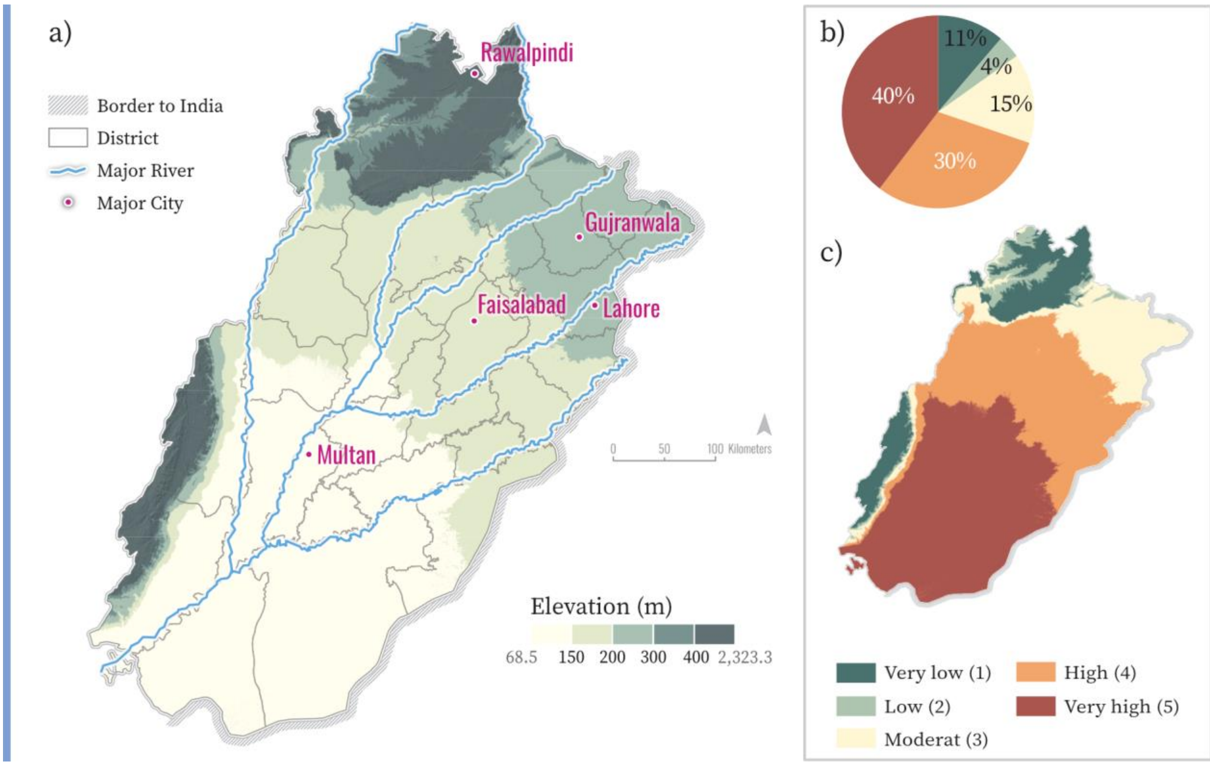


**Figure 18** (a) Elevation map, (b) percentages of classes, and (c) distribution of classes in Punjab.

#### 7.1.1.1.5 Land Use Land Cover

The LULC layer was classified into five classes (Table 13, p. 56), water bodies, herbaceous wetland (very high), built-up, cropland (high), bare/sparse vegetation (moderate), grassland (low), shrubland, and tree cover (very low). As Punjab is an agricultural center of the country, most of the provinces are covered with cropland. Shrubland and base/sparse vegetation can be found in the southeastern and western parts, as well as in one central area in the northwestern direction. Trees are mostly in the northern part, at high elevation. Built-up areas can mostly be found in the major cities (Figure 19a). The classification describes 14.91% (30,662.53 km²) of the study area as very low, 4.62% (9,495.62 km²) as low, 21.62% (44,460.48 km²) as moderate, 57.54% (118,358.67 km²) as high, and 1.32% (2,719.73 km²) as very high (Figure 19b, c).

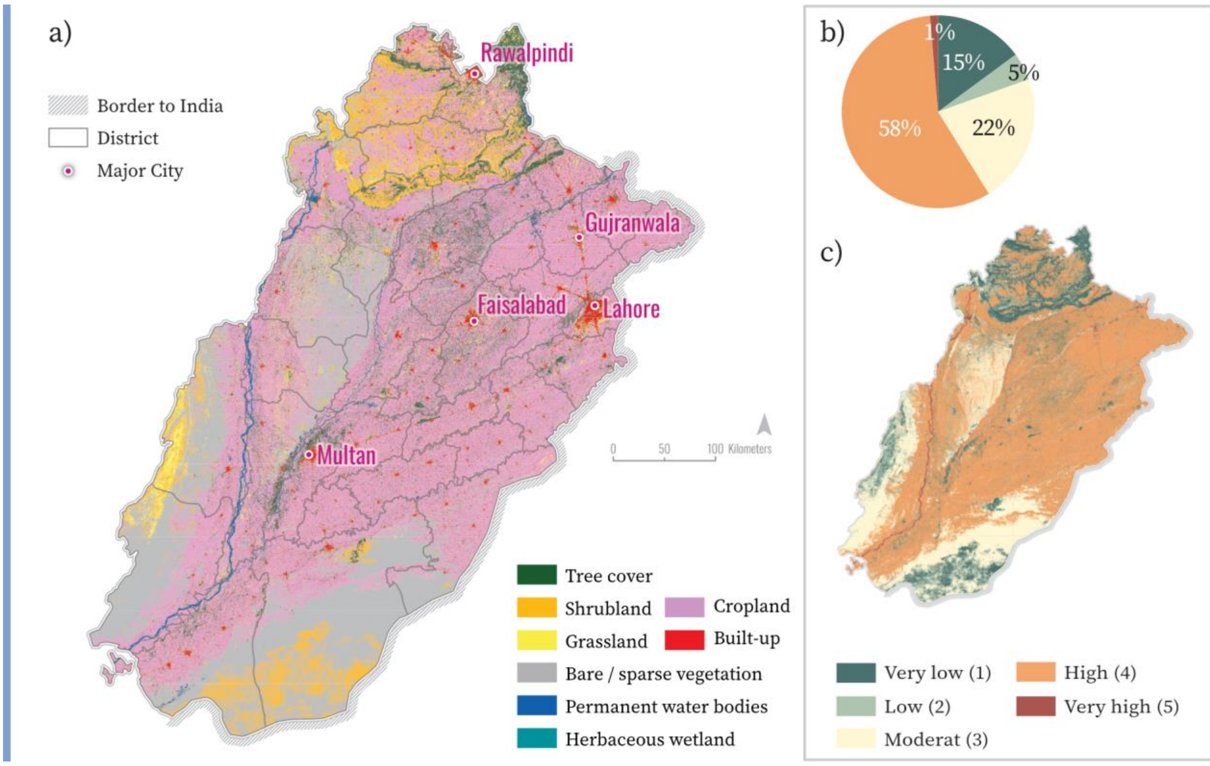


**Figure 19** (a) Land use land cover map, (b) percentages of classes, and (c) distribution of classes in Punjab.

#### 7.1.1.1.6 Slope

The SL layer was classified into five classes (Table 13, p. 56): ≤ 1.5° (very high), 1.5°–5° (high), 5°–15° (moderate), 15°–30° (low), > 30° (very low). High degrees of slope can be found in the mountainous areas of the province, while low degrees are in the flat land (Figure 20a). As Punjab is characterized by large areas with flat terrain, which are more prone to flooding (Gigović *et al.*, 2017), according to the classification, 0.59% (1213.16 km²) of the study area falls in very low, 2.59% (5333.28 km²) in low, 4.52% (9298.84 km²) in moderate, 7.63% (15,702.85 km²) in high, and 84.66% (174,148.89 km²) in very high classes (Figure 20b, c).

#### 7.1.1.1.7 Topographic Wetness Index

The TWI layer was classified into five classes (Table 13, p. 56): ≤ 5.12 (very low), 5.12–6.67 (low), 6.67–7.94 (moderate), 7.94–10.75 (high), > 10.75 (very high). Higher values pose more flood-prone (Roy and Dhar, 2024). Higher TWI values can be found at waterbodies and rivers, while lower values are in the higher elevated areas of the province (Figure 21a). The classification describes 19.49% (40,093.62 km²) of the study area as very low, 19.88%

(40,900.81 km²) as low, 21.94% (45,128.56 km²) as moderate, 20.07% (41,283.85 km²) as high, and 18.61% (38,290.19 km²) as very high (Figure 21b, c).

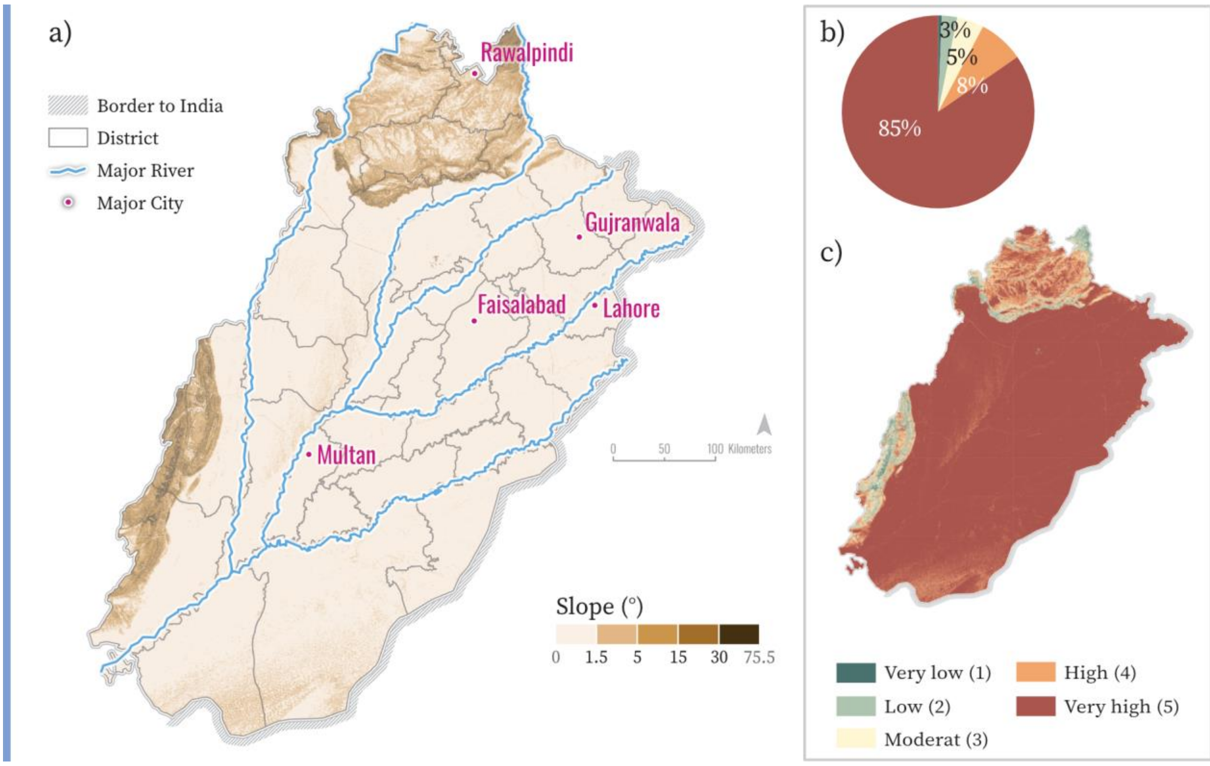


**Figure 20** (a) Slope map, (b) percentages of risk classes (values rounded), and (c) distribution of risk classes in Punjab.

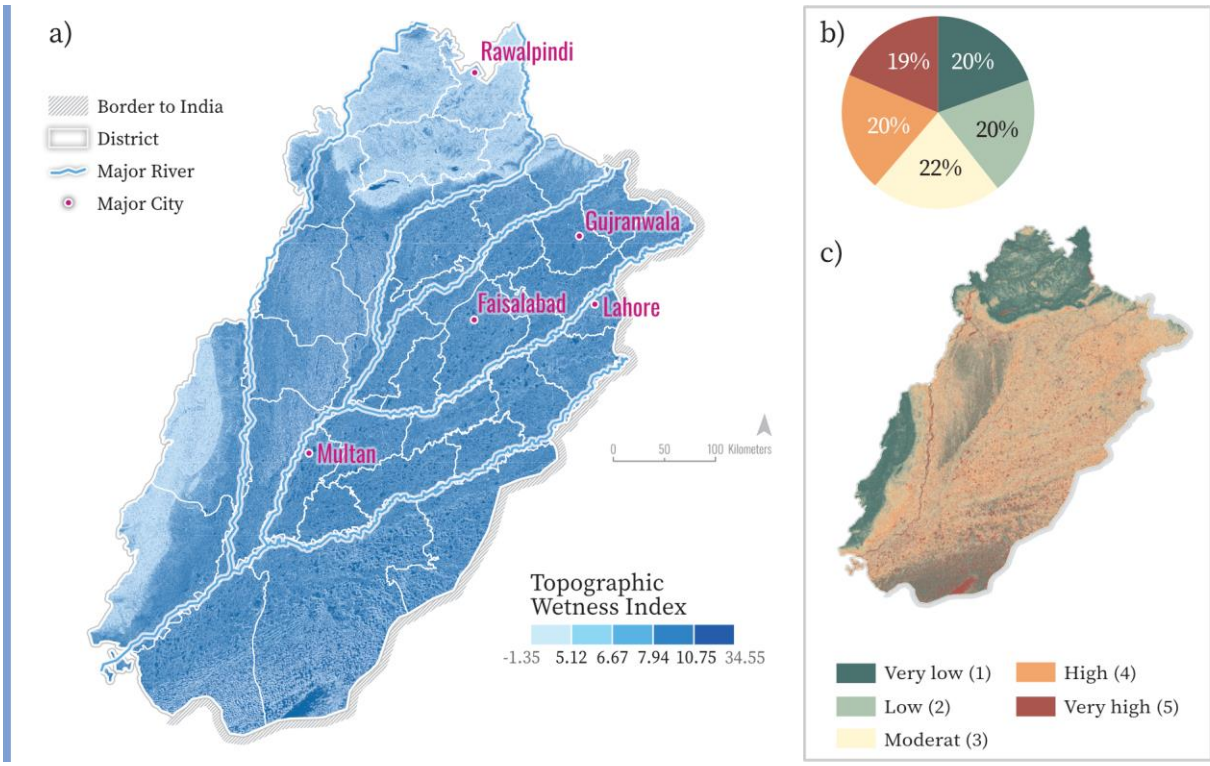


**Figure 21** (a) Topographic wetness index, (b) percentages of classes, and (c) distribution of classes in Punjab.

### 7.1.1.2 Population Susceptibility Component

#### 7.1.1.2.1 Dependent Population

The DeP values were classified into five classes (Table 13, p. 56): ≤ 41.41% (very low), 41.41–43.54% (low), 43.54–45.70% (moderate), 45.70–49.11% (high), > 49.11% (very high). Dependent Population is dependent on their family members (Hoque *et al.*, 2019). A lot of DeP are in the south-western rural areas, while in the northern part, as well as in the City Tehsils it is less (Figure 22a).

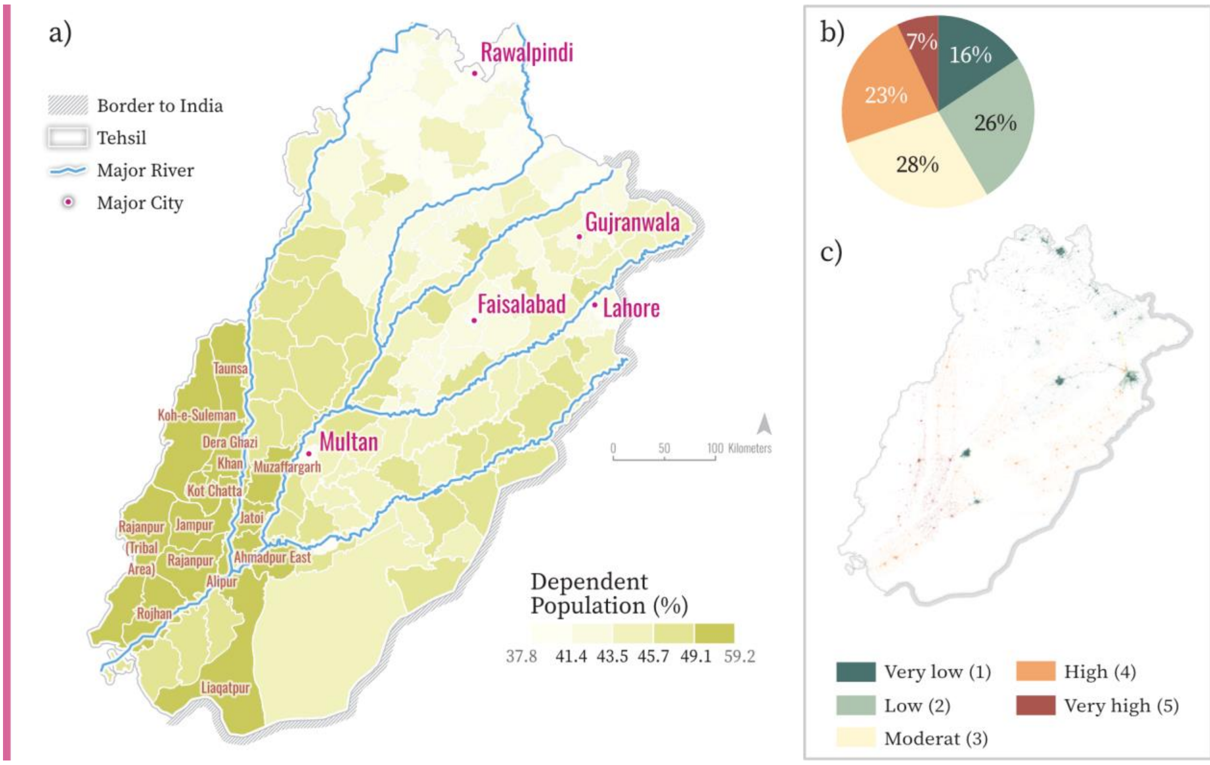


**Figure 22** (a) Percentage of dependent population (Tehsils with very high risk labeled), (b) percentages of classes in inhabited places, and (c) distribution of classes in Punjab based on settlements.

Considering the dasymetric map, masked out with settlements (Figure 22c), the classification describes 15.64% (1107.68 km²) of the study area as very low, 25.90% (1834.30 km²) as low, 28.18% (1995.62 km²) as moderate, 23.29% as high (1649.31 km²), and 6.99% (494.74 km²) as very high in inhabited places (Figure 22b, c). Areas with a higher dependent population face greater challenges because babies, children, and elderly people might be more vulnerable when flooding occurs. The Tehsils with the highest values are Ahmadpur East, Alipur, Dera Ghazi Khan, Jampur, Jatoi, Koh-e-Suleman, Kot Chatta, Liaqatpur, Muzaffargarh, Rajanpur, Rajanpur (Tribal Area), Rojhan, and Taunsa.

#### 7.1.1.2.2 Disabled Population

The DiP values were classified into five classes (Table 13, p. 56): ≤ 2.65% (very low), 2.65–3.86% (low), 3.86–5.70% (moderate), 5.70–9.40% (high), > 9.40% (very high). The distribution of the DiP in the Tehsils is fairly even, however, a slight distribution with a higher percentage can be seen in the north-western part. Furthermore, the highest amount is in the Tehsil in the south-west, as well as in the northern part; the Tehsil of Rajanpur (Tribal Area), as well as Kahuta (Figure 23a). Disabled populations might face challenges during an emergency situation (Hoque *et al.*, 2019). The classification describes 20.51% (1452.29 km²) in very low, 46.10% (3264.80 km²) in low, 24.92% (1764.74 km²) in moderate, 8.21% (581.29 km²) as high, and 0.26% (18.54 km²) as very high in inhabited places (Figure 23b, c). These findings suggest that, although the areas in the higher ranges are modest, some areas are characterized by very high share of disabled population, making them highly vulnerable during flood events.

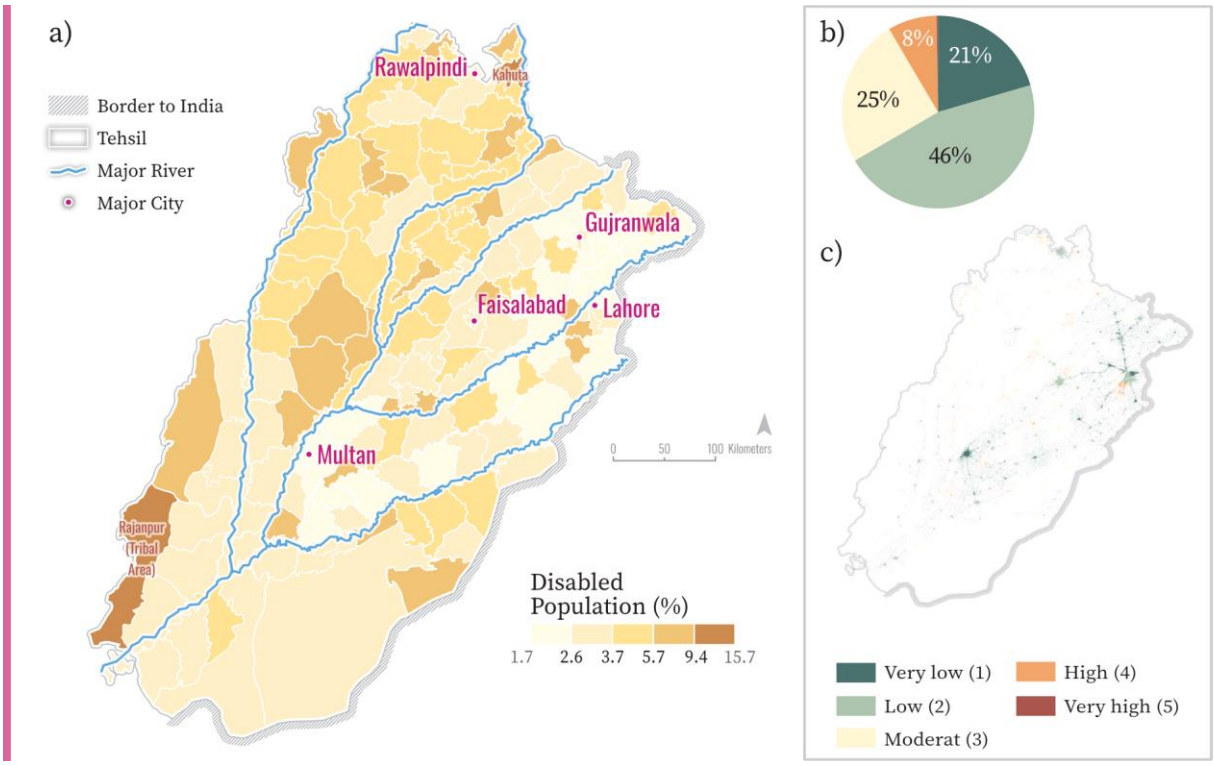


**Figure 23** (a) Percentage of disabled population (Tehsils with very high risk labeled), (b) percentages of classes in inhabited places, and (c) distribution of classes in Punjab based on settlements.

### 7.1.1.2.3 Female Population

The FP values were classified into five classes (Table 13, p. 56): ≤ 48.02% (very low), 48.02–48.77% (low), 48.77–49.40% (moderate), 49.40–50.20% (high), > 50.20% (very high). The higher percentage can be seen in the northern part in the Tehsils of Bhalwal, Chakwal, Gujar Khan, Jand, Kahuta, Kallar Sayaddan, Naushera (Figure 24a). Women have difficulties in flooding events (Neumayer and Plümper, 2007). The classification describes 22.58% (1598.95 km²) in very low, 23.56% (1668.64 km²) in low, 30.58% (2165.22 km²) in moderate, 20.11% (1423.83 km²) as high, and 3.18% (225.01 km²) as very high in inhabited areas (Figure 24b, c).

### 7.1.1.2.4 Population Density

The PD layer is categorized into five classes (Table 13, p. 56): ≤ 600 pop./km² (very low), 600–2000 pop./km² (low), 2000–4000 pop./km² (moderate), 4000–9000 pop./km² (high), > 9000 pop./km² (very high). The classification describes 28.61% (2025.85 km²) in very low, 53.92% (3818.63 km²) in low, 8.74% (619.24 km²) in moderate, 3.06% (216.62 km²) as high, and 5.67% (401.31 km²) as very high in inhabited places (Figure 25b, c). Higher population density is suggested as more vulnerable (Hoque *et al.*, 2019). The higher PD can be seen in the city Tehsils, especially in Faisalabad City, Gujranwala City, Model Town, and Lahore City (Figure 25a). However, since the AHP identified the PD as the least influential parameter of the PSC, its impact will be smaller than the other ones.

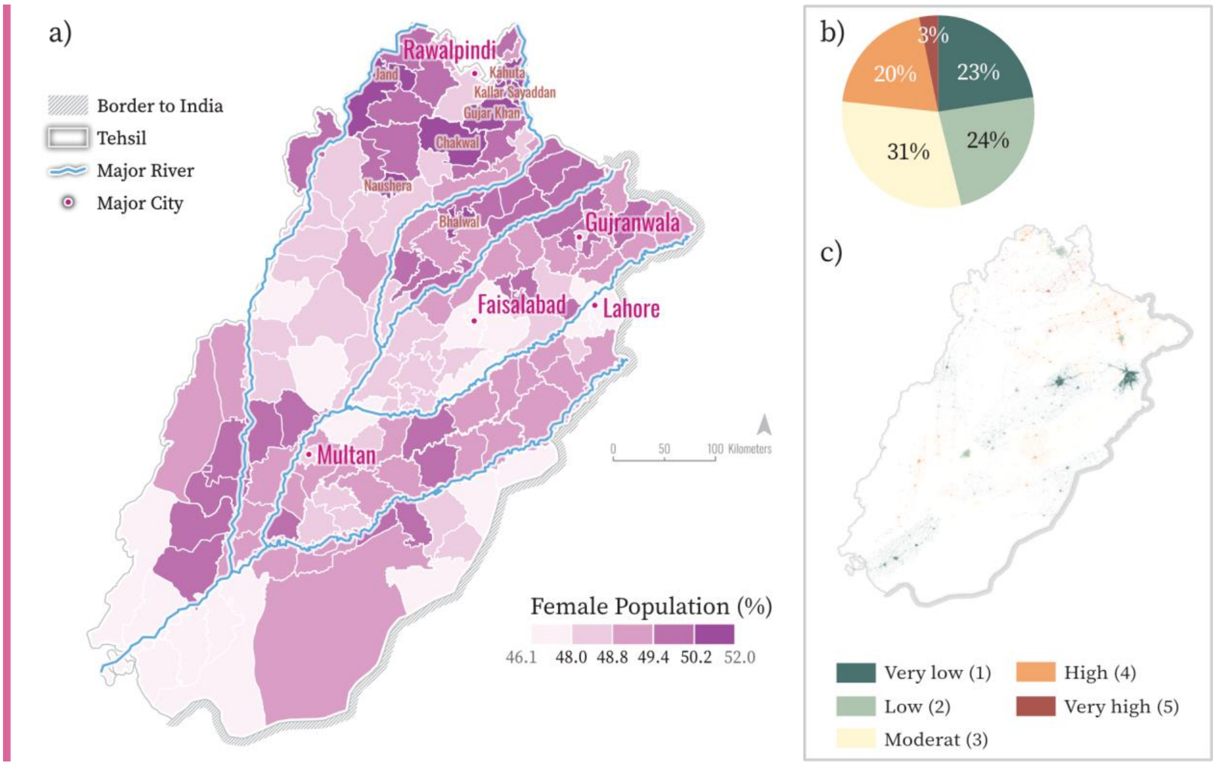


**Figure 24** (a) Percentage of female population (Tehsils with very high risk labeled), (b) percentages of classes, and (c) distribution of classes in Punjab based on settlements.

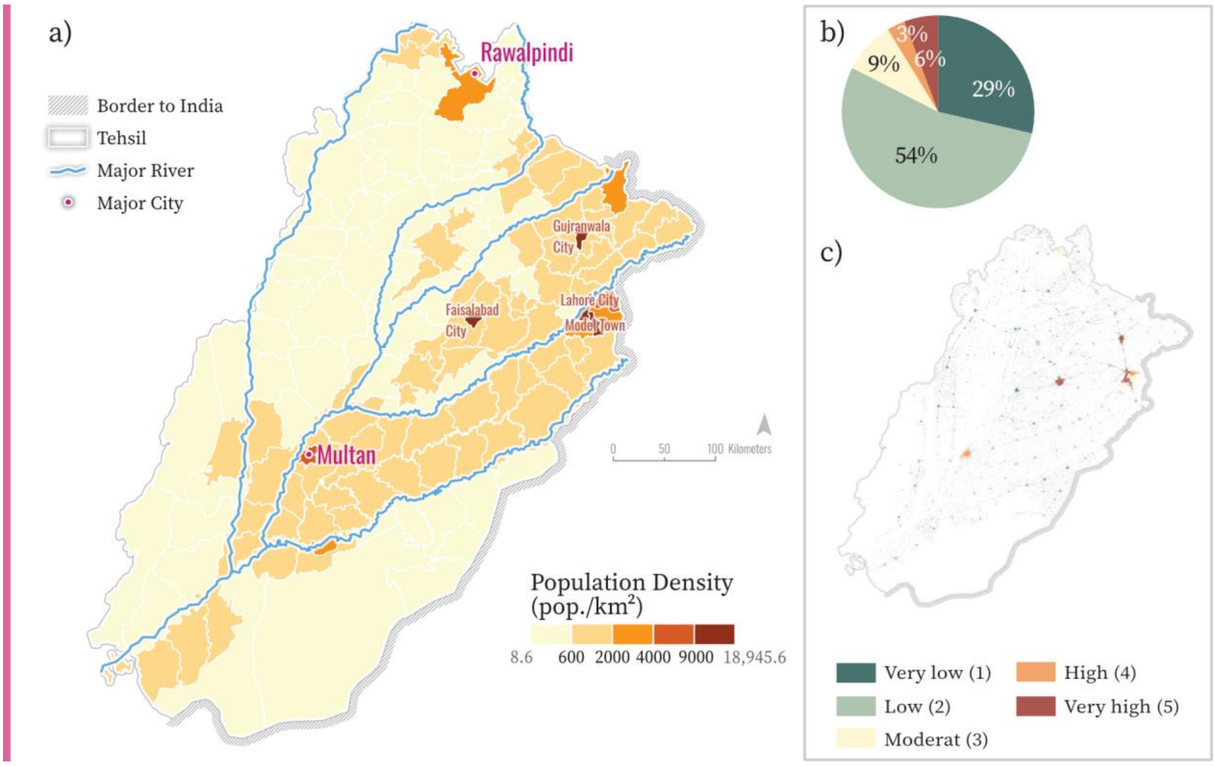


**Figure 25** (a) Population density (Tehsils with very high risk labeled), (b) percentages of risk classes (values rounded) in inhabited places, and (c) distribution of risk classes in Punjab based on settlements.

### 7.1.1.3 Coping Capacity Component

#### 7.1.1.3.1 Distance to Health Facilities

The DH values were classified into five classes (Table 13, p. 56): ≤ 2000 m (very high), 2000–4000 m (high), 4000–6000 m (moderate), 6000–8000 m (low), > 8000 m (very low). Especially in the major cities of Punjab, health facilities can be found (Figure 26a). The classification describes 50.04% (3897.82 km²) in very low, 6.77% (479.66 km²) in low, 7.18% (508.60 km²) in moderate, 9.76% (691.45 km²) as high, and 21.24% (1504.12 km²) as very high in inhabited places (Figure 26b, c). The distribution highlights that urban areas have better connections to health facilities. Urban areas, with distances often more than 8000 m, may be more vulnerable to flood events as they may face difficulties in flood events in accessing essential emergency services.

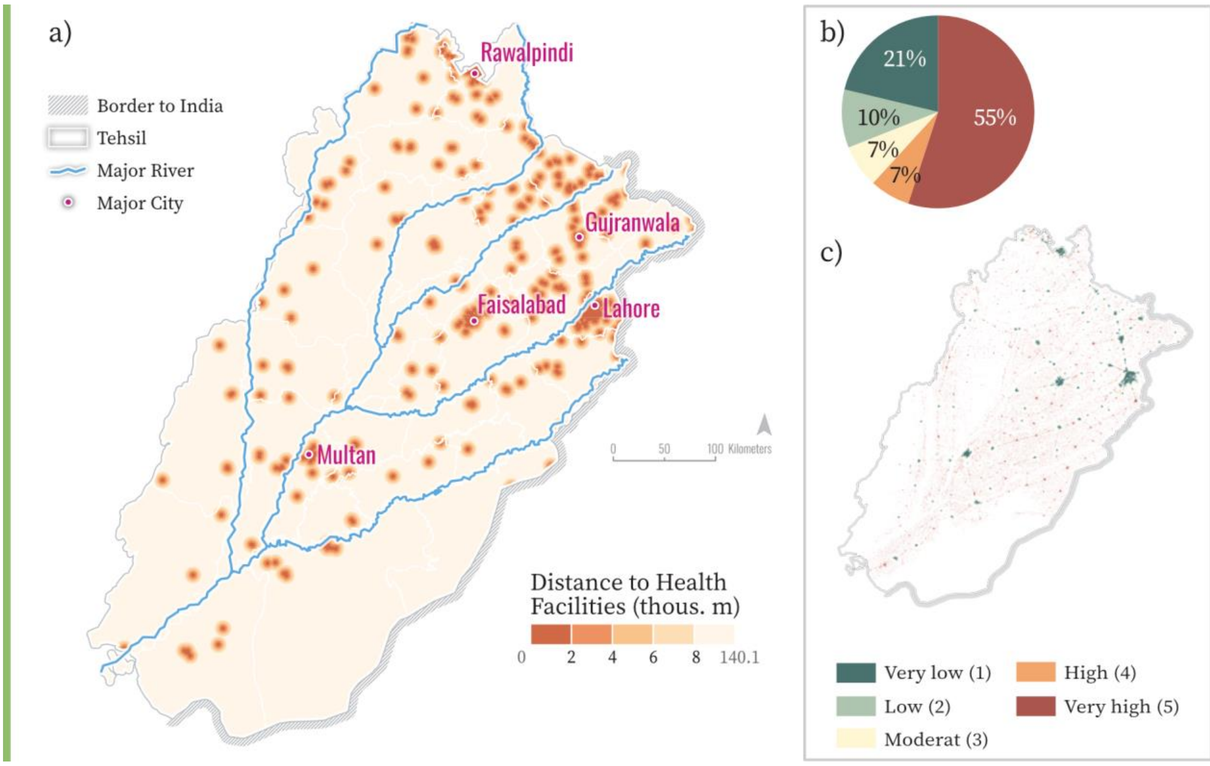


**Figure 26** (a) Distance to health facilities, (b) percentages of risk classes in inhabited places, and (c) distribution of classes in Punjab based on settlements.

#### 7.1.1.3.2 Literacy Rate

The LR layer was classified into five classes (Table 13, p. 56): ≤ 44.05% (very low), 44.05–59.02% (low), 59.02–67.55% (moderate), 67.55–76.28% (high), > 76.28% (very high). Low literacy rates can be found in the southwestern part of the province, and in the rural areas, while in the cities and in the northern part, high LR is drawn (Figure 27a). Warnings can be missed with low literacy rate (Hagenlocher *et al.*, 2016). The classification describes 5.41% (383.26 km²) in very low, 28.17% (1995.21 km²) in low, 23.47% (1662.22 km²) in moderate, 20.10% (1423.17 km²) as high, and 22.84% (1617.79 km²) in very high literacy rate in inhabited places (Figure 27b, c). The Tehsils with the lowest values are Ahmadpur East, Alipur, Jalalpur Pirwala, Jampur, Jatoi, Koh-e-Suleman, Kot Chatta, Liaqatpur, Minchinabad, Rajanpur, Rajanpur (Tribal Area), Rojhan. This distribution shows that areas with limited literacy, mainly the rural areas, may face challenges when flood warnings are communicated.

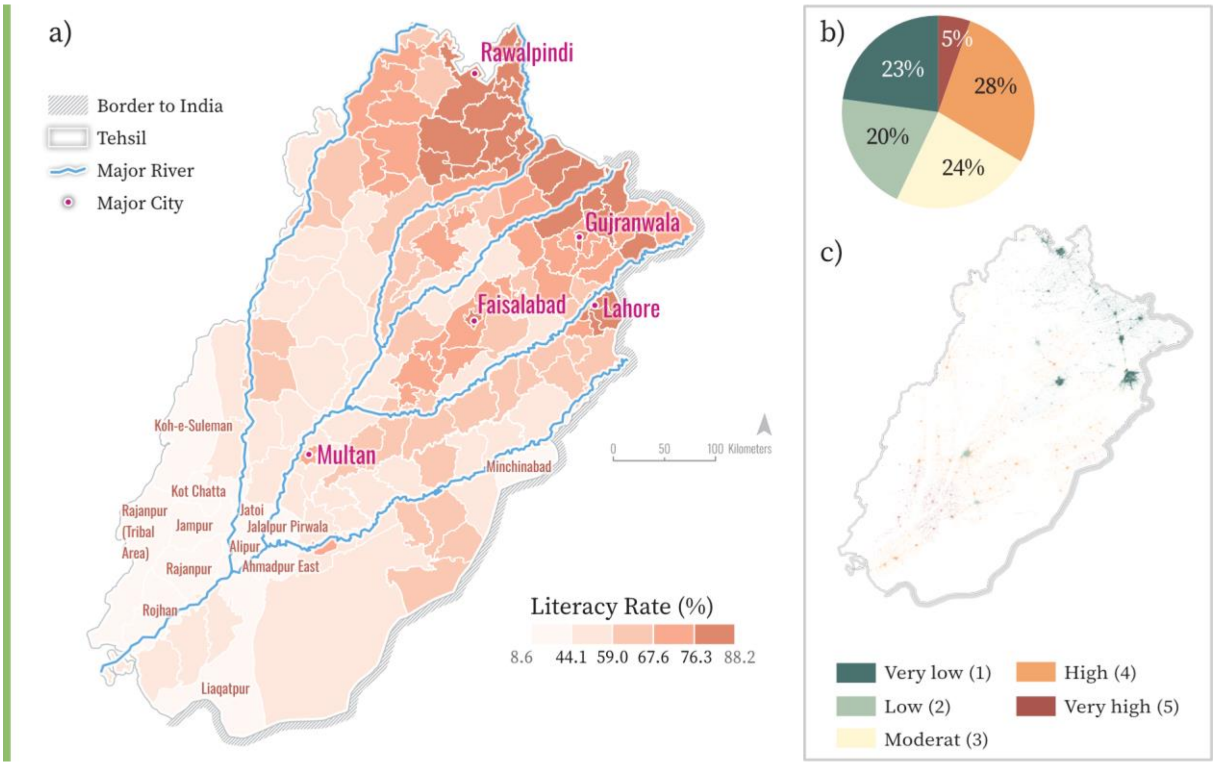


**Figure 27** (a) Percentage of literacy rate, (b) percentages of risk classes (values rounded) in inhabited places, and (c) distribution of risk classes in Punjab based on settlements.

**Table 13** Raking of the Parameters.

| Component | Parameter | Class | Class ratings | Class rankings |
|---|---|---|---|---|
| **Flood-Prone Component (FPC)** | | | | |
| | Annual Rainfall (mm/year) | < 400 | Very low | 1 |
| | | 400 - 500 | Low | 2 |
| | | 500 - 600 | Moderate | 3 |
| | | 600 - 700 | High | 4 |
| | | > 700 | Very high | 5 |
| | Distance to River (m) | < 1000 | Very high | 5 |
| | | 1000–3000 | High | 4 |
| | | 3000–6000 | Moderate | 3 |
| | | 6000–10,000 | Low | 2 |
| | | > 10,000 | Very low | 1 |
| | Drainage Density ($m/km^2$) | ≤ 6.34 | Very low | 1 |
| | | 6.34–27.76 | Low | 2 |
| | | 27.76–39.25 | Moderate | 3 |
| | | 39.25–56.96 | High | 4 |
| | | > 65.96 | Very high | 5 |
| | Elevation (m) | ≤ 150 | Very high | 5 |
| | | 150–200 | High | 4 |
| | | 200–300 | Moderate | 3 |
| | | 300–400 | Low | 2 |
| | | > 400 | Very low | 1 |
| | LULC | Shrubland, tree cover | Very low | 1 |
| | | Grassland | Low | 2 |
| | | Bare/sparse Vegetation | Moderate | 3 |
| | | Built-up, Cropland | High | 4 |
| | | Water bodies, Herbaceous wetland | Very high | 5 |
| | Slope (°) | ≤ 1.5 | Very high | 5 |
| | | 1.5–5 | High | 4 |
| | | 5–15 | Moderate | 3 |
| | | 15–30 | Low | 2 |
| | | > 30 | Very low | 1 |

| | | | |
|---|---|---|---|
| TWI (level) | ≤ 5.12 | Very low | 1 |
| | 5.12–6.67 | Low | 2 |
| | 6.67–7.94 | Moderate | 3 |
| | 7.94–10.75 | High | 4 |
| | > 10.75 | Very high | 5 |
| **Population Susceptibility Component (PSC)** | | | |
| Dependent Population (%) | ≤ 41.41 | Very low | 1 |
| | 41-40–43,54 | Low | 2 |
| | 43,54–45,70 | Moderate | 3 |
| | 45,70–49,11 | High | 4 |
| | > 49,11 | Very high | 5 |
| Disabled Population (%) | ≤ 2.65 | Very low | 1 |
| | 2.65–3.86 | Low | 2 |
| | 3.86–5.70 | Moderate | 3 |
| | 5.70–9.40 | High | 4 |
| | > 9.40 | Very high | 5 |
| Female Population (%) | ≤ 48.02 | Very low | 1 |
| | 48.02–48.77 | Low | 2 |
| | 48.77–49.40 | Moderate | 3 |
| | 49.40–50.20 | High | 4 |
| | > 50.20 | Very high | 5 |
| | ≤ 600 | Very low | 1 |
| Population Density (pop./km²) | 600–2000 | Low | 2 |
| | 2000–4000 | Moderate | 3 |
| | 4000–9000 | High | 4 |
| | > 9000 | Very high | 5 |
| **Coping Capacity Component (CCC)** | | | |
| Distance To Health Facilities (m) | ≤ 2000 | Very low | 1 |
| | 2000–4000 | Low | 2 |
| | 4000–6000 | Moderate | 3 |
| | 6000–10,000 | High | 4 |
| | > 10,000 | Very high | 5 |
| Literacy Rate (%) | ≤ 44.05 | Very high | 5 |
| | 44.05–59.02 | High | 4 |
| | 59.02–67.55 | Moderate | 3 |
| | 67.55–76.28 | Low | 2 |
| | > 76.28 | Very low | 1 |

## 7.1.2 Analytical Hierarchy Process

### 7.1.2.1 Flood-Prone Component

According to the AHP the DD is the most influential parameter in the FPC (21%), followed by LULC (18%), AR (15%), DR (13%), EL (12%), TWI (11%), and SL (10%).

### 7.1.2.2 Population Susceptibility Component

Based on the AHP DiP is the most influential parameter in the PSC (41%), followed by DeP (34%), FP (17%), and PD (8%).

### 7.1.2.3 Coping Capacity Component

According to the AHP the DH (67%) is the most influential parameter, followed by LR (33%).

## 7.1.3 Overlay Analysis of FPC, PSC, and CCC and FVI calculation

The FVI consists of three components: FPC, PSC, and CCC. While the FPC represents the physical flood hazard calculated over the whole area, the PSC shows the social vulnerability of populations, and the CCC, representing their ability to respond, is derived from the settlement location. First, the results of the three component maps will be analyzed and then the FVI.

After each FVI parameter was mapped and ranked as previously described, and the importance of each parameter was determined through the AHP, the different component maps were generated with overlay analysis.

### 7.1.3.1 Flood-Prone Component

Using the parameters and the respective weights derived from the AHP, the overlay analysis generated the FPC Map. The output of the FPC ranged from 1 (very low flood-prone) to 5 (very high flood-prone); while 8.22% (16,889.62 km²) in low, 48.74% (100,266.5 km²) in moderate, 42.72% (87,882.86 km²) in high, and 0.32% (654.96 km²) is very high flood-prone areas in the study area in the FPC pixel map (Figure 28a).

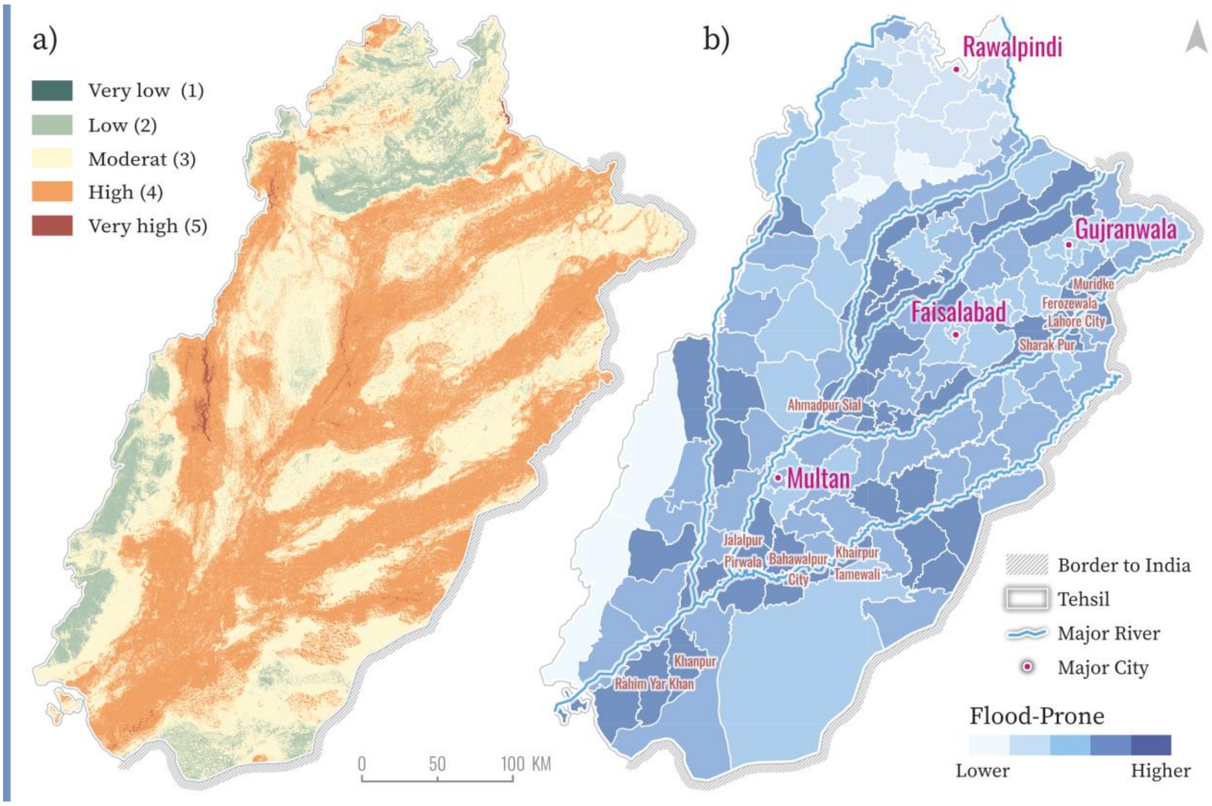


**Figure 28** (a) Flood-Prone Component Map, and (b) aggregated to Tehsils (The top 10 Tehsils with the highest flood-prone score are labelled).

The results indicate that almost half of the study area falls within the moderate flood-prone category, while a smaller portion of ~43% is classified as high and very high. This confirmed the high flood of catastrophic susceptibilities in the Punjab region. The high classes can especially be found near river basins, characterized by high drainage density, high proximity to rivers, flat terrain, and low slopes. While areas, characterized by high elevation, higher slope, and no river basins are classified as low, as well as moderate. Moderate areas are also especially found in flat terrain and lower slopes, However, the topographical characteristics of riverine areas in particular make them higher flood-prone areas. The FPC aggregated to Tehsils (Figure 28b) confirmed these findings. Especially areas in river basins are highly affected. Furthermore, based on the average FPC class value highest affected Tehsils are identified (Table 14); these values ranged from 2.26 to 3.99. Lahore City has an average FPC class value of 3.99 with 96.23% of its area classified as high and very high flood-prone. The Ahmadpur Sial and Ferozewala also show values around 3.98 with over 96% of their area in high and very high. Through these Tehsils, major rivers flow through, and almost the entire settlement area is exposed as the high percentage suggested.

**Table 14** Top 10 Tehsils are sorted with the highest average FP classes.

| Rank | Tehsil | Total Tehsil Area (km²) | High FP Area (km²) | Very High FP Area (km²) | Combined FP Area (km²) | % of Tehsil in High & Very High FP | Average FPC Class |
|---|---|---|---|---|---|---|---|
| 1 | Lahore City | 237.48 | 222.37 | 6.15 | 228.53 | 96.23% | 3.99 |
| 2 | Ahmadpur Sial | 758.67 | 722.73 | 13.10 | 735.83 | 96.99% | 3.99 |
| 3 | Ferozewala | 576.54 | 553.51 | 3.84 | 557.35 | 96.67% | 3.97 |
| 4 | Muridke | 832.60 | 782.49 | 0.30 | 782.79 | 94.02% | 3.94 |
| 5 | Khanpur | 1727.94 | 1609.15 | 0.13 | 1609.28 | 93.13% | 3.93 |
| 6 | Bahawalpur City | 385.42 | 355.63 | 0.01 | 355.64 | 92.27% | 3.92 |
| 7 | Sharak Pur | 386.06 | 349.98 | 0.80 | 350.78 | 90.86% | 3.91 |
| 8 | Khairpur Tamewali | 720.83 | 647.54 | 0.65 | 648.19 | 89.92% | 3.90 |
| 9 | Jalalpur Pirwala | 878.36 | 784.10 | 0.00 | 784.10 | 89.27% | 3.89 |
| 10 | Rahim Yar Khan | 2126.86 | 1843.92 | 10.99 | 1854.90 | 87.21% | 3.88 |

### 7.1.3.2 Population Susceptibility Component

The PSC Map was created with overlay analyses based on its parameters and the weights. The map ranged from 1 (very low population susceptibility) to 4 (high population susceptibility); while 1.89% (133.86 km²) in very low, 48.78% (3454.19 km²) is low, 47.91% (3392.97 km²) is moderate, and 1.42% (100.63 km²) in high population susceptibility in inhabited places in the PSC pixel map (Figure 29a).

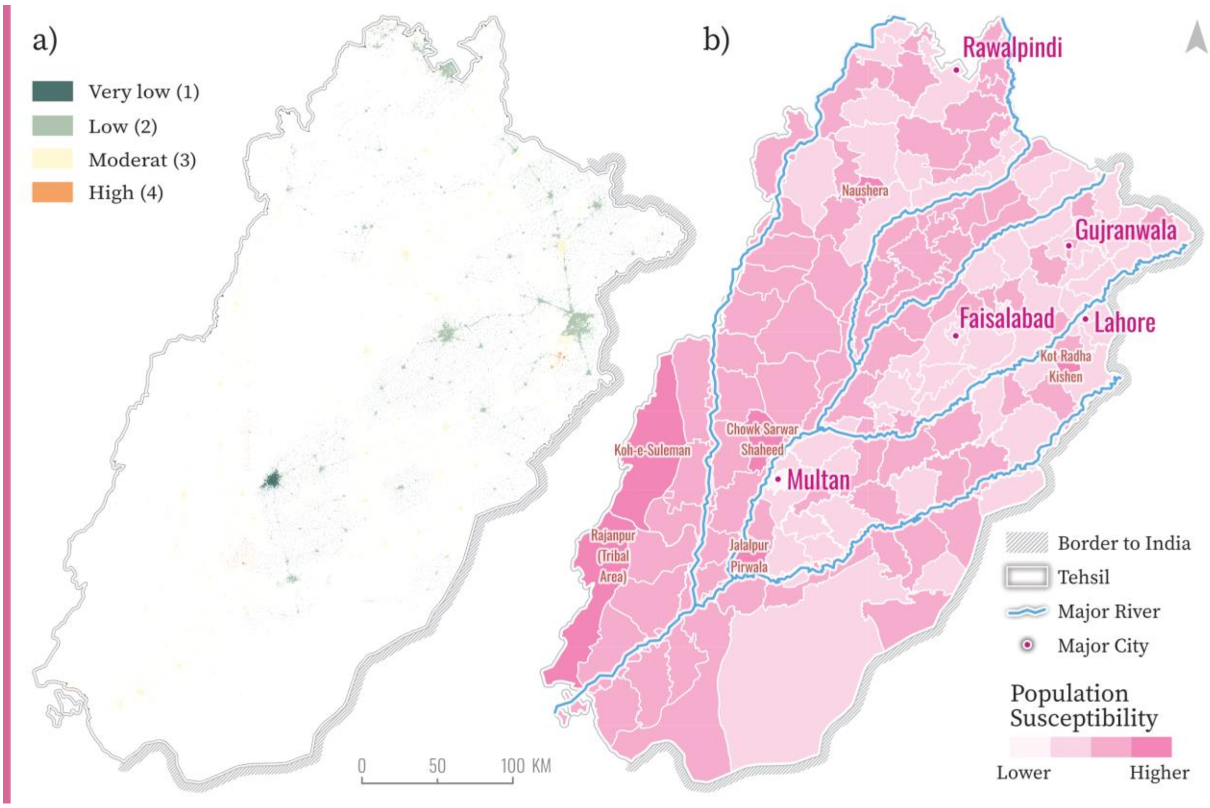


**Figure 29** (a) Population Susceptibility Component Map, and (b) aggregated to Tehsils (The top 10 Tehsils with the highest flood-prone score are labelled).

The PSC aggregated to Tehsils (Figure 29b) showed that the Tehsils Jalalpur Pirwala, Kot Radha Kishen, Chowk Sarwar Shaheed, Naushera, Rajanpur (Tribal Area), and Koh-e-Suleman are identified as the highest population susceptibility. These Tehsils are mostly located in rural areas, while areas with less population susceptibility are in urban areas. As the AHP evaluated the population density as the lowest influential factor (8%) it makes sense, that the rural areas achieved higher values, as they are characterized by a higher percentage of dependent and disabled population.

Table 15, shows the values of the average PSC values, which range from 1.00 to 4.00. As the data was available as Tehsil census data, the average data values are at whole numbers when aggregating the Tehsil. However, comparing Figure 29a and Figure 29b the importance of dasymetric mapping becomes clear. Dasysmetic mapping plays a crucial role in ensuring accuracy throughout the study. Without it, large Tehsils (Figure 29b, e.g., the large Tehsil in the southeast corner) would appear highly vulnerable in the calculation of the Flood Vulnerability Index (FVI) pixel map, as every pixel of this large area would have data from the census data. While each settlement pixel within a Tehsil was assigned the same PSC value this approach offers a higher resolution and better interpretability than full-scaled aggregated data. The most accurate method would be to assign the individual pixel location the exact value based on household survey data for instance but given the unavailability of such data for the entire region, the adopted approach remains an effective and practical alternative. This is the same for the CCC, respectively.

**Table 15** Top 10 Tehsils are sorted with the highest average PS classes.

| Rank | Tehsil | Total Settlement Area (km²) | Moderate PS Settlement Area (km²) | High PS Settlement Area (km²) | % of High | Average PSC Class |
|---|---|---|---|---|---|---|
| 1 | Jalalpur Pirwala | 34.43 | 0.00 | 34.43 | 100.00% | 4.00 |
| 2 | Kot Radha Kishen | 33.72 | 0.00 | 33.72 | 100.00% | 4.00 |
| 3 | Chowk Sarwar Shaheed | 22.18 | 0.00 | 22.18 | 100.00% | 4.00 |
| 4 | Naushera | 5.33 | 0.00 | 5.33 | 100.00% | 4.00 |
| 5 | Rajanpur (Tribal Area) | 3.49 | 0.00 | 3.49 | 100.00% | 4.00 |
| 6 | Koh-e-Suleman | 1.47 | 0.00 | 1.47 | 100.00% | 4.00 |
| 7 | Zafarwal | 27.56 | 27.56 | 0.00 | 0.00% | 3.00 |
| 8 | Vehari | 73.74 | 73.74 | 0.00 | 0.00% | 3.00 |
| 9 | Taunsa | 32.33 | 32.33 | 0.00 | 0.00% | 3.00 |
| 10 | Sohawa | 20.18 | 20.18 | 0.00 | 0.00% | 3.00 |

#### 7.1.3.3 Coping Capacity Component

The CCC map was generated with overlay analysis and the obtained weights The CCC map ranged from 1 (very low coping capacity) to 5 (very high coping capacity); while 26.64% (1886.33 km²) of the study area is very low, 32.14% (2275.78 km²) is low, 9.74% (689.99 km²) is moderate, 15.00% (1061.94 km²) in high, and 16.49% (1167.60 km²) in very high coping capacity in inhabited places (Figure 30a). Urban areas are characterized by higher coping capacity, as cities have a higher presence of health facilities, and they were ranked as highest in the AHP (67%). Furthermore, the literacy rate is also higher in urban areas and to the north.

The CCC aggregated to Tehsils (Figure 30b) emphasizes it. Especially in urban areas, the ability to cope is high. Several Tehsils are identified with the lowest coping capacity (Table 16): Athara Hazari, Bahawalnagar, Isakhel, Jalalpur Pirwala, Jatoi, Kalur Kot, Liaqatpur, Pakpattan, Quaidabad, Noorpur, Shorkot, Kot Chatta. The average CCC values ranged from 1.00 to 4.92.

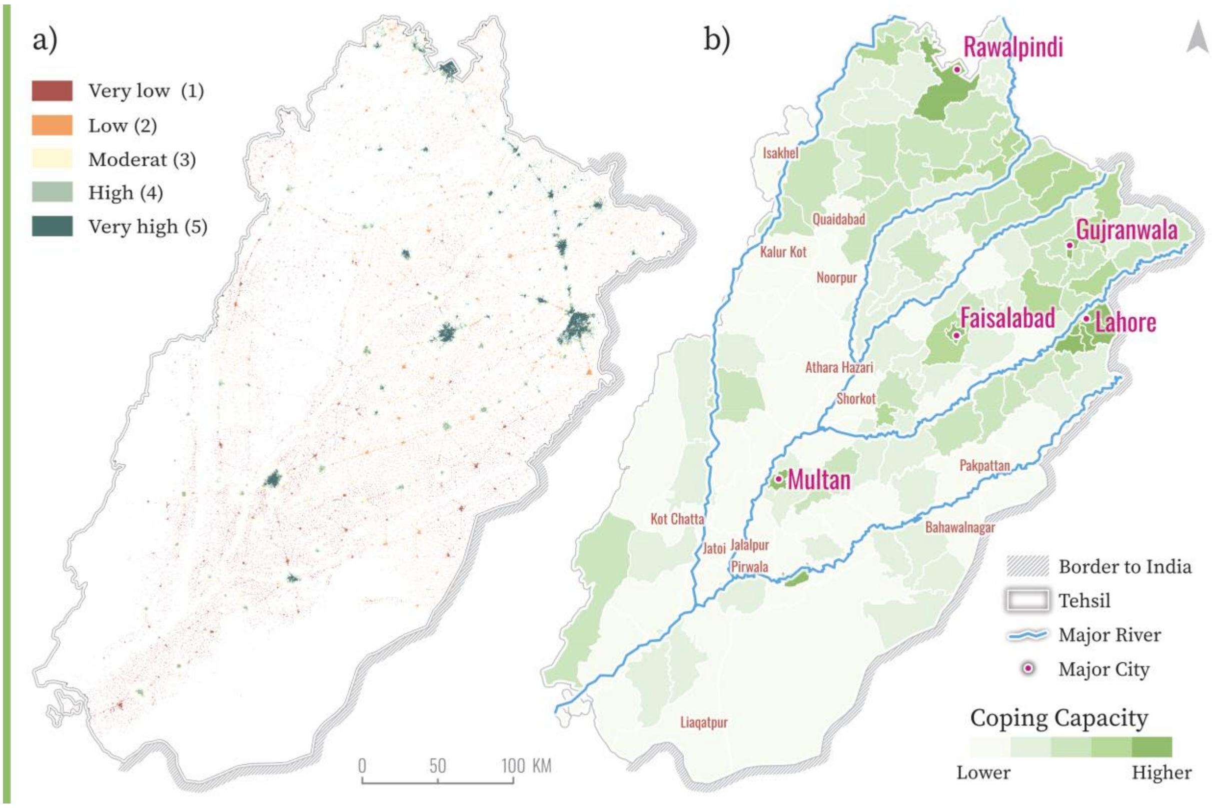


**Figure 30** (a) Coping Capacity Component Map, and (b) aggregated to Tehsils (The top 12 Tehsils with the highest flood-prone score are labelled).

**Table 16** Top 20 Tehsils are sorted with the lowest average CC classes.

| Rank | Tehsil | Total Settlement Area (km²) | Very low CC Settlement (km²) | Low CC Area (km²) | Combined CC Settlement (km²) | % of Very low + Low | Average CC Class |
|---|---|---|---|---|---|---|---|
| 1 | Athara Hazari | 20.17 | 20.17 | 0.00 | 20.17 | 100.00% | 1.00 |
| 2 | Bahawalnagar | 64.36 | 64.36 | 0.00 | 64.36 | 100.00% | 1.00 |
| 3 | Isakhel | 37.86 | 37.86 | 0.00 | 37.86 | 100.00% | 1.00 |
| 4 | Jalalpur Pirwala | 34.43 | 34.43 | 0.00 | 34.43 | 100.00% | 1.00 |
| 5 | Jatoi | 30.62 | 30.62 | 0.00 | 30.62 | 100.00% | 1.00 |
| 6 | Kalur Kot | 26.20 | 26.20 | 0.00 | 26.20 | 100.00% | 1.00 |
| 7 | Liaqatpur | 68.71 | 68.71 | 0.00 | 68.71 | 100.00% | 1.00 |
| 8 | Pakpattan | 52.76 | 52.76 | 0.00 | 52.76 | 100.00% | 1.00 |
| 9 | Quaidabad | 12.18 | 12.18 | 0.00 | 12.18 | 100.00% | 1.00 |
| 10 | Noorpur | 25.71 | 25.68 | 0.03 | 25.71 | 100.00% | 1.00 |
| 11 | Shorkot | 49.97 | 49.80 | 0.17 | 49.97 | 100.00% | 1.00 |
| 12 | Kot Chatta | 26.16 | 26.04 | 0.13 | 26.16 | 100.00% | 1.00 |
| 13 | Sadiqabad | 86.18 | 85.44 | 0.71 | 86.15 | 99.97% | 1.01 |
| 14 | Rojhan | 12.07 | 11.99 | 0.07 | 12.05 | 99.82% | 1.01 |
| 15 | Dunyapur | 37.40 | 37.05 | 0.35 | 37.40 | 100.00% | 1.01 |
| 16 | Depalpur | 77.02 | 76.37 | 0.41 | 76.78 | 99.68% | 1.01 |
| 17 | Khairpur Tamewali | 21.16 | 20.81 | 0.35 | 21.16 | 100.00% | 1.02 |
| 18 | Lodhran | 55.52 | 54.56 | 0.91 | 55.48 | 99.92% | 1.02 |
| 19 | Kabirwala | 72.18 | 69.90 | 2.04 | 71.94 | 99.67% | 1.03 |
| 20 | Minchinabad | 29.27 | 28.07 | 1.09 | 29.16 | 99.62% | 1.05 |

#### 7.1.3.4 Flood Vulnerability Index

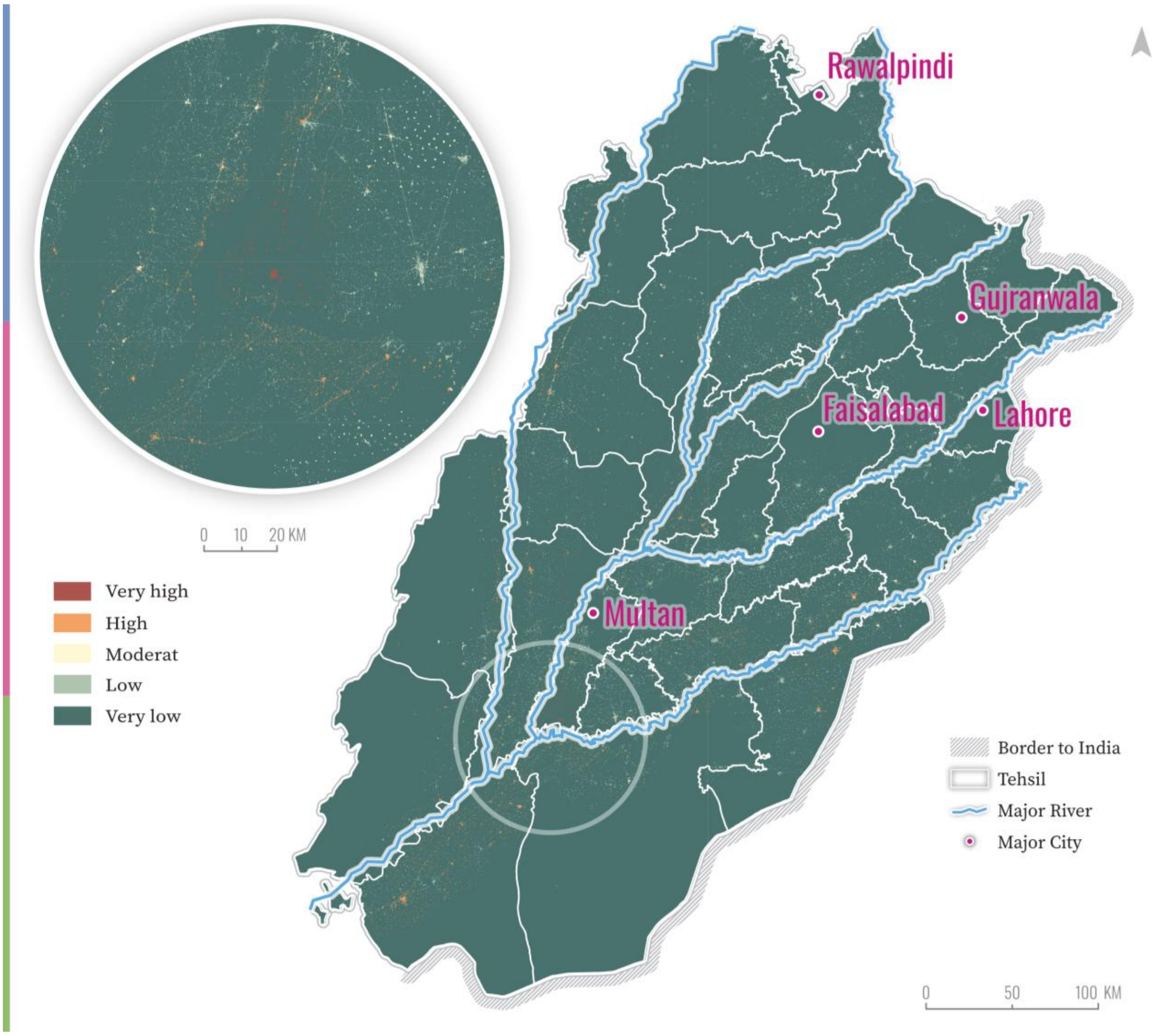


**Figure 31** FVI map.

The FVI was calculated by multiplying the PFC by the PSC and dividing by the CCC. The FVI was classified using the Equal Interval method. The calculation of the FVI revealed that 13.28% (941 km$^2$) of the study area is in very high and high vulnerability areas in inhabited places in the FVI pixel map. The FVI emphasizes that areas characterized by large FPC and large PSC values, as well as low CCC, are highly vulnerable. The FVI aggregated to Tehsils (Table 17; map on page 36, Figure 6) revealed that Jalalpur Pirwala is the area with the highest flood vulnerability. This Tehsil has an average FPC of 3.89, an average PSC of 4.00, and an average CCC of 1.00, resulting in a raw FVI of around 15.57, which normalizes to 1.00, making it the most vulnerable. The Tehsils identified as the most vulnerable are Jalalpur Pirwala, Shorkot, Khairpur Tamewali, Bahawalnagar, Sadiqabad, Athara Hazari, Pakpattan, Jatoi, Chowk Sarwar Shaheed, and Liaqatpur. While Tehsils like Koh-e-Suleman (avg. PSC 4.00) have high population susceptibility and a lower coping capacity (avg. CCC 1.65), their PFC is lower (avg. PFC 2.51) than other areas, making it less vulnerable when computed by the formula.

In contrast, Tehsils with higher CCC averages, like Multan City, have a high average of CCC (4.68), but low PSC (1.00) and high PFC (3.63), however, vulnerability is still low due to the high CCC. This emphasizes that even urban areas are more prone to flooding overall, due to distance to rivers, but as the ability to cope is higher and the population is less exposed, they are less affected.

**Table 17** Top 10 Tehsils sorted with the highest normalized FVI at the Tehsil.

| Rank | Tehsil | Total Settlement Area (km²) | Av. PFC Settl. Tehsil | Av. PSC Settl. Tehsil | Av. CCC Settl. Tehsil | FVI norm. | Raw FVI |
|---|---|---|---|---|---|---|---|
| 1 | Jalalpur Pirwala | 34.43 | 3.89 | 4.00 | 1.00 | 1.00 | 15.57 |
| 2 | Shorkot | 49.96 | 3.87 | 3.00 | 1.00 | 0.73 | 11.58 |
| 3 | Khairpur Tamewali | 21.16 | 3.90 | 3.00 | 1.02 | 0.73 | 11.51 |
| 4 | Bahawalnagar | 64.36 | 3.83 | 3.00 | 1.00 | 0.72 | 11.48 |
| 5 | Sadiqabad | 86.18 | 3.64 | 3.00 | 1.01 | 0.68 | 10.83 |
| 6 | Athara Hazari | 20.17 | 3.54 | 3.00 | 1.00 | 0.66 | 10.61 |
| 7 | Pakpattan | 52.76 | 3.49 | 3.00 | 1.00 | 0.65 | 10.46 |
| 8 | Jatoi | 30.62 | 3.47 | 3.00 | 1.00 | 0.65 | 10.41 |
| 9 | Chowk Sarwar Shaheed | 22.18 | 3.44 | 4.00 | 1.35 | 0.63 | 10.15 |
| 10 | Liaqatpur | 68.71 | 3.34 | 3.00 | 1.00 | 0.63 | 10.03 |

These findings are important and can help policy implementation. Areas with high FVI values, such as the Jalalpur Pirwala Tehsil, should be prioritized for flood mitigation and flood resilience plans. Furthermore, the drawn picture that rural areas, which are often affected by flood events, are highly vulnerable as in contrast, urban areas are less vulnerable, emphasizes that flood mitigation strategies are just as important in rural areas, even if there may be fewer people living.

### 7.1.4 Validation of the FPC

The validation of the FPC showed that the previous flood occurred in 71.22% of very high and high vulnerability classified areas; 26.47% were in the moderate vulnerability class, while 2.31 % were in the low vulnerability class. The results indicate that the assessment of flood-prone areas in this model is accurate and reliable.

## 7.2 Geographic Design and User Testing

### 7.2.1 Visualization Approaches

Different mapping approaches were visualized. The FVI is aggregated to Tehsils (Chapter 5.2.1) and interpolated (Chapter 5.2.4). Furthermore, the FPC was mapped in the background, and PSC and CCC were visualized with pie charts (Chapter 5.2.2), half-circles (Chapter 5.2.3), and Wurman dots (Chapter 5.2.5). The maps can be seen in Chapter 5.4. These maps were tested in the user testing.

### 7.2.2 Rating of the different mapping approaches

The users were asked to rate the different maps based on their level of spatial detail and their ease of understanding (Figure 32). The FVI map across Tehsils (a) clearly shows that users in both groups found this approach easy to understand, although it lacks spatial detail. The Kriging Map of FVI (b) shows a similar result; however, a higher detail was evaluated. This makes sense, as due to the interpolation technique approach, the vulnerability does not stop at boundaries and has weird cuts between Tehsils. However, opinions are divided when it comes to the next maps, where the components are visualized separately. Users evaluate the FPC background with pie charts of people exposed across Tehsils (c) with a higher spatial detail as before, justified by many respondents that this gives more information it the three components and their influence on vulnerability. However, this means that simple understanding is lost for several participants, and given more time for understanding, the complexity of the map can be overcome. Similar things were said about the FPC background with half-circles of people exposed across Tehsils (d) map. Interestingly were the responses to the Kriging Map of FPC with Wurman Dots of people exposed (e). The spatial detail was rated high; however, for some analysts, the Wurman dots were difficult to understand, as their legend title was misleading.

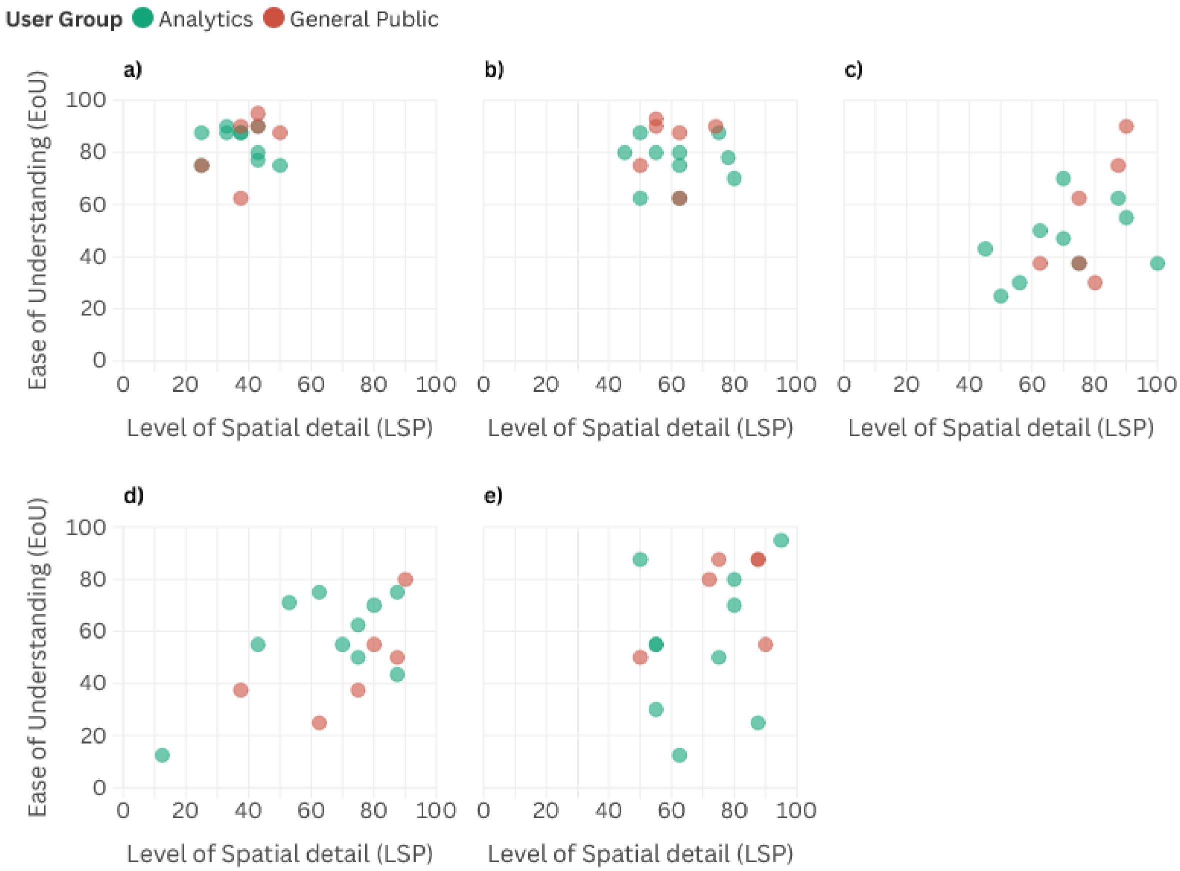


**Figure 32** User responses of climate risk analyzers and general public; (a) FVI across Tehsils, (b) and interpolated, (c) FPC background with pie charts of people exposed across Tehsils, (d) FPC background with half-circles of people exposed across Tehsils, (e) Kriging Map of FPC with Wurman Dots of people exposed; overlapping points exists.

Considering the average of the users' responses, although the FVI map across Tehsils (a) was the easiest to understand, it was also the one with the lowest spatial detail (Figure 33). This map received a score of 37.00 for Level of Spatial Detail (LSP) and 83.70 for Ease of Understanding (EoU) by the climate risk analysts user group, 39.33 LSP, and 83.33 EoU by the general public (Table 18). The Kriging Map of FVI (b) was rated as having higher spatial detail but with a slightly less ability to understand: 62.05 LSP and 76.30 EoU by the climate risk analysts, and 59.83 LSP and 83.00 EoU by the general public; this visualization approach was therefore rated the best map in using the FVI formula, also highly rated overall. The FPC background with pie charts of people exposed across Tehsils (c) was rated better by the general public than the climate risk analysts. This makes sense, as analysts might understand the problem of the pie charts better and know that they cannot directly get an understanding of the underlying values. This visualization approach achieved 70.60 LSP and 45.75 EoU by the climate risk analysts, and 78.33 LSP and 55.42 EoU by the general public; indicating that this map provided the most information but was harder to interpret. The FPC background with half-circles of people exposed across Tehsils (d) was rated with 64.60 LSP and 56.95 EoU by the climate risk analysts, and 72.08 LSP and 47.50 EoU by the general public; this map was quite similar to (c) but better understood by analysts. The Kriging Map of FPC with Wurman Dots of people exposed (e) was rated with best values in the maps by visualizing the components separately: 69.50 LSP and 56.00 EoU by the climate risk analysts, and 77.00 LSP and 74.58 EoU by the general public.

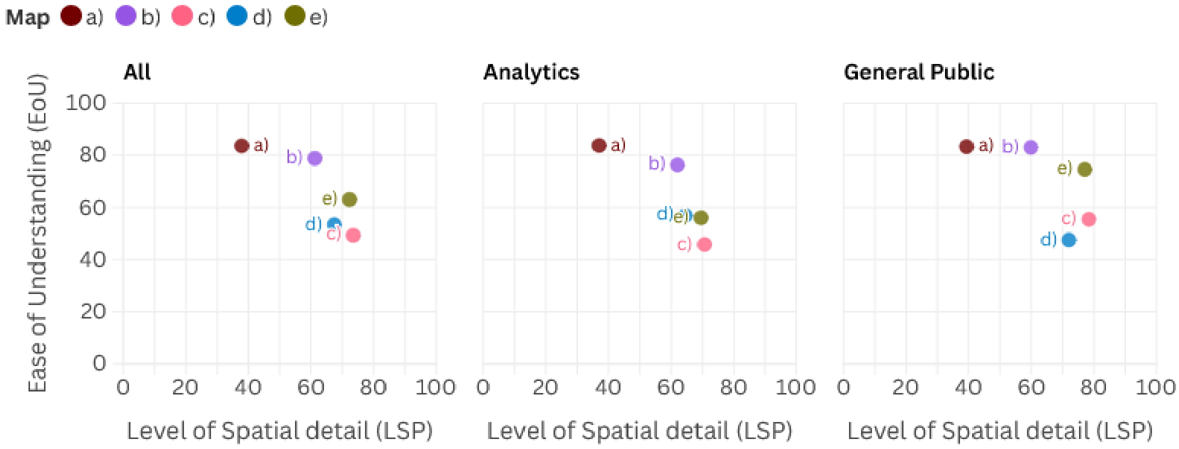


**Figure 33** Average user responses of all interviewees, climate risk analyzers, and of the general public; (a) FVI across Tehsils, (b) and interpolated, c) FPC background with pie charts of people exposed across Tehsils, (d) FPC background with half-circles of people exposed across Tehsils, (e) Kriging Map of FPC with Wurman Dots of people exposed.

Given the rating, the Kriging Map of FVI (b) achieved the highest score of 140.03 in total (summing both dimensions together) in combining the user groups, with 61.22 LSP and 78.81 EOU. Followed by the Kriging Map of FPC with Wurman Dots of people exposed (e), with a value of 135.28, with 72.31 LSP and 62.97 EoU. As Map (b) was highlighted to understand it easier, and that it makes more sense and reflects the vulnerability compared to the aggregation in Tehsils, this map should be given when using the formula. This statement is supported by different participants, who stated that this map would be good to show to the public; also, some people stated that this map is also good for decision making, to get a quick overview of where exactly in the Tehsils help is needed. As some people mentioned the interpolation resolution, different resolutions should be given, to give the user different views for Tehsil, or settlement scale views. Although map (e) did not achieve the highest scores, it was still the best-rated map in separately visualizing the vulnerability components and receiving feedback on how to improve it. Several participants rated this map as a lack of understanding as the legend title of the Wurman Dots was misleading; would this explanation had been given on the map, or the title better, they might have rated it better. The resolution could also be considered here. Furthermore, the feedback, adding the number of people in the Wurman dots, might draw a better picture to get more insight into vulnerability. A bivariate mapping method could be used: the size shows the risk values (calculated by dividing PSC by CCC), and the color intensity of the dots tells something about how many people live there. This would give a good overview of the final flood vulnerability while being easy to understand as well as giving also information on the people, as well as their level of vulnerability. Also changing the color background slightly, making it not so prominent, to increase the readability. Given that the interpolation makes consumption, for the atlas, maps with finer hexagon resolution should be provided, and with the above-mentioned feedback. With that, the user has the possibility to get a broader overview of vulnerability in the province and can look more specifically at different maps capturing a smaller scale, and a higher resolution in a particular area. Overall, general feedback from the risk analysts was that they really appreciated the different approaches to mapping, as they are usually confronted with GIS Outputs.

**Table 18** Mean values of user testing.

| Map | User Group | Level of Spatial detail (LSP) | Ease of Understanding (EoU) | Total |
|---|---|---|---|---|
| **a)** | All | 37,88 | 83,56 | 121,44 |
| | Analytics | 37,00 | 83,70 | 120,70 |
| | General Public | 39,33 | 83,33 | 122,67 |
| **b)** | All | 61,22 | 78,81 | 140,03 |
| | Analytics | 62,05 | 76,30 | 138,35 |
| | General Public | 59,83 | 83,00 | 142,83 |
| **c)** | All | 73,50 | 49,38 | 122,88 |
| | Analytics | 70,60 | 45,75 | 116,35 |
| | General Public | 78,33 | 55,42 | 133,75 |
| **d)** | All | 67,41 | 53,41 | 120,81 |
| | Analytics | 64,60 | 56,95 | 121,55 |
| | General Public | 72,08 | 47,50 | 119,58 |
| **e)** | All | 72,31 | 62,97 | 135,28 |
| | Analytics | 69,50 | 56,00 | 125,50 |
| | General Public | 77,00 | 74,58 | 151,58 |

In summary, through the user feedback, the following changes were made:

- changing the color scheme of the FPC;
- making the description better, to increase the understanding of the methodology;
- correct legend titles, which led to misleading;
- changing colors of the symbology to increase readability and clarity;
- providing different resolutions of interpolation maps;
- adding inset maps to the atlas, to zoom into particular important areas;
- improving the Wurman dots map by adding additional information.

## 7.3 Cartographic Project of the Atlas

### 7.3.1 Atlas

According to the layout structure presented in Chapter 6.1 the atlas was designed. The parameters are visualized covering two pages (Figure 34). This gives the possibility to present the spatial distribution of the classes in one map, while a figure shows the covered area. Another map shows the distribution of the values. The mapping approaches are mainly visualized on two pages (Figure 35). Providing more space for explanation and for inset maps.

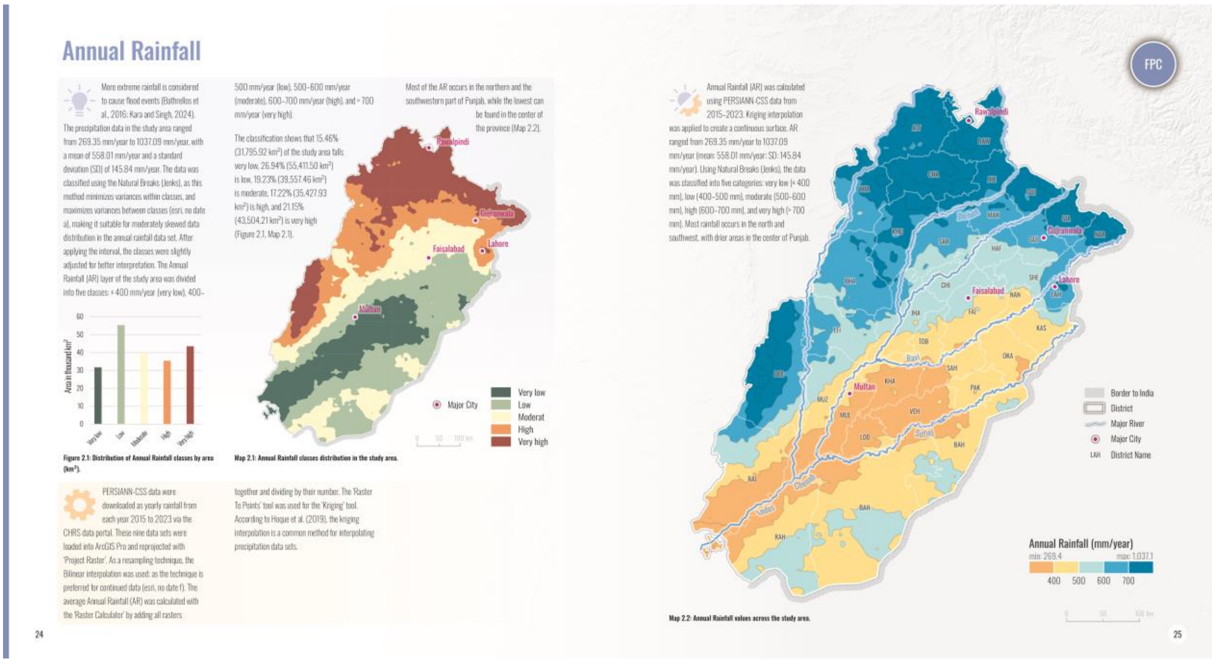


**Figure 34** Sample image of two pages of the atlas; here the AR parameter.

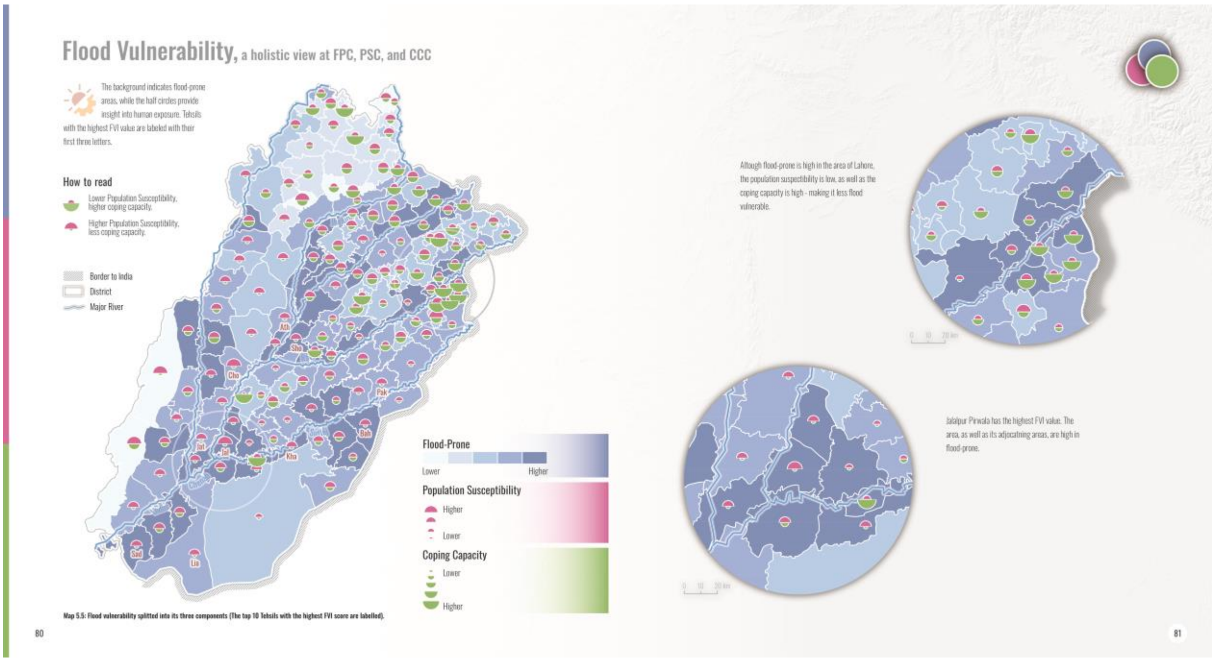


**Figure 35** Sample image of two pages of the atlas; here FVI drawn with FPC in the background and PSC and CCC as half-circles.

During the user testing, a question mark symbol was used on the different maps, identifying an explanation text about the map creation and the data. In the atlas layout, a different visualizing approach was used, one symbol indicates the used methods and data (Figure 36a), while another gives information about the results (Figure 36b), and a combination of both provides a quick summary (Figure 36c).


**Figure 36** (a) methods, (b) results, (c) summary.

The improved maps, based on the feedback from the user testing, can be seen in the atlas at https://gernotnikolaus.github.io/MasterThesis_FloodVulnerabilityPunjab.

### 7.3.2 Digital Product

The digital product was developed in Leaflet and hosted on a GitHub page (https://gernotnikolaus.github.io/FVI_Punjab/). This interactive dashboard allows the user to explore the layers of FVI and its three different components, aggregated to the Tehsil level (Figure 37). The explanation text on the left side gives a summary of the study analysis. While the different layers can be switched on or off, the user can zoom to a specific Tehsil and investigate the different values of the analysis by hovering over the respective administrative boundary.

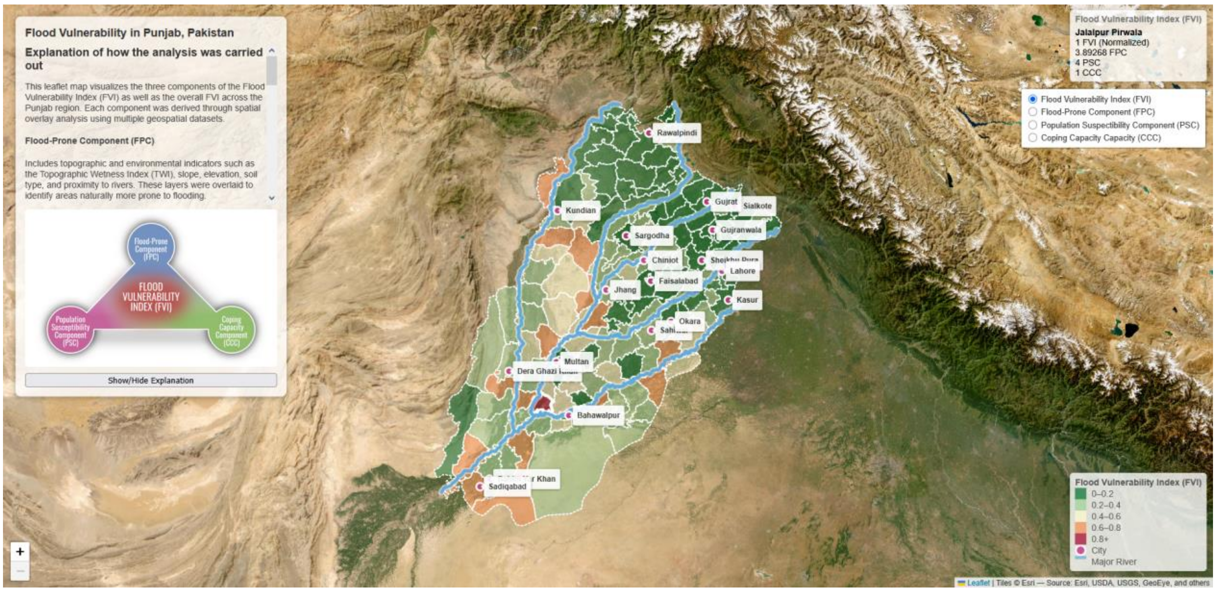


**Figure 37** Screenshot of the interactive dashboard.

# 8 DISCUSSION

The master's thesis deals with the flooding problem in Pakistan. The Punjab province was chosen as a study area, as this region is prone to flooding and people are yearly affected. To address these issues, the study developed a framework that aims to analyze the area with a multi-layer approach. In contrast to Ullah *et al.* (2024), this research not only concentrates on the identification of flood-prone areas but also takes the population into account. This Flood Vulnerability Index (FVI) framework consists of three components: the Flood-Prone Component (FPC), the Population Susceptibility Component (PSC), and the Coping Capacity Component (CCC). By integrating demographic and adaptive capacity factors, the study delivers insights that were not considered in previous studies in the Punjab region. Although the use of geospatial techniques, the Analytical Hierarchy Process (AHP), and the creation of user-friendly visualizations offer a practical way to evaluate the risk of flooding, some limitations must be considered. There are also some methodological points that must be discussed, which might have influenced the outcome of this study. Also, improvements are worth mentioning, which might pave the way for future research.

## 8.1 Data Sources, Processing, Resolution, Validation, and Scaling Issues

One thing that stood out was the huge study area, which has advantages and disadvantages. It has the benefit that a large area is covered by the assessment, but the analysis might not be able to capture small nuances. Classification of some parameters might be generalized, as the study areas are characterized by different topographic conditions. For example, Punjab reaches from high mountains in the north to flat terrain in the south. This results in a large range of values (e.g., meters in the Elevation), which can influence the classification and therefore, the outcome of the study. Nevertheless, the analysis provides general patterns of flood vulnerability. The determined hotspots can serve for future studies to analyze the most affected areas in greater detail. Future researchers can build on the results of this study and include data with higher resolution and more precise information in smaller and more localized study areas, as described below.

Existing limitations in the data and the processing must be discussed. The data for the health facilities and the rivers were obtained from OpenStreetMap (OSM). Although this data is freely available, the information is provided by users, and inaccuracies and gaps can occur. While Kablan *et al* (2017) uses census data based on sub-district level, the study uses a dasymetric mapping technique to enhance the data's localization of the PSC and the CCC. Future studies that might have access to data on the house survey level would provide better accuracy than the technique used in this study. Although the dasymetric mapping technique masked the census data to settlements, so as a proxy for where people live, each pixel in the administrative value still has the same value. However, as more precise data was not available, this technique still provided better precision in the FVI calculation than if the data had not been masked out. Had this not been done, each pixel of the whole administrative boundary would have had one pixel and would have distorted the results. The availability and up-to-date population data would improve future studies. As future studies might focus on smaller areas, highlighted as endangered areas in this study, it might be easier to obtain this data.

Resolution and the scaling of the data also have to be added to the consideration. All layers were scaled to 30m to guarantee consistency between the parameters. Although the 30m matched the resolution of the DEM, the Sentinel-1 and the Land Use Land Cover data had to be downscaled. Finer resolution of data might improve the accuracy of the study because smaller nuances in the topography might be captured. However, as discussed earlier, given the large study area, these nuances could be absorbed, and hence, higher resolution might be considered for smaller study areas. Furthermore, the use of 30m gives a good balance of computational efficiency and spatial resolution. What really has to be pointed out here is the precipitation data. This data was available with a resolution of 4 km and had to be upscaled. The data was processed with interpolation and resampling, that it matches the 30m and ensures consistency between the data sets. Therefore, this coarse resolution might have gaps which might be important in some local conditions and cannot be excused by the size of the study area. Nevertheless, it provided general patterns of the annual rainfall in the province. Despite the available resolution, rainfall is a driver of flooding (Bates *et al.*, 2008), and hence, it should not be neglected, as it gives crucial information about where most rainfall fell.

Furthermore, methodological limitations exist. As the AHP is rated based on opinion, it is rated with subjectivity. The low consistency ratio of below 0.1 suggests consistency, but a different group of experts might assign different relative importance to the parameters. The robustness of the AHP could be assessed with Sensitivity Analysis (Ullah *et al.*, 2024). A single-parameter sensitivity analysis (SPSA) could be performed to evaluate how each parameter layer influences the FVI, providing valuable information about their impact. While the map removal sensitivity analysis (MRSA) might assess the significance of each parameter when each layer is systematically removed at a time to determine whether significant changes occur in the model output. Moreover, the classification of the parameters was mostly based on literature and interval methods. Precise adjustment of the indicators based on fieldwork or discussion with locals might enhance the model further.

Another point worth mentioning is the limitations in the validation process. The result of the FPC was validated with multiple flooding extents derived from Sentinel-1 covering five years. Adding more years to the validation step might improve the representation of the flood-prone analysis and the validation result. Furthermore, validating the whole FVI results would provide valuable information about the model's reliability. Similar to Hoque *et al.* (2019) the results of the FVI could be evaluated by people in the study area. Based on a survey, people affected and the experts from Pakistan who rated the AHP would give important feedback on the accuracy of the model's mapping result.

## 8.2 Mapping Approaches, FVI, and User Testing Feedback

While Hoque et al. (2019), Ullah *et al.* (2024), Roy and Dhar (2024), and Mshelia et al. (2024) produced raster-based maps for visualizing flood-prone and vulnerable areas, this study developed different mapping approaches for visualizing flood vulnerability. The user testing concluded that the FVI aggregated to the Tehsils is easier to understand and good for comparing regions with others. However, it also created artificial boundaries. The interpolated FVI might be more precise, but different resolutions should be provided because data could be lost, or misleading information could be added in the interpolation step. One thing that stood out is that mapping the components separately gives more insight into vulnerability, but it is more complex to understand. Although different visualization approaches offer various ways of reading the analyzed vulnerability, the formula-based method needs some discussion. A challenge that emerged here is that the FVI model uses different dimensions. While the FPC covers the whole area, the PSC and CCC cover pixels where settlements are located. Thus, visualizing the components separately gives the possibility to avoid this problem. The pie charts, half-circles, and the Wurman dots present a good way of combining the thematic content and at the same time deliver important information about their interplay in flood vulnerability in the respective areas.

The user testing was conducted with a relatively small sample size (n=16), and no user from Punjab was included. Different user groups are important in the user testing. While the climate risk analyzers gave feedback on technical aspects, the user of the general public ensured that the maps are also understandable for a broader audience. Also, if they are usually not in touch with such topics. Hence, adding an additional user group might enhance the findings. Cartographers will observe the maps with their professional perspective and provide information on cartographic rules. People in Punjab could be added to the general public group. They might look at the maps more specifically, due to their experiences, and different findings can be collected. Furthermore, only five maps were included in the user testing. Future studies, that also put effort into visual creation, might test the whole product. While the atlas was not tested in the user testing, the layout was discussed with experts in the atlas creation to ensure its correctness.

Overall, the mapping approaches were well received. Especially, the feedback from climate risk analysts was valuable, as they usually work with GIS outputs and pixel maps. They emphasize how important it is to find new ways of communicating and presenting the results. This study contributes to their research and can be directly used in flood management. Furthermore, the feedback highlighted a clear legend and additional text on how the data was processed and mapped. The user testing ensured that the final results are accurate, accessible, and understandable not only for decision makers but also for the public. Although the aggregation process from pixel maps to vector-based maps increases the readability, it also generalizes the results. Future studies might search for different mapping approaches or might focus more on the creation of an interactive pixel map. However, as the study’s main focus lay in visualizing maps which are easy to understand and to interpret, the study’s approach is still appropriate.

# 9 CONCLUSION

This study was motivated by the flood danger in Punjab and the research gap that exists in the area. This issue was addressed in two parts. Firstly, flood-vulnerable areas were identified and analyzed. For this, the study developed a Flood Vulnerability Index (FVI) which integrates various physical and environmental factors, and demographic and coping capacity parameters. Geospatial tools and an Analytical Hierarchy Process (AHP) were combined. The use of FVI's three components the study offered a multi-dimensional perspective of flood vulnerability. Secondly, the results obtained were visualized with different mapping approaches. The different visualization techniques were compiled to an atlas, making the results not only accessible for decision-makers, but also for a broader audience.

The study followed a structured workflow for geospatial analysis and mapping creation. First, literature research on flooding was conducted, and indicators were identified. Seven parameters frame the Flood-Prone Component (FPC), including the Annual Rainfall, Distance to the River, Drainage Density, Elevation, Land Use Land Cover, Slope, and Topographic Wetness Index. Secondly, the Population Susceptibility Component (PSC) consists of four indicators, such as the Dependent Population, Disabled Population, Female Population, and Population Density. Lastly, two parameters, the Distance to Health Facilities and the Literacy Rate, create the Coping Capacity Component (CCC). This data was obtained from various open-data sources and platforms, such as Sentinel-1, ESA WorldCover, FABDEM, and OpenStreetMap. For every parameter, a map was created, classified into 5 categories ranging from very low to very high, and weighed based on experts' opinion with the AHP. The participants consisted of eight experts in Pakistan and five climate risk analysts from the United Nations University – Institute for Environment and Human Security (UNU-EHS). Pairwise comparison matrices helped with detecting the influence of each parameter. Furthermore, the consistency was determined. Each component map was then generated with an overlay analysis.

The research delivered methodical and thematic contributions to geospatial flood mapping. Furthermore, valuable results for the study program of geoinformatics, earth observation, geovisualization, and geocommunication were obtained. The FPC identified flood-prone areas, which lay generally in flat terrain near river basins. The PSC and the CCC determined regions where human susceptibility is high and coping capacity is lacking. However, the most important result of the study is the FVI itself and the different maps. Therefore, another contribution lies in the cartographic results. The different mapping approaches used, combined with the user testing, delivered valuable insights on how to create maps that are easy to understand while providing the required level of detail for decision making. The atlas created in this thesis thus provides legible visualizations and tools for decision-making, which are also understandable by non-experts.

At the same time, the study also delivers thematic contributions to the assessment and strategies for flooding. Using climate and environmental parameters, such as precipitation and elevation, the study not only determines current but also future flooding scenarios. By integrating population susceptibility and coping capacity, the study also offers another perspective on how the population might be affected. The major benefit of this study lies in the methodology, which can be scaled to another region of the world. All data in this study were open access. If some data might be limited or not available, the FVI can be adopted for the respective area. Future studies can build on the FVI framework to analyze flood vulnerabilities, especially when taking the limitations and improvements into account considered in Chapter 8. If data is available, information about housing quality, economic status, and access to resources can draw a clearer picture of flood vulnerability. Taking these limitations and improvements into consideration, and adopting the framework to the study area, this study's methodology supports long-term climate planning and the analysis of risk induced by climate.

In summary, this study achieves its aims and delivered a useful contribution to flood assessment. Especially its visualizations. The study not only deals with the methodical possibilities of mapping but also provides practical tools. The integration of geospatial analysis with visual user-centered design enhances the potential of the study to serve as a model for future studies. The printed atlas and the digital product can help with decision-making and to make communities more resilient and contribute to flood management and climate adaptation globally. While climate-related catastrophes arise and millions of people get affected, the need for frameworks like in this study grows too. Combining open access data, geodata data and user-centric design, research is getting more and more important for building strong communities and to be prepared for the climate-induced challenges we already face, and we will face in the coming years.

# REFERENCES AND INFORMATION SOURCES


Ajtai, I. *et al.* (2023) 'Mapping social vulnerability to floods. A comprehensive framework using a vulnerability index approach and PCA analysis', *Ecological Indicators*, 154, p. 110838. Available at: https://doi.org/10.1016/j.ecolind.2023.110838.

Aldous, A. *et al.* (2011) 'Droughts, floods and freshwater ecosystems: evaluating climate change impacts and developing adaptation strategies', *Marine and Freshwater Research*, 62, pp. 223–231. Available at: https://doi.org/10.1071/MF09285.

Allafta, H. and Opp, C. (2021) 'GIS-based multi-criteria analysis for flood prone areas mapping in the trans-boundary Shatt Al-Arab basin, Iraq-Iran', *Geomatics, Natural Hazards and Risk*, 12(1), pp. 2087–2116. Available at: https://doi.org/10.1080/19475705.2021.1955755.

Arnell, N.W. and Gosling, S.N. (2013) 'The impacts of climate change on river flow regimes at the global scale', *Journal of Hydrology*, 486, pp. 351–364. Available at: https://doi.org/10.1016/j.jhydrol.2013.02.010.

Aydin, M.C. and Sevgi Birincioğlu, E. (2022) 'Flood risk analysis using gis-based analytical hierarchy process: a case study of Bitlis Province', *Applied Water Science*, 12(6), p. 122. Available at: https://doi.org/10.1007/s13201-022-01655-x.

Balica, S., Douben, N. and Wright, N. (2009) 'Flood vulnerability indices at varying spatial scales', *Water science and technology : a journal of the International Association on Water Pollution Research*, 60, pp. 2571–80. Available at: https://doi.org/10.2166/wst.2009.183.

Balica, S. and Wright, N. (2009) 'A network of knowledge on applying an indicator-based methodology for minimizing flood vulnerability', *Hydrological Processes*, 23, pp. 2983–2986. Available at: https://doi.org/10.1002/hyp.7424.

Balica, S. and Wright, N. (2010) 'Reducing the complexity of the flood vulnerability index', *Environmental Hazards*, 9(4), pp. 321–339. Available at: https://doi.org/10.3763/ehaz.2010.0043.

Baptista, S. (2014) 'Design and Use of Composite Indices in Assessment of Climate Change Vulnerability and Resilience, Tetra Tech ARD'. Available at: https://pdf.usaid.gov/pdf_docs/PA00K67Z.pdf (Accessed: 30 November 2024).

Bates, B. *et al.* (2008) 'Climate Change and Water. Technical Paper of the Intergovernmental Panel on Climate Change'.

Bathrellos, G.D. *et al.* (2016) 'Urban flood hazard assessment in the basin of Athens Metropolitan city, Greece', *Environmental Earth Sciences*, 75(4), p. 319. Available at: https://doi.org/10.1007/s12665-015-5157-1.

Bathrellos, G.D. *et al.* (2018) 'Temporal and Spatial Analysis of Flood Occurrences in the Drainage Basin of Pinios River (Thessaly, Central Greece)', *Land*, 7(3), p. 106. Available at: https://doi.org/10.3390/land7030106.

Beven, K.J. and Kirkby, M.J. (1979) 'A physically based, variable contributing area model of basin hydrology / Un modèle à base physique de zone d'appel variable de l'hydrologie du bassin versant', *Hydrological Sciences Bulletin*, 24(1), pp. 43–69. Available at: https://doi.org/10.1080/02626667909491834.

Brewer, C. (1999) *Color Use Guidelines for Data Representation*, *Proceedings of the Section on Statistical Graphics*.

Brunelli, M. (2015) 'Introduction to the Analytic Hierarchy Process', Springer International Publishing. Available at: https://doi.org/10.1007/978-3-319-12502-2.

Burayu, D.G., Karuppannan, S. and Shuniye, G. (2023) 'Identifying flood vulnerable and risk areas using the integration of analytical hierarchy process (AHP), GIS, and remote sensing: A case study of southern Oromia region', *Urban Climate*, 51, p. 101640. Available at: https://doi.org/10.1016/j.uclim.2023.101640.

Chen, F. *et al.* (2024) 'Pakistan's 2022 floods: Spatial distribution, causes and future trends from Sentinel-1 SAR observations', *Remote Sensing of Environment*, 304, p. 114055. Available at: https://doi.org/10.1016/j.rse.2024.114055.

CHRS (no date) *CHRS Data Portal*. Available at: https://chrsdata.eng.uci.edu/ (Accessed: 16 January 2025).

Connor, R. and Hiroki, K. (2005) 'Development of a method for assessing flood vulnerability', *Water science and technology : a journal of the International Association on Water Pollution Research*, 51, pp. 61–7. Available at: https://doi.org/10.2166/wst.2005.0109.

'Copernicus Sentinel data, 2021-2024' (no date). Retrieved via Google Earth Engine. https://earthengine.google.com/.

Coveney, S. and Roberts, K. (2017) 'Lightweight UAV digital elevation models and orthoimagery for environmental applications: data accuracy evaluation and potential for river flood risk modelling', *International Journal of Remote Sensing*, 38(8–10), pp. 3159–3180. Available at: https://doi.org/10.1080/01431161.2017.1292074.

Cutter, S.L., Boruff, B.J. and Shirley, W.L. (2003) 'Social Vulnerability to Environmental Hazards', *Social Science Quarterly*, 84(2), pp. 242–261.

Eicher, C. and Brewer, C. (2001) 'Dasymetric Mapping and Areal Interpolation: Implementation and Evaluation', *Cartography and Geographic Information Science - CARTOGR GEOGR INF SCI*, 28, pp. 125–138. Available at: https://doi.org/10.1559/152304001782173727.

esri (no date a) *Data classification methods*. Available at: https://pro.arcgis.com/en/pro-app/latest/help/mapping/layer-properties/data-classification-methods.htm (Accessed: 7 February 2025).

esri (no date b) *Distance Accumulation (Spatial Analyst)*. Available at: https://pro.arcgis.com/en/pro-app/3.2/tool-reference/spatial-analyst/distance-accumulation.htm (Accessed: 7 February 2025).

esri (no date c) *Fill (Spatial Analyst)—ArcGIS Pro | Documentation*. Available at: https://pro.arcgis.com/en/pro-app/latest/tool-reference/spatial-analyst/fill.htm (Accessed: 24 January 2025).

esri (no date d) *Flow Accumulation (Spatial Analyst)—ArcGIS Pro | Documentation*. Available at: https://pro.arcgis.com/en/pro-app/latest/tool-reference/spatial-analyst/flow-accumulation.htm (Accessed: 24 January 2025).

esri (no date e) *Flow Direction (Spatial Analyst)—ArcGIS Pro | Documentation*. Available at: https://pro.arcgis.com/en/pro-app/latest/tool-reference/spatial-analyst/flow-direction.htm (Accessed: 24 January 2025).

esri (no date f) *Resample (Data Management)—ArcGIS Pro | Documentation*. Available at: https://pro.arcgis.com/en/pro-app/3.2/tool-reference/data-management/resample.htm (Accessed: 24 January 2025).

esri (no date g) *Slope (3D Analyst)—ArcGIS Pro | Documentation*. Available at: https://pro.arcgis.com/en/pro-app/3.2/tool-reference/3d-analyst/slope.htm (Accessed: 24 January 2025).

Evers, M., Almoradie, A. and de Brito, M. (2018) 'Enhancing Flood Resilience Through Collaborative Modelling and Multi-criteria Decision Analysis (MCDA)', in *Urban Book Series*, pp. 221–236. Available at: https://doi.org/10.1007/978-3-319-68606-6_14.

Fernández, D.S. and Lutz, M.A. (2010) 'Urban flood hazard zoning in Tucumán Province, Argentina, using GIS and multicriteria decision analysis', *Engineering Geology*, 111(1), pp. 90–98. Available at: https://doi.org/10.1016/j.enggeo.2009.12.006.

Fernandez, P., Mourato, S. and Moreira, M. (2016) 'Social vulnerability assessment of flood risk using GIS-based multicriteria decision analysis. A case study of Vila Nova de Gaia (Portugal)', *Geomatics, Natural Hazards and Risk* [Preprint].

Ghorbani, S. *et al.* (2015) 'Delineation of groundwater potential zones using remote sensing and GIS-based data driven models', *Geocarto International*, 32. Available at: https://doi.org/10.1080/10106049.2015.1132481.

Gigović, L. *et al.* (2017) 'Application of GIS-Interval Rough AHP Methodology for Flood Hazard Mapping in Urban Areas', *Water*, 9, pp. 1–26. Available at: https://doi.org/10.3390/w9060360.

Hagenlocher, M. *et al.* (2016) 'Spatial assessment of social vulnerability in the context of landmines and explosive remnants of war in Battambang province, Cambodia', *International Journal of Disaster Risk Reduction*, 15, pp. 148–161. Available at: https://doi.org/10.1016/j.ijdrr.2015.11.003.

Hamidi, A.R. *et al.* (2022) 'Flood Exposure and Social Vulnerability Analysis in Rural Areas of Developing Countries: An Empirical Study of Charsadda District, Pakistan', *Water*, 14(7), p. 1176. Available at: https://doi.org/10.3390/w14071176.

Hawker, L. *et al.* (2022) 'A 30 m global map of elevation with forests and buildings removed', *Environmental Research Letters*, 17(2), p. 024016. Available at: https://doi.org/10.1088/1748-9326/ac4d4f.

Hoque, M.A.-A. *et al.* (2019) 'Assessing Spatial Flood Vulnerability at Kalapara Upazila in Bangladesh Using an Analytic Hierarchy Process', *Sensors*, 19(6), p. 1302. Available at: https://doi.org/10.3390/s19061302.

Hossain, Md.N. and Mumu, U.H. (2024) 'Flood susceptibility modelling of the Teesta River Basin through the AHP-MCDA process using GIS and remote sensing', *Natural Hazards*, 120(13), pp. 12137–12161. Available at: https://doi.org/10.1007/s11069-024-06677-z.

Huang, D. *et al.* (2012) 'An assessment of multidimensional flood vulnerability at the provincial scale in China based on the DEA method', *Natural Hazards*, 64. Available at: https://doi.org/10.1007/s11069-012-0323-1.

Ibrahim, M. *et al.* (2024) 'Flood vulnerability assessment in the flood prone area of Khyber Pakhtunkhwa, Pakistan', *Frontiers in Environmental Science*, 12, p. 13. Available at: https://doi.org/10.3389/fenvs.2024.1303976.

IPCC (2001) 'Climate Change 2001: Impacts, Adaptation, and Vulnerability'. Available at: https://www.ipcc.ch/site/assets/uploads/2018/03/WGII_TAR_full_report-2.pdf.

IPCC (2012) *Managing the Risks of Extreme Events and Disasters to Advance Climate Change Adaptation: Special Report of the Intergovernmental Panel on Climate Change*. 1st edn. Edited by C.B. Field et al. Cambridge University Press. Available at: https://doi.org/10.1017/CBO9781139177245.

IPCC (2014) *Climate Change 2014: impacts, adaptation, and vulnerability Working Group II contribution to the fifth assessment report of the Intergovernmental panel on climate change*. New York: Cambridge University Press, Cambridge, United Kingdom and New York, NY, USA, 1132 pp. ([Field, C.B., V.R. Barros, D.J. Dokken, K.J. Mach, M.D. Mastrandrea, T.E. Bilir, M. Chatterjee, K.L. Ebi, Y.O. Estrada, R.C. Genova, B. Girma, E.S. Kissel, A.N. Levy, S. MacCracken, P.R. Mastrandrea, and L.L. White (eds.)].).

IPCC (2022) *Climate Change 2022: Impacts, Adaptation and Vulnerability. Contribution of Working Group II to the Sixth Assessment Report of the Intergovernmental Panel on Climate Change*. ([H.-O. Pörtner, D.C. Roberts, M. Tignor, E.S. Poloczanska, K. Mintenbeck, A. Alegría, M. Craig, S. Langsdorf, S. Löschke, V. Möller, A. Okem, B. Rama (eds.)]. Cambridge University Press. Cambridge University Press, Cambridge, UK and New York, NY, USA, 3056 pp., doi:10.1017/9781009325844.). Available at: https://www.ipcc.ch/report/ar6/wg2/downloads/report/IPCC_AR6_WGII_FullReport.pdf.

Islamic Relief (2024) *Pakistan Monsoon Floods 2024 Situation Report - August 29, 2024 - Pakistan*. Available at: https://reliefweb.int/report/pakistan/pakistan-monsoon-floods-2024-situation-report-august-29-2024 (Accessed: 14 February 2025).

Jahandideh-Tehrani, M. *et al.* (2020) 'Hydrodynamic modelling of a flood-prone tidal river using the 1D model MIKE HYDRO River: calibration and sensitivity analysis', *Environmental Monitoring and Assessment*, 192(2), p. 97. Available at: https://doi.org/10.1007/s10661-019-8049-0.

Kabenge, M. *et al.* (2017) 'Characterizing flood hazard risk in data-scarce areas, using a remote sensing and GIS-based flood hazard index', *Natural Hazards*, 89(3), pp. 1369–1387. Available at: https://doi.org/10.1007/s11069-017-3024-y.

Kablan, M.K.A., Dongo, K. and Coulibaly, M. (2017) 'Assessment of Social Vulnerability to Flood in Urban Côte d'Ivoire Using the MOVE Framework', *Water*, 9(4), p. 292. Available at: https://doi.org/10.3390/w9040292.

Kara, R. and Singh, P. (2024) 'Flood assessment for Lower Godavari basin by using the application of GIS-based analytical hierarchy process', *International Journal of System Assurance Engineering and Management* [Preprint]. Available at: https://doi.org/10.1007/s13198-024-02595-2.

Kumar, V. *et al.* (2023) 'Comprehensive Overview of Flood Modeling Approaches: A Review of Recent Advances', *Hydrology*, 10(7), p. 141. Available at: https://doi.org/10.3390/hydrology10070141.

Kundzewicz, Z.W. *et al.* (2014) 'Flood risk and climate change: global and regional perspectives', *Hydrological Sciences Journal*, 59(1), pp. 1–28. Available at: https://doi.org/10.1080/02626667.2013.857411.

Latif, R.M.A. and He, J. (2025) 'Flood Susceptibility Mapping in Punjab, Pakistan: A Hybrid Approach Integrating Remote Sensing and Analytical Hierarchy Process', *Atmosphere*, 16(1), p. 22. Available at: https://doi.org/10.3390/atmos16010022.

Mojaddadi, H. *et al.* (2017) 'Ensemble machine-learning-based geospatial approach for flood risk assessment using multi-sensor remote-sensing data and GIS', *Geomatics, Natural Hazards and Risk*, 8(2), pp. 1080–1102. Available at: https://doi.org/10.1080/19475705.2017.1294113.

Molinari, D. *et al.* (2019) 'Validation of flood risk models: Current practice and possible improvements', *International Journal of Disaster Risk Reduction*, 33, pp. 441–448. Available at: https://doi.org/10.1016/j.ijdrr.2018.10.022.

Nasiri, H., Mohd Yusof, M.J. and Ali, T. (2016) 'An overview to flood vulnerability assessment methods', *Sustainable Water Resources Management*, 2. Available at: https://doi.org/10.1007/s40899-016-0051-x.

Neumayer, E. and Plümper, T. (2007) 'The Gendered Nature of Natural Disasters: The Impact of Catastrophic Events on the Gender Gap in Life Expectancy, 1981–2002', *Annals of the Association of American Geographers*, 97(3), pp. 551–566. Available at: https://doi.org/10.1111/j.1467-8306.2007.00563.x.

Ogato, G.S. *et al.* (2020) 'Geographic information system (GIS)-Based multicriteria analysis of flooding hazard and risk in Ambo Town and its watershed, West shoa zone, oromia regional State, Ethiopia', *Journal of Hydrology: Regional Studies*, 27, p. 100659. Available at: https://doi.org/10.1016/j.ejrh.2019.100659.

Ouma, Y.O. and Tateishi, R. (2014) 'Urban Flood Vulnerability and Risk Mapping Using Integrated Multi-Parametric AHP and GIS: Methodological Overview and Case Study Assessment', *Water*, 6(6), pp. 1515–1545. Available at: https://doi.org/10.3390/w6061515.

Owuor, S.O. *et al.* (2016) 'Groundwater recharge rates and surface runoff response to land use and land cover changes in semi-arid environments', *Ecological Processes*, 5(1), p. 16. Available at: https://doi.org/10.1186/s13717-016-0060-6.

Padhan, N. and Madheswaran, S. (2023) 'An integrated assessment of vulnerability to floods in coastal Odisha: a district-level analysis', *Natural Hazards*, 115(3), pp. 2351–2382. Available at: https://doi.org/10.1007/s11069-022-05641-z.

PBS (2023) *Pakistan Bureau of Statistics, 7th Population and Housing Census - Detailed Results*. Available at: https://www.pbs.gov.pk/digital-census/detailed-results (Accessed: 20 January 2025).

PMD (2024) *Pakistan Meteorological Department - Pakistan Monsoon 2024 Analysis*. Available at: https://cdpc.pmd.gov.pk/Monsoon_2024_update/Pakistan_Monsoon_2024_Rainfall_Update.pdf (Accessed: 15 February 2025).

Price, K., Jackson, C.R. and Parker, A.J. (2010) 'Variation of surficial soil hydraulic properties across land uses in the southern Blue Ridge Mountains, North Carolina, USA', *Journal of Hydrology*, 383(3), pp. 256–268. Available at: https://doi.org/10.1016/j.jhydrol.2009.12.041.

Proag, V. (2014) 'The Concept of Vulnerability and Resilience', *Procedia Economics and Finance*, 18, pp. 369–376. Available at: https://doi.org/10.1016/S2212-5671(14)00952-6.

Rahman, G. *et al.* (2017) 'Socio-Economic Damages caused by the 2014 Flood in Punjab Province, Pakistan', *Proceedings of the Pakistan Academy of Sciences*, 54, pp. 365–374.

Rahman, M. *et al.* (2019) 'Flood Susceptibility Assessment in Bangladesh Using Machine Learning and Multi-criteria Decision Analysis', *Earth Systems and Environment*, 3(3), pp. 585–601. Available at: https://doi.org/10.1007/s41748-019-00123-y.

Rentschler, J., Salhab, M. and Jafino, B.A. (2022) 'Flood exposure and poverty in 188 countries', *Nature Communications*, 13(1), p. 3527. Available at: https://doi.org/10.1038/s41467-022-30727-4.

Roy, A. and Dhar, S. (2024) 'Assessment of flood vulnerability and identification of flood footprint in Keleghai River basin in India: a geo-spatial approach', *Natural Hazards*, 120. Available at: https://doi.org/10.1007/s11069-024-06411-9.

Saaty, R.W. (1987) 'The analytic hierarchy process—what it is and how it is used', *Mathematical Modelling*, 9(3), pp. 161–176. Available at: https://doi.org/10.1016/0270-0255(87)90473-8.

Saaty, T.L. (1990) 'How to make a decision: The analytic hierarchy process', *European Journal of Operational Research*, 48(1), pp. 9–26. Available at: https://doi.org/10.1016/0377-2217(90)90057-I.

Saaty, T.L. (1994) 'How to Make a Decision: The Analytic Hierarchy Process', *Aestimum*, 24. Available at: https://doi.org/10.13128/Aestimum-7138.

Sanders, B.F. *et al.* (2020) 'Collaborative Modeling With Fine-Resolution Data Enhances Flood Awareness, Minimizes Differences in Flood Perception, and Produces Actionable Flood Maps', *Earth's Future*, 8(1), p. e2019EF001391. Available at: https://doi.org/10.1029/2019EF001391.

Sanyal, J. and Lu, X.X. (2006) 'GIS-based flood hazard mapping at different administrative scales: A case study in Gangetic West Bengal, India', *Singapore Journal of Tropical Geography*, 27, pp. 207–220. Available at: https://doi.org/10.1111/j.1467-9493.2006.00254.x.

Seneviratne, S. *et al.* (2021) 'IPCC AR6 WGI Chapter11: Weather and Climate Extreme Events in a Changing Climate', Cambridge University Press, Cambridge, United Kingdom and New York, NY, USA, pp. 1513–1766. Available at: https://doi.org/10.1017/9781009157896.013.

Subbarayan, S. and Saravanan, S. (2020) 'Modelling of Flood Susceptibility Based on GIS and Analytical Hierarchy Process—A Case Study of Adayar River Basin, Tamilnadu, India', in, pp. 91–110. Available at: https://doi.org/10.1007/978-981-32-9527-8_6.

Thomas, K. *et al.* (2018) 'Explaining differential vulnerability to climate change: A social science review', *Wiley Interdisciplinary Reviews: Climate Change*, 10, p. e565. Available at: https://doi.org/10.1002/wcc.565.

Ullah, N. *et al.* (2024) 'Geospatial analysis and AHP for flood risk mapping in Quetta, Pakistan: a tool for disaster management and mitigation', *Applied Water Science*, 14(11), p. 236. Available at: https://doi.org/10.1007/s13201-024-02293-1.

UNDP (2004) *Reducing disaster risk a challenge for development. United Nations Development Programme Bureau for Crisis Prevention and Recovery*. Edited by M. Pelling. New York: United Nations Development Programme.

UNDRR (2009) *Definition: Exposure | UNDRR*. Available at: https://www.undrr.org/terminology/exposure (Accessed: 1 December 2024).

UNISDR (2009) 'UNISDR terminology for disaster risk reduction'.

Waseem, H.B. and Rana, I.A. (2023) 'Floods in Pakistan: A state-of-the-art review', *Natural Hazards Research*, 3(3), pp. 359–373. Available at: https://doi.org/10.1016/j.nhres.2023.06.005.

WFP (2024) *WFP Pakistan Floods Situation Report (August 2022 - December 2023) - Final report (January 2024) - Pakistan*. Available at: https://reliefweb.int/report/pakistan/wfp-pakistan-floods-situation-report-august-2022-december-2023-final-report-january-2024 (Accessed: 14 February 2025).

Youssef, A. *et al.* (2021) 'The devastating flood in the arid region a consequence of rainfall and dam failure: Case study, Al-Lith flood on 23th November 2018, Kingdom of Saudi Arabia', *Zeitschrift für Geomorphologie*, 63. Available at: https://doi.org/10.1127/zfg/2021/0672.

Zanaga, D. *et al.* (2022) 'ESA WorldCover 10 m 2021 v200'. Zenodo. Available at: https://doi.org/10.5281/zenodo.7254221.

Zhran, M. *et al.* (2024) 'Exploring a GIS-based analytic hierarchy process for spatial flood risk assessment in Egypt: a case study of the Damietta branch', *Environmental Sciences Europe*, 36(1), p. 184. Available at: https://doi.org/10.1186/s12302-024-01001-9.

# LIST OF ATTACHMENTS

## Free attachments

| | |
|---|---|
| Attachment 1 | Thesis Poster (Printed A2 Format) |
| Attachment 2 | Atlas (Printed Book) |
| Attachment 3 | Digital Product |
| Attachment 4 | Website |

The atlas and the digital product can be found here:
https://gernotnikolaus.github.io/MasterThesis_FloodVulnerabilityPunjab

The poster can be found on the website:

https://www.geoinformatics.upol.cz/dprace/magisterske/nikolaus25/